Covenant Journal of Engineering Technology (CJET) Vol.5 No.1, June, 2021
ISSN: p. 2682-5317 e. 2682-5325

An Open Access Journal Available Online

Covenant Journal of Engineering Technology (CJET)

Vol. 5 No. 1, June 2021

Publication of the College of Engineering, Covenant University, Canaanland.

Editor-in-Chief: **Dr. Imhade Princess Okokpujie**
editorcjet@covenantuniversity.edu.ng

URL: ***http://journals.covenantuniversity.edu.ng/index.php/cjet***

ISSN: p. 2682-5317 e. 2682-5325

Published by Covenant University Journals,
Covenant University, Canaanland, Km 10, Idiroko Road,
P.M.B. 1023, Ota, Ogun State, Nigeria

Printed by Covenant University Press

Articles

Particulate Mollusc Shells as Reinforcements
for Aluminium Matrix Composites: A Review
Kolapo Olawale Ibrahim **1**

Statistical Model for Predicting Slump and Strength of
Concrete Containing Date Seeds
Yusuf, A.; Jamal, J. O.; Abubakar, M.[1] & Aminulai, H. O. **12**

Effects of the Partial Replacement of Cement with Cassava
Peel Ash and Rice Husk Ash on Concrete
John Oloche Obute, Oluwatobi Olufemi Akin,
Yusuf Dada Amartey, Stephen Pinder Ejeh **20**

Effect of Temperature and Catalyst on Biofuel Yields
from Pyrolysis of African Copaiba Balsam (*Daniellia Oliveri*) Sawdust
Pious O. Okekunle*, Abdulrasaq O. Olasupo and Ibrahim A. Adeyemi **29**

Development of a New Air Compressor System for Ship Operations
Thaddeus C. Nwaoha* and Fabian I. Idubor **37**

Emission Comparison of Air-Fuel Mixtures for Pure Gasoline
and Bioethanol Fuel Blend (E20) Combustion on Sparking-Ignition Engine
M.A. Muregi, M.S. Abolarin, O.J. Okegbile, E.J. Eterigho, I.P. Okokpujie **46**

Mechanical and Chemical Properties of Reinforcement Bars Manufactured in Nigeria
Oluwaseun B. Hassan, Oluwatobi O. Akin, Adamu Lawan and Yusuf D. Amartey **56**

Covenant Journal of Engineering Technology (CJET) Vol.5 No.1, June, 2021
ISSN: p. 2682-5317 e. 2682-5325 DOI: xxxxxxxxxx

An Open Access Journal Available Online

Particulate Mollusc Shells as Reinforcements for Aluminium Matrix Composites: A Review

Kolapo Olawale Ibrahim

Department of Mechanical and Aerospace Engineering, University of Uyo, P. M. B. 1017, Uyo, Akwa Ibom State, Nigeria.
kolapoolawale1@gmail.com

Received: 26.01.2021 Accepted: 06.05.2021 Published: 30.06.2021

Abstract: In recent times, the global need for high-performance, affordable and topnotch materials has necessitated a shift in research from unreinforced to composite materials. Metal matrix composites (MMCs) are relatively novel and highly promising materials that continually attract researchers' attention. They are constantly being developed, and their applications in various industries are on the increase. Aluminium matrix composites (AMCs) are the most commonly studied MMCs because of their many desirable properties, especially high strength and lightweight. These properties make them find extended use commercially. Also, AMCs can be manufactured via cost-effective and straightforward methods. However, the conventional ceramic reinforcements commonly used to reinforce aluminium matrix pose high costs and limited availability. This has triggered other renewable and cheap materials such as agro and industrial wastes as alternatives for reinforcing aluminium alloys. This work attempts to review some particulate mollusc shells that have been used as reinforcements for the fabrication of AMCs. The processes used for the fabrication of AMCs are briefly discussed. Finally, further research for the improvement of AMCs is suggested.

Keywords: composites, mollusc shells, aluminium, reinforcements

1. Introduction

Materials such as steel, aluminium, copper, cast iron, and many more have, over the years, been of high interest in the world of engineering. These materials find extensive use in automotive, aerospace, chemical processing, military, petroleum processing, biomedical, sports. And many other industries where they are used to suit different purposes. However, the global demand for reduced weight, top quality, high performance, and low-cost materials is causing a shift of focus from these unreinforced materials to composite materials [1-4].

The new era engineering systems demand materials with a wide spectrum of properties, which are rarely met using unreinforced materials [5]. Also, the present reality regarding human material demands has necessitated industries to use materials of a better class that are sustainable and environmentally friendly [6]. Metal matrix

composites (MMCs) have been discovered to offer uniquely combined properties required in a wide range of engineering applications [5,7]. High specific strength, high thermal resistance, good damping capacities, improved wear resistance, high specific stiffness, and good corrosion resistance are some of the properties offered by MMCs [8-10]. Due to these much-improved properties, MMCs that were hitherto predominantly used in aerospace and automobile industries are now fast replacing metals. And their alloys in the vast majority of other applications, including defense, sports, marine, and recreation industries [11].

MMCs can be defined as metallic alloys reinforced mostly with hard ceramic material particles to produce desired specifications. Alloys of light metals like Aluminum (Al), Magnesium (Mg), and Titanium (Ti) are commonly used as based metals in the production of MMCs. However, other metals like copper (Cu) and Zinc (Zn) have also been used [12-16]. Despite having some drawbacks in their mechanical properties, aluminum and its alloys have been the most widely utilized as matrix materials in the fabrication of MMCs amongst the competing alternatives [8,11,13,17].

Aluminium matrix composites (AMCs) have a unique combination of physical, chemical, and mechanical properties. This property is rarely obtained when unreinforced materials are used to compete strongly with steel and other alloys in various engineering applications [18-21]. Also, AMCs have other advantages such as low cost of processing and being complaint to production using the techniques for processing monolithic metallic alloys [22,23].

Presently, mollusc farming on a commercial scale is an essential component of the aquaculture industry globally. It represents about 23% of the world's total aquaculture production. It is growing gradually because of its small investment requirement and relatively low energy consumption. Molluscs are sources of cheap and healthy food for the growing world population [24]. Shells of some molluscs can amount to up to 75% of their total body weight. An estimated seven million tons of mollusc shells are disposed of yearly. These shells are usually dumped into public waters and landfills, making them pose some environmental discomfort [25]. Using these shells to reinforce metals will solve environmental problems and serve as a cheap alternative to synthetic reinforcements characterized by high cost and limited supply [26]. In this work, an effort has been made to review some particulate mollusc shells used as reinforcements for the fabrication of AMCs. However, they influence some properties in the composites

2 Materials used to Reinforce AMCs

Materials used to reinforce metal matrix play essential roles because they determine the fabrication methods used for the syntheses of AMCs and the nature of the alloy matrix being reinforced [12, 27-29]. Likewise, most parameters such as reinforcement type, shape, size, modulus of elasticity, hardness, and distribution in the matrix are strongly linked to reinforcing materials [30]

Considering the literature studied while preparing this review, different reinforcing materials that have been used in the development of AMCs can be classified into three broad categories. These are synthetic ceramic particulates, industrial wastes, and agro-waste derivatives [30]. Silicon carbide, silicon nitride, silica, aluminium oxide (alumina), titanium carbide, titanium nitride, graphite, zirconium, boron carbide, tungsten carbide, carbon nanotubes are some of the synthetic ceramic particulates that have been widely studied [31,32]. Nonetheless, silicon carbide and alumina have been the most utilized compared to other synthetic reinforcing particulates [32]. Fly ash and red mud, which are the waste products of power plants and aluminium industries, are the

industrial wastes that have been investigated by various authors [33]. Among many other agro-wastes, bamboo leaf ash (BLA), rice husk ash (RHA), sugarcane bagasse ash (SCBA). Maize stalk ash (MSA), groundnut shell ash (GSA), and coconut shell ash have been used respectively by [34],[35],[36],[37],[38], and [39] to reinforce various aluminium alloys. Seashell wastes that are products of aquaculture or mariculture in recent times are fast gaining interest in the use as reinforcement for aluminium matrix. They are the major focus of this review.

3 Using Particulate Mollusk Shells as Reinforcement phase

Particulate mollusc shells have over the years been used to serve different reinforcement purposes. Various authors have widely studied their reinforcement ability, most especially in concrete and polymers. Mollusc shells are materials that offer advantages of modulus improvement and cost reduction without notably increasing the specific gravity of the composites when compared with the commonly used inorganic fillers [40].

Many authors, including [41],[42],[43], and [44], have used mollusc powder to reinforce polymers such as polypropylene and polyester, and they all affirmed improved mechanical properties. Efforts have been made to use mollusc shells in the reinforcement of AMCs. Based on the published articles studied, the most investigated mollusc shells in aluminium matrixes are those of land snails, periwinkles, mussels, and oysters which are considered in this review

3.1 Snail Shells

The main constituent of the shell is calcium carbonates which can be one of two crystalline forms; calcite or aragonite. The remainder is organic matrixes that constitute a protein known as conchiolin, which usually makes up to 5% of the shell [45-47]. Snail shells are usually present as discarded bio-waste remnants of restaurants, households, eateries, and snail sellers. They constitute environmental threats with little or no economic significance [48,49]. As observed by [49], the Snail shell has about 9.4-25.9 lesser density compared with other agro or industrial reinforcement materials such as fly ash, coconut shell ash, bagasse, and maize husk.

Kolawole et al. [49] have studied the potentials of snail shells as a low-cost reinforcement material in AMCs utilizing a characterization technique. The mineralogical composition and physical properties of particulate snail shells were carried out using density determination. And the thermogravimetric analysis (TGA), refractoriness, dispersive energy X-ray (SEM/EDX), X-ray fluorescent (XRF). The X-ray diffraction (XRD) analyses at 0^{o}C, 800^{o}C, 850^{o}C and 900^{o}C calcination temperatures for 3hrs. The results obtained affirmed that the particulate snail shell had chemical hard phase oxides such as Al_2O_3, Fe_2O_3, SiO_2, CaO, Cr_2O_3, MnO, and NiO. Therefore, at all calcination temperature values with the maximum amount of these phases formed at a 900^{o}C calcination temperature. The XRD analysis indicated the presence of lime (Ca_4O_4), calcite ($Ca_6C_6O_8$), and portlandite (CaO_2H_2) as major hard phases of the particulate snail shells at 900^{o}C calcination temperature. The study also indicated that the density and refractoriness temperature of the snail shell particles are 1.63 g/cm^3 and 1400^{o}C, respectively. The result of the TGA showed that the particulate snail shells attained their thermal stability at 840^{o}C. It was concluded from the results that particulate snail shell was a promising reinforcing material in the production of lightweight metal matrix composites at low costs. Additionally, the high refractoriness temperature of the snail shell particle indicated that it was a suitable reinforcement material in the production of MMCs that are stable at elevated temperatures. And could find use in

automotive components such as pistons connecting rods.

Asafa et al. [50] experimentally studied the potentials of particulate snail shells as reinforcement for discarded aluminum-based materials. Particulate snail shells of 16 to 48 wt% and 200, 400, and 600 μm were added to discarded aluminium pistons using a double stir-casting method. After casting, a microstructural study was carried out on the resultant composites using a metallurgical microscope. Also, the hardness and tensile strength of the composites were examined. The microstructure of the unreinforced sample indicated significant pores of different sizes and shapes. The reinforced samples, however, showed snail shell particles uniformly distributed in the aluminium matrix. The sample containing 48 wt% and 600 μm particle size gave the maximum tensile strength and hardness with the values of 236 MPa and 48.3 HRF, respectively. In contrast, the unreinforced sample gave 92.4 MPa in tensile strength and hardness of 29.2 HRF. The notable increase in tensile strength and hardness was attributed to the uniform distribution of snail shells in the aluminium matrix.

Olawuni et al. [51], to reduce the cost of reinforcement and minimize waste disposal challenges, used discarded aluminium piston reinforced with alumina and snail shells to produce hybrid composite piston material. Discarded motorcycle pistons were melted and then reinforced with alumina and snail shells at different proportions using the D-optimal approach of the Design of Experiment. The microstructure is shown in Figure 1, and elemental composition was determined using a Scanning Electron Microscope (SEM). Mechanical tests such as tensile strength, hardness, and wear were conducted. A corrosion test was also done. The results indicated that hardness, yield point, and tensile strength increased with increased snail shell particles to aluminium alloy. Also, wear loss was greatly minimized as a result of improved mechanical properties. However, the corrosion rate of the composite was higher than that of unreinforced alloy. The reason for this was not stated. It was concluded that alumina and snail shells improved aluminum pistons' mechanical properties, which can be helpful in various engineering applications.

Table1. Chemical Composition of Snail shell ash obtained at 800°C [52]

Constituent	**SiO_2**	**Al_2O_3**	**Fe_2O_3**	**CaO**	**MgO**	**SO_3**	**TiO_2**	**Na_2O**	**P_2O_5**	**MnO_3**	**K_2O**
wt%	10.20	4.81	3.15	61.95	0.18	0.03	0.05	0.04	0.01	0.01	0.01

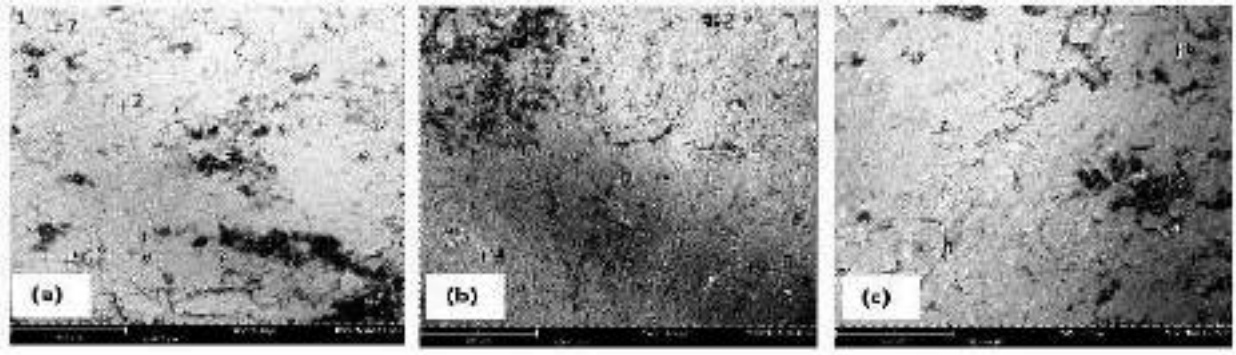

Figure1. SEM Micrographs of (a) Aluminium alloy + 10% Al_2O_3 + 10% snail shell (b) Aluminium alloy + 5% Al_2O_3 + 20% Snail shell (c) Unreinforced Aluminium alloy. Source [51]

3.2 Periwinkle Shells

Periwinkle shells are hard, generally light, and readily available in sizeable quantities. They are also inexpensive [53]. Umunakwe et al. [54] have accessed some mechanical properties and microstructure of particulate periwinkle shell-aluminum 6063 metal matrix composite (PPS-AlMMC) produced through a two-step casting route. After being washed and boiled in water for 40 minutes at 100°C, Periwinkle shells were subsequently sundried. They were further dried in an oven at 110^0C for 30mins to remove all moistures. The shells were crushed, pulverized, and sieved to 75µm and 150µm particle sizes. A software-driven optical metallurgical microscope was used to study the microstructure of the specimens. The tensile and hardness tests were also conducted. The microstructural examination results indicated that particulate periwinkle shells distributed uniformly in AA6063 alloy and refined grains from coarse grains to fine grains at smaller particle sizes. Consequently, due to the ability of particulate periwinkle shells to refine AA6063 alloy grains, the strength and hardness of the composites were improved when compared with the unreinforced alloy. It was deduced that the composites could be used in areas where lighter weight and higher strength were required.

The effect of isothermal heat treatment on the hardness and microstructure of aluminum-periwinkle shell ash biocomposite was experimentally studied by Umaru et al. [55]. Using a stir casting method, the aluminium alloy was reinforced with periwinkle shell ash (PSA) from 5% - 25% in step 5. The composites were subsequently heat treated. It was revealed that periwinkle shell ash distributed homogenously in some aluminium specimens, as shown in Figure 2. These composites had better thermal conductivity and hardness compared to the unreinforced specimen.

The density and mechanical properties of particulate periwinkle shell aluminium 6063 metal matrix composite (PPS-AlMMC) were also investigated by Umunakwe et al. [56]. Particulate periwinkle shell sizes of 75µm and 150µm were used to produce the composite at 1,5,10 and 15wt% using two-step casting. It was observed that the filler was distributed uniformly in the aluminium matrix. The composites had lower density, improved strength, ductility, and hardness. The better mechanical properties were ascribed to the ability of periwinkle shell ash particles to refine the grains of Al6063. It was concluded that the composites could find use in the areas where lighter weight and higher strength were required.

Table 2. Chemical Composition of periwinkle shell ash obtained at 800°C[52]

Constituent	**SiO_2**	**Al_2O_3**	**Fe_2O_3**	**CaO**	**MgO**	**SO_3**	**TiO_2**	**Na_2O**	**P_2O_5**	**MnO_3**	**K_2O**
wt%	26.26	8.79	4.82	55.53	0.4	0.18	0.20	0.25	0.05	0.05	0.07

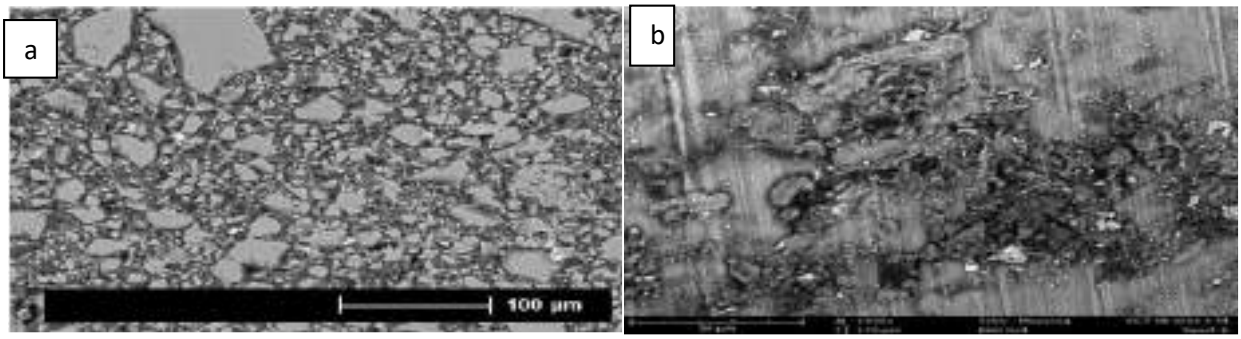

Figure 2: SEM micrograph of (a) unreinforced Al (b) Al/25%PSA. Source [55].

3.3 Mussel Shells

In 2016 alone, an estimated 1827.27 metric tonnes of green mussels were produced worldwide, and it has been increasing yearly. About 33% of mussels are made up of shells, which are usually discarded. With that, they also contribute sizably to waste generation. [57,58]

Surendra et al. [59] have fabricated composites using Al6061 reinforced with mussel shell particulate with the primary aim of studying the dry sliding wear of the composites.2, 4, 6, 8, and 10 weight percent (wt%) of mussel shell particulate was used to reinforce the aluminium matrix. The microstructural study revealed that the particles distributed fairly in the matrix, with 6 wt% having the maximum particle filling capacity. Also, mussel shell particulates progressively increased the overall hardness and wear resistance of the composites up to 6 wt%, demonstrating the best properties. The increase in hardness was attributed to differences in the thermal properties of the reinforcement and matrix phase. This mismatch led to an increase in dislocation densities during solidification.

3.4 Oyster Shells

The corrosion behaviour of Aluminium alloy 6063-Seashell (oyster shell) composites in acidic and alkaline environments was studied by Abdulkareem et al. [60]. The composites were fabricated by varying particulate oyster reinforcements in steps of 1.5 wt% from 1.5 - 7.5 wt % and particle size of 100, 150, and 200 μm in the aluminium 6063 alloy matrix double stir casting method. The static immersion weight loss technique was used to determine the corrosion rate with the weights measured at 72 hours intervals for 18 days in line with the ASTM G31-12 standard. The acidic and alkaline media used were Sulphuric acid (H_2SO_4) and Sodium hydroxide (NaOH), respectively. The results indicated that oyster reinforcement relatively improved the corrosion resistance of the composites, with the sample containing 6.0 wt% and 100 μm particle size. The result shows the best corrosion property in both acidic and alkaline environments. However, all the composites exhibited better corrosion characteristics in the alkaline medium than the acidic medium. The reason for this occurrence was not stated.

Table 3. Chemical Composition of Oyster Shell Ash Obtained at 800°C [52]

Constituent	SiO_2	Al_2O_3	Fe_2O_3	CaO	MgO	SO_3	TiO_2	Na_2O	P_2O_5	MnO_3	K_2O
wt%	13.41	4.95	3.80	57.95	0.19	0.12	0.02	0.22	0.01	0.01	0.01

4. Fabrication Methods for Aluminium Matrix Composites

Various methods have been used to manufacture AMCs. These methods are broadly classified based on the temperature of the metallic matrix while processing [61]. They are solid-state methods and liquid state methods [30,62]. In liquid state routes, the particulates are distributed mechanically over the liquid metal before casting and solidification. These routes are particularly cost-effective [63]. Liquid state routes include stir casting, compocasting, squeeze casting, spray forming, In-Situ Synthesis, and liquid metal infiltration [61].

For liquid state routes of manufacturing AMCs, the stir casting method has been the most investigated. This is because of its simplicity, being commercially viable, and flexibility [64,65]. Nonetheless, it is not without its downsides, including problems of homogenous distribution of reinforcing particles, wettability, porosity, clustering of particles, segregation, interfacial reactions, and the formation of detrimental secondary phases. Methods to contain these challenges have been reported [30]. To solve the wettability between reinforcing particles and aluminium matrix, reinforcement coatings and wetting agents such as K_2TiF_6 are used [66,67]. Clustering and

particle segregation can be avoided by optimizing mixing parameters, including rotation of stirrer, stirring speed, and blade angle to stirrer axis [68]. Formation of secondary phases and interfacial reactions, which are of high detriment to the performance of the composites during the development process. It can be prevented by selecting reinforcing materials that do not undergo interfacial reactions, such as boron carbide and alumina [69]. Employing cold deformation and hot isostatic pressing, and porosity can be substantially reduced in cast AMCs [70,71].

Solid route fabrication includes powder metallurgy (PM), high-energy ball milling, diffusion bonding, and ultrasonic probe assisted method [62]. The fabrication of MMCs via PM has been widely reported. It involves mixing reinforcements uniformly with metal alloy, and the powders are blended. The product, after solidification in a vacuum, is sintered under high temperatures [62]. Many researchers have adopted PM to eliminate the defects encountered in MMCs prepared through conventional methods like stir casting, squeeze casting, and other liquid molten metal techniques. Through this, the mechanical properties of the composites have been increased. It is also one of the much-improved ways to prepare composites and nanocomposites [72].

5. Conclusions and Recommendations

This study has reviewed various works on mollusc shells reinforced metal matrix composites, and the following conclusions have been drawn:

(i) Mollusk shells available in sizeable quantity, are usually considered wastes with little or no economic value.

(ii) Particulate mollusc shells at calcination temperatures produced chemicals hard phases oxides such as Fe_2O_3, CaO, Al_2O_3, and SiO_2, which improved the composites' mechanical properties and made them attain stability at elevated temperatures. This has made them highly promising for the production of AMC's at reduced costs.

(iii) Mollusc shells can distribute uniformly in the aluminium matrix, with the ability to refine matrix materials from coarse grains to fine grains.

It is recommended that further works should be done to determine in details:

(i) The corrosion behaviours of the mollusc shells reinforced AMCs, especially under different conditions since there were conflicting corrosion results from the reviewed articles.

(ii) Further studies also should be focused on how to optimize the production process to ascertain the optimum processing parameters for mollusc shells reinforced AMCs

References

[1] Panwar, N. and Chauhan, A. (2018). Fabrication Methods of Particulate Reinforced Aluminium Metal Matrix, Composite -A Review. Mater Today 5, 5933–5939.

[2] Venugopal, A. and Manoharan, N. (2015). Evaluation Of Mechanical Properties of Aluminium Metal Matrix Composite for Marine Applications. ARPN J. Eng. Appl. Sci. 10, 5557–5559.

[3] Ranjith, R., Kumar, G.S and Seenivasan, N. (2016) A Review on Advancements in Aluminium Matrix Composites. Int. J. Adv. Eng. Technol. VII, 173–176.

[4] Ghasali, E., Shirvanimoghaddam, K., Pakseresht, A.H., Alizadeh, M, and Ebadzadeh, T. (2017) Evaluation of Microstructure and Mechanical Properties of Al-Tac Composites Prepared By Spark Plasma Sintering Process. J. Alloys Compd. 705, 283–289.

[5] Rino, J.J., Chandramohan D., Sucitharan K.S and Jebin V.D. (2012) An overview on

the development of aluminium metal matrix composites with hybrid reinforcement. IJSR India OnlineISSN :2319–7064.

[6] Qin, S. Y., Chen, C. R., Zhang, G. D., Wang W. L. and Wang, Z. G. (1999) "Characterization of Thermal Residual Strain in Sicp/6061 Al Composites By Ultramicrohardness", Journal of Mater. Sci. Lett., Vol. 18, no. 14, pp. 363-370.

[7] Tjong, S.C. (2014) Processing and deformation characteristics of metals reinforced with ceramic nanoparticles. In: Tjong S-C, editor. Nanocrystalline materials [Internet]. 2nd ed. Oxford: Elsevier. p. 269–304 [cited 2020 Aug 25].

[8] Alaneme, K.K, and Bodunrin M.O. (2011) Corrosion Behavior of Alumina Reinforced Aluminium (6063) Metal Matrix Composites. J Miner Mater Charact Eng 2011;10(12):1153.

[9] Surappa M.K. (2003) Aluminium matrix composites: challenges and opportunities. Sadhana;28(1–2):319–34.

[10] Kok M. (2005) Production and mechanical properties of Al_2O_3 particle-reinforced 2024 aluminium alloy composites. J Mater Process Technol;161(3):381–7.

[11] Das D.K., Mishra, P.C, Singh S and Pattanaik S. (2014) Fabrication and Heat Treatment of Ceramic-Reinforced Aluminium Matrix Composites – A Review. Int J Mech Mater Eng;9(1):1–15.

[12] Casati, R. and Vedani, M. (2014) Metal Matrix Composites Reinforced by Nano-Particles- A Review. Metals;4(1):65–83.

[13] Alaneme K.K. and Olubambi P.A. (2013) Corrosion and Wear Behaviour of Rice Husk Ash-Alumina Reinforced Al-Mg-Si Alloy Matrix Hybrid Composites. J Mater Res Technol;2(2):188–94.

[14] Maleque, M.A., Radhi, M and Rahman, M.M. (2016) Wear study of Mg-SiCp reinforcement aluminium metal matrix composite. Journal of Mechanical Engineering and Sciences.;10:1758-64.

[15] Meena, K., Manna, A., Banwait, S., and Jaswanti. An Analysis of Mechanical Properties of the Developed Al/SiC-MMC's. American Journal of Mechanical Engineering.1:14-9.

[16] Abu Bakar M.H., Raja Abdullah R.I., Md. Ali M.A., Kasim M.S., Sulaiman, M.A., and Ahmad S.S.N., et al. (2014) Surface integrity of LM6 aluminium metal matrix composite when machined with high-speed steel and uncoated carbide cutting tools. Journal of Mechanical Engineering and Sciences. 6:854-62.

[17] Lai, M. O. (2009) "Development of Ductile Mg Composite Material Using Ti Reinforcement," Journal of Mater. Sci., Vol. 31, pp. 2155-2167.

[18] Alaneme, K. K. and Olubambi, P. A. (2013) "Corrosion and wear behaviour of rice husk ash Alumina reinforced Al-Mg-Si alloy matrix hybrid composites", j mater res tech-nol., Vol. 2(2), page. 188-189,.

[19] Christy, T.V., Murugan, N. and Kumar S. A, (2010) "Comparative Study on The Microstructures and Mechanical Properties Of Al 6061 Alloy And The MMC Al 6061/Tib2/12". JMMCE pages 57-65.

[20] Alaneme, K.K.(2012) Influence of Thermo-Mechanical Treatment on the Tensile Behaviour And CNT Evaluated Fracture Toughness Of Borax Premixed Sicp Reinforced Aluminium (6063) Composites", IJMME, Vol. 7, page 96-100.

[21] Rohatgi, P. and Schultz B., (2007) "Light Weight Metal Matrix Compo-Sites-Stretching The Boundaries of Metals", Mater Matt, Vol. 2, page 16-9.

[22] Surappa, M.K., and Sadhana, (2003) "Aluminium Matrix Composites: Challenges And Opportunities", page 281-282, 319-334.

[23] Adiamak, M. (2006) "Selected Properties of Aluminium Alloy Based Composites Reinforced With Intermetallic Particles", JAMME, Vol. 14, pages 43-47.

[24] Jović, M., Mandić, M., Šljivić-Ivanović, M., and Smičiklas I (2019) "Recent Trends In Application Of Shell Waste From Mariculture" Studia Marina 32 (1): 47-62

[25] Hou, Y., A. Shavandi, A. Carne, A.A. Bekhit, T.B. Ng, R.C.F. Cheung and A.E.A. Bekhit (2016): Marine shells: Potential opportunities for extraction of

functional and health-promoting materials. Critical Reviews in Environmental Science and Technology 46, 1047–1116

[26] Oghenevweta J.E., Aigbodion V.S., Nyior G.B. and Asuke F. (2014) Mechanical Properties and Microstructural Analysis of Al-Si-Mg/Carbonized Maize Stalk Waste Particulate Composites. J King Saud Univ – Eng Sci [Internet] [cited 2014 Aug 25], available from: http://www.sciencedirect.com/science/article/pii/S1018363914000245.

[27] Alaneme K.K. and Bodunrin M.O. (2013) Mechanical Behaviour of Alumina Reinforced AA 6063 Metal Matrix Composites Developed By Two-Step – Stir Casting Process. Acta Tech Corvininesis – Bull Eng;6(3) [cited 2014 Aug 25], [Internet] Available from:

[28] Alaneme K.K and Aluko A.O. (2012) Production And Age-Hardening Behaviour Of Borax Premixed Sic Reinforced Al-Mg-Si Alloy Composites Developed By Double Stir-Casting Technique. West Indian J Eng;34(1–2):80–5.

[29] Alaneme K.K. (2011) Corrosion behaviour of heat-treated Al-6063/SiCp composites immersed in 5 wt% NaCl solution. Leonardo J Sci;18(18):55–64.

[30] Bodunrin, M. O., Alaneme, K. K and Chown L. H. "Aluminium Matrix Hybrid Composites: A Review Of Reinforcement Philosophies; Mechanical, Corrosion And Tribological Characteristics" J MATER RES TECH N O L .2 0 1 5;4(4):434–445

[31] Yaspal, Jawalkar, C. S., Verma, A. S., and Suri, N. M. (2017). Fabrication of Aluminium MMC with Particulate Reinforcement: A Review. Materials Today: Proceedings 4(2), 2927-2936.

[32] SirahbizuYigezu B., Mahapatra, M.M. and Jha, P.K. (2013) Influence of reinforcement type on microstructure, hardness, and tensile properties of an aluminium alloy metal matrix composite. J Miner Mater Charact Eng;1(4):124–30.

[33] Nagender K. C., Yashpal K. and Chandrashekhar S.J. (2017) "Review on Analysis of Stir Cast Aluminium Metal Matrix Composite from Agro-Industrial Wastes" Article *in* i-manager's Journal on Material Science · January

[34] Alaneme, K. K., Ademilua, B. O., and Bodunrin, M. O. (2013). Mechanical Properties and Corrosion Behaviour of Aluminium Hybrid Composites Reinforced with Silicon Carbide and Bamboo Leaf Ash. Tribology in Industry, 35(1).

[35] Prasad, D. S. and Krishna, R. A. (2011). Production and mechanical properties of A356. 2/RHA composites.International Journal of Advanced Science and Technology, 33, 51-58.

[36] Aigbodion, V. S., Hassan, S. B., Dauda, E. T., and Mohammed, R. A. (2010). The development of the mathematical model for the prediction of ageing behaviour for Al-Cu-Mg/bagasse ash particulate composites. Journal

[37] Oghenevweta, J. E., Aigbodion, V. S., Nyior, G. B., & Asuke, F. (2016). Mechanical properties and microstructural analysis of Al-Si–Mg/carbonized maize stalk waste particulate composites. Journal of King SaudUniversity-Engineering Sciences, 28(2), 222-229.

[38] Alaneme, K. K., Bodunrin, M. O. and Awe, A. A. (2016). Microstructure, mechanical, and fracture properties of groundnut shell ash and silicon carbide dispersion strengthened aluminium matrix composites. Journal King Saud University-Engineering Sciences.

[39] Apasi, A., Madakson, P. B., Yawas, D. S., and Aigbodion, V. S. (2012). Wear behaviour of Al-Si-Fe alloy/coconut shell ash particulate composites. *Tribology in Industry*, 1(34), 36-43

[40] Yao, Z., M. Xia, H. Li, T. Chen, Y. Ye and Zheng H. (2014): Bivalve Shell: Not An Abundant Useless Waste But A Functional And Versatile Biomaterial. Critical Reviews in Environmental Science and Technology 44: 2502–2530.

[41] Muhammad Shabery Sainudin *et al* 2019 *IOP Conf. Ser.: Mater. Sci. Eng.* 601 012033

[42] Adeosun, S. O., Akpan E., and Akanegbu H. A. (2015) Thermo-Mechanical Properties of Unsaturated Polyester

Reinforced with Coconut and Snail Shells Shells International Journal of Composite Materials 5(3): 52-64 DOI:10.5923/j.cmaterials.20150503.02

[43] Atta ur Rehman Shah, M.N. Prabhakar, Dong-woo Lee, Byung-sun and Kim Jung Il Song(2014) Development and Characterization of Oyster Shell Powder Filled Polypropylene Composite Vol. 27, No. 5, 201-206 DOI:http://dx.doi.org/10.7234/composres.2014.27.5.201 ISSN 2288-2103(Print), ISSN 2288 2111(Online)

[44] Onuoha, C., Onyemaobi, O.O., Anyakwo, C.N. and Onuegbu, G.C. (2017)Effect of Filler Loading and Particle Size on The Mechanical Properties Of Periwinkle Shell-Filled Recycled Polypropylene Composites. American Journal of Engineering Research (AJER) American Journal of Engineering Research (AJER) e-ISSN: 2320-0847 p-ISSN: 2320-0936 Volume-6, Issue-4, pp-72-79 www.ajer.org

[45] Abhulimen E. A. And Orumwense F. F. O. (2017)" Characterization and Development of Asbestos-Free Brake Pad, Using Snail Shell and Rubber Seed Husk" African Journal of Engineering Research Vol. 5(2), pp. 24-34, ISSN: 2354-2144

[46] Anieti-mfon E. I. and Benjamin R. E. (2016) "The Effect of Calcination Temperature on the Chemical Composition of Oyster, Periwinkle and Snail Shell Ash" IJRET: International Journal Of Research In Engineering And Technology eISSN: 2319-1163 | pISSN: 2321-7308

[47] Benjamin, R. E., Idongesit F. E. and Linus O. A. (2012) "Feasibility of Using Sea Shells Ash as Admixtures for Concrete" Journal of Environmental Science and Engineering A 1 121-127

[48] Tobins, Ferguson H., Abubakre, Oladiran. K., Muriana, Raseed, A., Abdulrahman, Salawu. A (2018) "Snail Shell As An Inspiring Engineering Material in Science and Technology Development: A Review" International Journal of Contemporary Research And Review Issn 0976 – 4852.

[49] Kolawole, M.Y., Aweda, J.O. and Abdulkareem S. (2017) "Archachatina marginata bio-shells as reinforcement material in metal matrix composites" International Journal of Automotive and Mechanical Engineering ISSN: 2229-8649 (Print); ISSN: 2180-1606 (Online); Volume 14, Issue 1 pp. 4068-4079 March

[50] Asafa, T. B., Durowoju, M. O., Oyewole, A. A., Solomon, S. O., Adegoke, R. M. and Aremu O. J.(2015) "Potentials of Snailshell as a Reinforcement for Discarded Aluminum Based Materials" International Journal of Advanced Science and Technology Vol.84 pp.1-8.

[51] Olawuni,E.O.,Drowoju,M. O., Asafa, T. B. and Mudashiru L. O.(2018) "Production of Piston Material from discarded Aluminum Piston reinforced with Alumina and Snailshells"Int. J. Adv. Sci. Eng. Vol.5 No.1 788-799

[52] Benjamin R. E., Idongesit F. E. and Linus O. A. (2012) Feasibility of Using Sea Shells Ash as Admixtures for Concrete Journal of Environmental Science and Engineering A 1 121-127 Formerly part of Journal of Environmental Science and Engineering, ISSN 1934-8932.

[53] Soneye, T., Ede, A.N., Bamigboye, G. O., Olukanni, D.O. (2016) "The Study of Periwinkle Shells as Fine and Coarse Aggregate in Concrete Work" (CU-ICADI) International Conference on African Development Issues May 9–11, Ota, Nigeria

[54] Umunakwe R., Olaleye, D. J., Oyetunji, A. O. Okoye, C. and Umunakwe I. J. (2017) "Assessment of Some Mechanical Properties And Microstructure Of Particulate Periwinkle Shell-Aluminium 6063 metal matrix Composite (PPS-AlMMC) Produced By Two-Step Casting" Nigerian Journal of Technology(NIJOTECH) Vol. 36, No. 2, April, pp. 421 – 427

[55] Umaru, O.B., Abdulwahab, M., Tokan, A., Onoriode, A.and Mohammed, Y. (2019) "Effect Of Isothermal Heat Treatment On The Hardness And Microstructural Study Of Aluminium/Periwinkle Shell Ash Bio Composite" International Journal of Research in Advanced Engineering and

Technology ISSN: 2455-0876 Volume 5; Issue 3; July; Page No. 77-81

[56] Umunakwe, R., Olaleye, D. J., Oyetunji, A., Okoye, O. C. and Umunakwe, I. J. (2017) "Assessment Of The Density And Mechanical Properties Of Particulate Periwinkle Shell-Aluminium 6063 Metal Matrix Composite (Pps-Almmc) Produced By Two-Step Casting" ACTA TECHNICA CORVINIENSIS Bulletin of Engineering Tome X Fascicule 1 [January – March] ISSN: 2067 – 380

[57] Muhammad, S. S., Nor, H. O.and Shahiron, S.(2019) Performance Of Concrete Containing Mussel Shell (Perna Viridis) Ash Under Effect Of Sodium Chloride CuringIOP Conf. Series: Materials Science and Engineering 601012033 IOP Publishing doi:10.1088/1757-899X/601/1/012033

[58] European Market Observatory for Fisheries and Aquaculture Products - Fresh Mussel In the EU www. eumofa.Eu Accessed in October 2020

[59] Surendra, K. D., Ashok, K. S. and Manoj, C. (2019)Fabrication and dry sliding wear study of Al6061/mussel-shell particulate composites Springer Nature Switzerland AG

[60] Abdulkareem, S., AwedaJ.O., Kolawole, M.Y., Akintunde, T.S. and Mohammed, M. O. (2020) Characteristic of Al-Alloy/Seashell (S_ES_B) Composites in Acidic and Alkaline Environments. Covenant Journal of Engineering Technology (CJET) Vol. 4 No.1

[61] Sahu, P. S. and Banchhor,R. (2016)Fabrication methods used to prepare Al metal matrix composites- A review International Research Journal of Engineering and Technology (IRJET) e-ISSN: 2395 -0056 p-ISSN: 2395-0072 Volume: 03 Issue: 10 |

[62] Surappa, M.K. (2003) Aluminium Matrix Composites: Challenges and Opportunities. Sadhana;28(1–2):319–34.

[63] Kerti, I. and Toptan, F. (2008) Microstructural Variations in Cast B4C-Reinforced Aluminium Matrix Composites (AMCs). Mater Lett;62:1215–8.

[64] Kaczmar, J.W., Pietrzak, K. and Włosi´nski W. (2000) The Production and Application of Metal Matrix Composite Materials. J MaterProcess Technol;106(1–3):58–67.

[65] Rohatgi, P. (1991) Cast Aluminum-Matrix Composites for Automotive Applications. J Manag;43(4):10–5.

[66] Rajan, T.P.D., Pillai R.M. and Pai, B.C. (1998) Reinforcement coatings and interfaces in aluminium metal matrix composites. J MaterSci;33(14):3491–503.

[67] Kalaiselvan K., Murugan, N.and Parameswaran S. (2011) Production and characterization of AA6061-B4C stir cast composite. MaterDes;32(7):4004–9.

[68] Ravi K.R., Sreekumar, V.M., Pillai, R.M., Mahato C., AmaranathanK.R. and Arul Kumar R, et al. Optimization Of Mixing Parameters Through a Water Model for Metal Matrix Composites Synthesis. Mater Des 2007;28(3):871–81.

[69] Shorowordi, K.M., Laoui and T., Haseeb (2003) ASMA, Celis JP, Froyen L.Microstructure and interface characteristics of B4C, SiC, and Al_2O_3Reinforced Al Matrix Composites: A Comparative Study. J Mater Process Technol;142(3):738–43.

[70] Zulfia A, Atkinson H.V., Jones H. and King S. (1999) Effect of Hot Isostatic Pressing on Cast A357 Aluminium Alloy With and Without Sic Particle Reinforcement. J Mater Sci;34(17):4305–10.

[71] Alaneme, K.K. Mechanical Behaviour of Cold Deformed and Solution Heat-Treated Alumina Reinforced AA 6063 Metal Matrix.

[72] Manohar, G., Dey, A., Pandey, K. M. and Maity S. R. (2018)Fabrication of metal matrix composites by powder metallurgy: A review AIP Conference Proceedings 1952, 020041 DOI: 10.1063/1.5032003

Covenant Journal of Engineering Technology (CJET) Vol.5 No.1, June, 2021
ISSN: p. 2682-5317 e. 2682-5325 DOI: xxxxxxxxxx

An Open Access Journal Available Online

Statistical Model for Predicting Slump and Strength of Concrete Containing Date Seeds

Yusuf, A.[1]; Jamal, J. O.[1]; Abubakar, M.[1] & Aminulai, H. O.[1]

[1]Civil Engineering Department, Federal University of Technology, P.M.B 65, Minna, Nigeria
E-mail: yusuf.abdul@futminna.edu.ng

Received: 17.11.2020 Accepted: 09.05.2021 Published: 30.06.2021

Abstract: Incorporating agro-based waste in concrete can reduce environmental pollution and lead to preserving the ecosystem. In order to reduce trial and error in achieving desired slump and compressive strength of concrete containing Date Seed (DS), this paper examines the slump and compressive strength of concrete using date seeds as a partial replacement for crushed granite. Preliminary tests were conducted on the aggregates to ascertain their suitability for concrete production. Concrete with DS-crushed granite ratios of 0:100, 5:95, 10:90, 15:85, and 20:80 were prepared using a mix ratio of 1:2:4 and a water-cement ratio of 0.5. Slump loss was used to estimate the workability of the fresh concrete. The freshly prepared concrete was cast in 150 x 150 x 150 mm and the compressive strength was determined after curing by full immersion in water for 7, 14, 21 and 28 days. Results showed that the slump of concrete increased with an increase in the content of date seed. The compressive strength was inversely proportional to the date seed content with a DS-crushed granite ratio of 20:80 recording the lowest compressive strength (20N/mm^2). Linear regression models for slump and compressive strength were developed and found to be sufficient in explaining the experimental data based on a Mean Square Error (MSE) of 0.37 and 0.029 and R^2 of 88% and 99% obtained for slump and compressive strength respectively. The study has concluded that DS can be used as a partial replacement for crushed granite in concrete and a linear model is sufficient in predicting the slump and strength of concrete containing date seeds.
Keywords: Compressive strength, Concrete, Date seed, Model, Slump

1. Introduction

Infrastructural development is essential for developing countries such as Nigeria, which records a spontaneous increase in population annually. Consequently, engineers have made efforts to develop sustainable and cost-effective materials for the Nigerian construction industry. Concrete is the major construction material used for various types of infrastructure in Nigeria due to the availability and affordability of its constituent materials. Concrete is a composite material made up of aggregates (fine and coarse aggregate), cement, and water in the required proportion [1][2]. Coarse aggregate which is the least expensive material in concrete accounts for about 55% of the total concrete volume and plays an active role in the workability, volume stability, strength and durability of concrete [3][4][5]. It is usually obtained from fragments of rocks (crushed granite) or gravels of different mineralogy. Due to the increasing population of Nigeria, construction materials are being overstretched. Intrinsically, efforts have been made to replace conventional crushed granite with sustainable and cost-effective materials obtained from agricultural, municipal, and construction wastes for the production of concrete [6][7][8] [9][10][11] [12][13].

Research has shown that Date Seed (DS) is a viable agricultural waste used to substitute crushed granite in concrete. DS is obtained as a waste product after date stoning when producing pitted dates or date paste. It is a hard-coated seed with a grooved oblong shape as depicted in Figure 1.

Figure 1: Date Seed

DS has been used in the production of concrete by lots of researchers in the past. [14] studied the durability of lightweight concrete made from date palm seeds using a mix ratio of 1:2.2:1.5. Similarly, [15] examined the compressive strength of concrete containing DS using replacement levels of 25, 50, 75, and 100% and recommended using DS as lightweight aggregate material. [16] also studied the compressive strength of concrete using coarse aggregate-date seed ratios of 100:0, 95:05, 90:10, 85:15, 80:20 and 75:25 for grades M20, M25 and M30 designated concrete. The study concluded that only 10% replacement of coarse aggregate with date seed showed acceptable compressive strength. Research into the modelling of compressive strength of concrete using DS as coarse aggregate is scarce in the literature. There seems therefore, to be a research gap in this regard. Hence, this research is focused on developing a statistical model for predicting the strength of concrete containing DS.

2. Materials and Methods

2.1 Materials

The properties of all the materials used in work are given in Table 1. These properties were tested based on guidelines contained in [17] and [18].

Coarse Aggregate: Crushed granite with a maximum size of 20mm used in this study was sourced from Pyata quarry in Bosso Local Government, Minna, Nigeria. The result of sieve analysis for the crushed granite is shown in Table 2.

Date seeds: The date seeds were obtained from local retailers and dried in the open air to reduce their moisture content. The result of sieve analysis for the DS is also presented in table 2.

River Sand: River sand not containing any particles of clay and silt obtained from Chanchaga river in Minna, Niger State, was used as fine aggregate in the study. The result of the sieve analysis is shown in Table 3.

Ordinary Portland Cement (OPC) classified as grade 42.5 in [18] possessing specific gravity (SG) of 3.14 sourced from retailers was used in the study.

Water: Potable water from the tap located at the laboratory of the Civil Engineering Department, Federal University of Technology, Minna, was used for mixing and curing.

Table 1: Properties of materials used.

Material	Specific Gravity	Moisture Content (%)	Bulk Density (kg/m^3) Compacted	Uncompacted	Aggregate Impact Value (%)
Cement	3.14	-	-	-	-
River Sand	2.60	3.8	1447	1310	
Crushed Granite	2.54	2	757	703	14.3
Date Seed	1.28	11.78	1470	1406	19.2

2.2 Methods and Experimental Programme

A mixed ratio of 1:2:4 with a water-cement ratio of 0.5 was adopted in the study. A DS replacement level of 5, 10, 15, and 20 percent by weight of crushed granite was added to the measured quantity of cement, sand and crushed granite in each case. The materials in the desired proportion were adequately mixed until a uniform blend was achieved. The required quantity of water was added to each blend and mixed thoroughly to achieve a consistent blend. A slump test was carried out on each of the freshly prepared concrete in accordance with [19] to determine the workability of each blend. Five representative cube

specimens of 150 x 150 x 150 mm size were cast for each replacement level. The cubes were demoulded after 24 hours and allowed to cure in a water curing tank for 7, 14, 21 and 28 days. In compliance with [20] guidelines, the compressive strength of the specimens was determined at the appropriate curing age using a 2000 kN compressive strength testing machine.

2.3 Model Development

Slump test results and 28 days compressive strength results were used as the response parameters, while the percentage of DS was used as the predictor in each case. The statistical models were developed and validated using the data analysis toolbox available in [21] following the procedure shown in Figure 2. Analysis of variance (ANOVA) was performed at a 95 % confidence interval and 0.05 significance level.

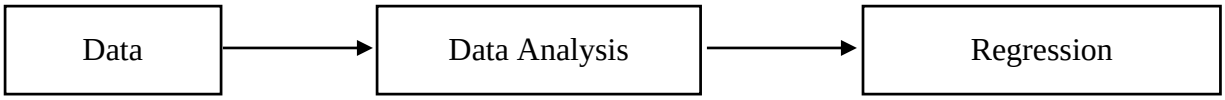

Figure 2: Procedure of Model Development in Excel

3. Results and Discussion

3.1 Sieve Analysis

Sieve analysis results of the DS and crushed granite used showed the distribution of the DS having the majority of the aggregate less than 14mm, while the crushed granite, on the other hand, contained particles ranging between 10 mm and 20 mm. The aggregates do not conform to limits prescribed by [22] for aggregates in concrete, as presented in Table 2.

The sieve analysis result of the river sand used is shown in Table 3. The fine sand satisfied grading limits prescribed by [22]. As such, the aggregate is suitable for concrete production.

Table 2: Sieve Analysis for Date Seed and Crushed Granite

Sieve Size (mm)	Mass Retained (g)	Percentage Mass Retained (%)	Cumulative Percentage Mass Retained (%)	Percentage Passing (%)	Grading Limits Prescribed by BS 882 (%)
			Date Seed		
20	0	0	0	100	90 - 100
14	0	0	0	100	40 - 80
10	130	13	13	87	30 - 60
6.3	840	84	97	3	
5	30	3	100	0	0 - 10
Total	**1000**				
			Crushed granite		
20	400.5	40.05	40.05	59.95	90 - 100
14	505.7	50.57	90.62	9.38	40 - 80
10	93.8	9.38	100	0	30 - 60
6.3	0	0	100	0	
5	0	0	100	0	0 - 10
Total	**1000**				

Table 3: Sieve Analysis of River Sand

Sieve size (mm)	weight of sieve + sample (g)	Percentage retained (%)	Cumulative percentage retained (%)	Percentage passing (%)	Grading Limits Prescribed by BS 882 (%)
5	5.4	1.08	1.08	98.92	98 - 100
3.35	16.5	3.3	4.38	95.62	
2.36	32.1	6.42	10.8	89.2	60 - 100
2	16.8	3.36	14.16	85.84	
1.18	71.3	14.26	28.42	71.58	30 - 100
850	53.3	10.66	39.08	60.92	
600	70.4	14.08	53.16	46.84	15 - 100
425	60.8	12.16	65.32	34.68	
300	32	6.4	71.72	28.28	5 to 70
150	92.6	18.52	90.24	9.76	0 - 15
75	38.6	7.72	97.96	2.04	
pan	304.7	1.42	99.9	0.1	

3.2 Slump and Compressive Strength

The slump test result (to the nearest 5 mm) of the fresh concrete and compressive strength of concrete cubes for different percentages of DS is presented in Table 4. From the results, there exists an increase in a slump as the percentage of DS increased. This may be due to the smooth surface texture of the DS, as aggregates with smooth surfaces have been reported to possess higher workability than aggregates with rough surfaces [23]. The slump test results agree with the slump values reported by [15] and [16]. The compressive strength decreased with an increase in the percentage of date seed used. Smooth surface aggregates are detrimental to the bond between aggregates and cement paste according to [4][23]. This can be attributed to why the compressive strength decreased with an increase in the percentage of DS at all curing ages. The trend in the compressive strength result conforms with compressive strength reported by [14], [15] and [16] (19.6 - 23.44 N/mm^2) using date seeds with similar properties.

Table 4. Slump and Compressive Strength

% Replacement of DS	Slump	Compressive Strength (N/mm^2)			
		7 days	14 days	21 days	28 days
0	30	13.3	16.4	20.8	23.5
5	30	12.9	15.4	20.3	22.9
10	30	12.5	14.9	19.9	21.6
15	30	11.9	14.1	19.2	20.9
20	35	11.0	13.6	18.1	20.0

3.3 Model Development

Regression models for slump and 28 days compressive strength were developed using data analysis in Microsoft Excel (2010). The percentage replacement of DS was selected as the independent variable labeled x while slumping and compressive strength results labeled Y1 and Y2 were used as the dependent variable, respectively. The regression equations obtained for the slump and compressive strength model are given in Equations 1 and 2 respectively while the regression statistics and Analysis of Variance (ANOVA) are presented in Tables 5 and 6. The coefficient of determination (R^2) ranges from 0 – 100%, where a percentage

close to 100% suggests adequate goodness of fit [24][25][26]. The R^2 obtained for the slump model was 88%. This affirms that 88% of the model parameters fit the model developed and 88% variance in the slump values in the neighborhood of the mean are described by the percentage increase in DS. Similarly, a very high R^2 of 99% was obtained for the compressive strength model as shown in Table 5. This proves that the percentage increase in DS explains 99% variation of the compressive strength data within the mean.

From the ANOVA result shown in Table 6, the slump model recorded a Mean Square Error (MSE) of 0.37 and a significance F of 0.02. MSE ranges from 0 to 1, with values closer to 0 suggesting a minimal error between the observed and predicted responses. Furthermore, the significance related to the p-value is less than the 0.05 significance level. An indication that the data has discrete means. In the same vein, the compressive strength model recorded MSE of 0.029 and significance F of 0.0005 which is less than 0.05 significance level. A suggestion that means of the compressive strength data is distinct.

$$Y1 = 0.18x + 27.18 \quad (1)$$

$$Y2 = 23.58 - 0.18x \quad (2)$$

Where,
Y1 = slump
Y2 = compressive strength and
x = percentage increase in DS

The residual, line and normal probability plots are presented in Figures 3, 4 and 5 for the slump model while Figures 6, 7 and 8 are for the compressive strength model. The residual plots show that the residuals are arbitrarily scattered over the negative and positive sides of zero. An indication that the residuals do not follow a regular path.

Table 5: Regression Statistics for slump and compressive strength models

	Slump	Compressive Strength
Multiple R	0.94	0.99
R Square	0.88	0.99
Adjusted R Square	0.84	0.99
Standard Error	0.61	0.17
Observations	5	5

Table 6: ANOVA for slump and compressive strength models

	df	*SS*	*MS*	*F*	*Significance F*
			Slump		
Regression	1	8.1	8.1	22.09	0.02
Residual	3	1.1	0.37		
Total	4	9.2			
			Compressive Strength		
	1	8.1	8.1	276.136	0.0005
	3	0.09	0.029		
	4	8.19			

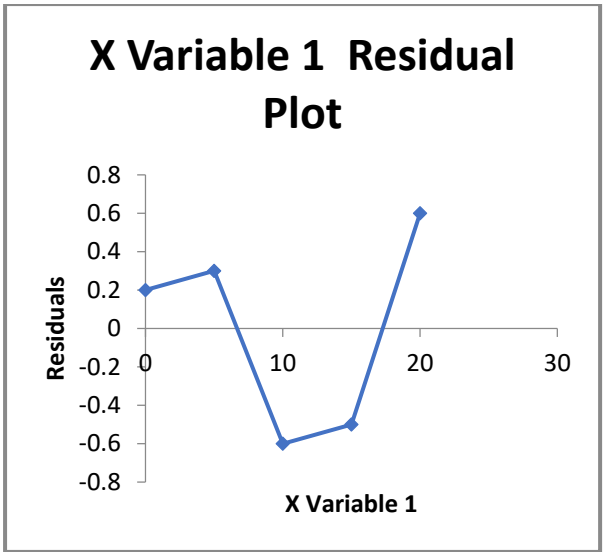

Figure 3: Residual Plot for Slump Model

The normal probability plot depicts that the residuals are not so far away from the straight line. This indicates that the residuals are normally distributed.

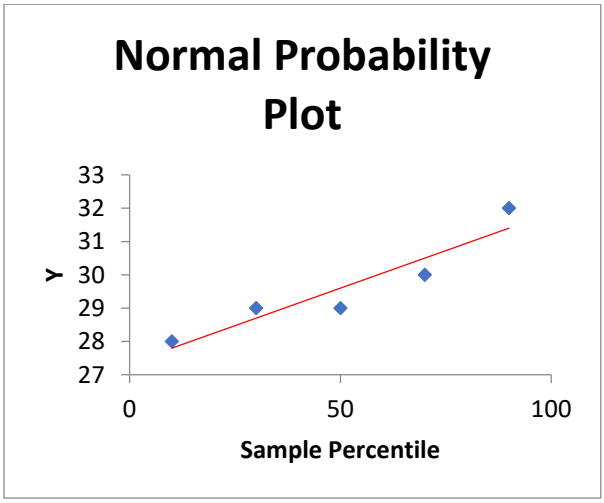

Figure 4: Normal Probability Plot for Slump Model

The experimental vs. model slump results are shown in Figure 5. The experimental slump data are not so close to the predicted slump results. This accounts for why it recorded an R^2 of 88% and MSE of 0.37. The slump model is therefore adequate to a reasonable extent in predicting the slump of concrete containing DS.

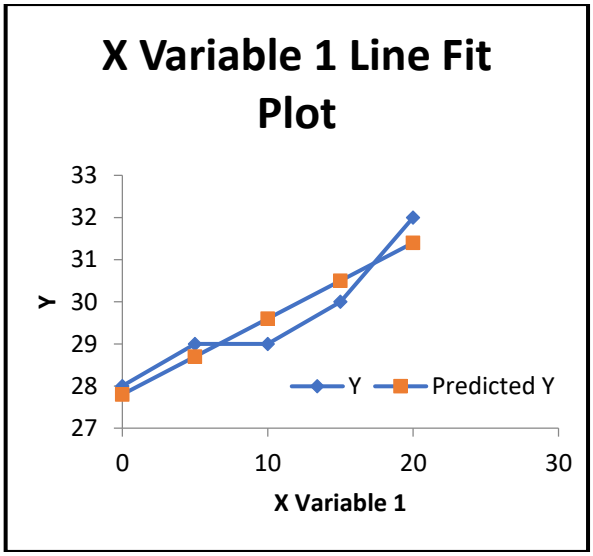

Figure 5: Experimental vs. Predicted Slump Result

The residual plots for the compressive strength model illustrate that the residuals are haphazardly represented on the negative and positive sides of zero. Therefore, the residuals do not follow a regular path.

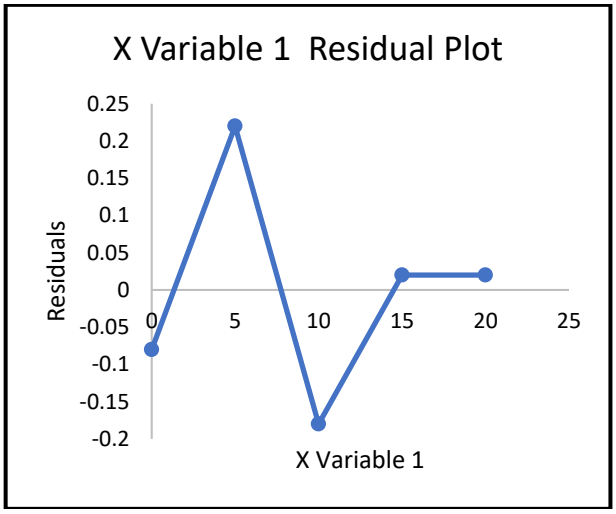

Figure 6: Residual Plot for Compressive Strength Model

The normal probability plot for the compressive strength model shown in Figure 7 indicates that the residuals are very close to the straight line. A clear signal that the residuals are normally distributed. This gives an insight as to why it recorded a very low MSE (0.029) and a very high R^2 (99%).

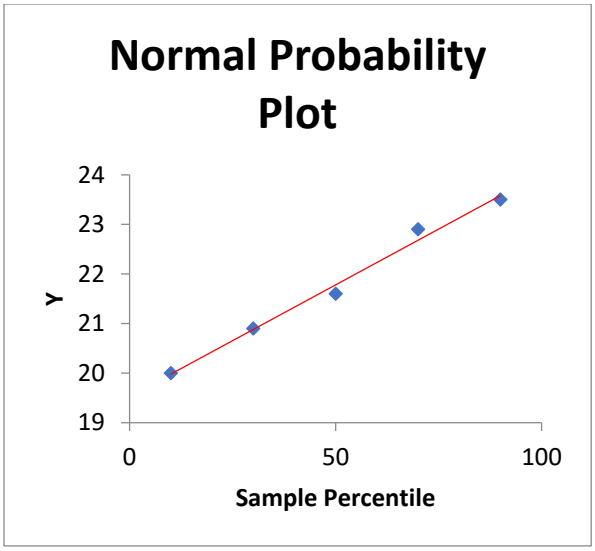

Figure 7: Normal Probability Plot for Compressive Strength Model

The result of the compressive strength vs model is shown in Figure 8. The observed compressive strength is very close to that of the predicted compressive strength. This is an indicator that the error between the actual and predicted compressive strength results is negligible. It is, therefore, safe to oblige that the model is adequate in predicting the compressive strength data.

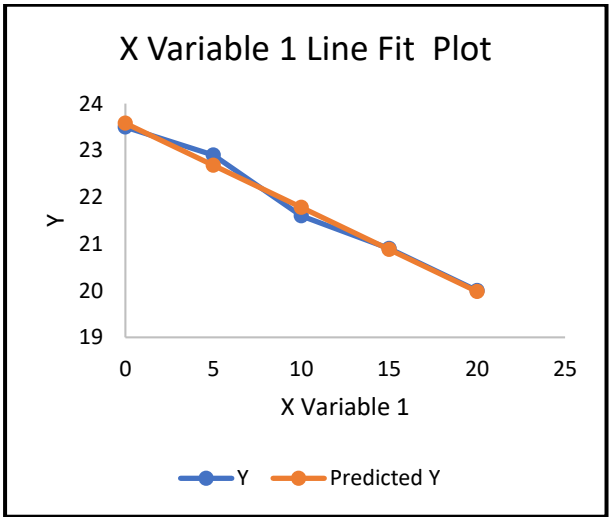

Figure 8: Experimental vs. Predicted Compressive Strength Result

4. Conclusion

The conclusion arrived at based on findings in this research are;

i. The higher the quantity of DS as partial replacement of coarse aggregate in concrete, the higher the slump of the resulting concrete.

ii. The compressive strength of concrete reduces with an increase in the percentage of date seed in concrete. A percentage increase in date seed of 20% recorded the lowest compressive strength of 20N/mm^2. Concrete with 5 - 20% replacement levels is thus suitable for structural applications.

iii. A linear regression model is sufficient in predicting the slump and 28 days compressive strength of concrete containing date seeds with an R^2 of 88% and 99% and MSE of 0.37 and 0.029 respectively.

iv. From the results of the compressive strength, DS is suitable for normal-weight concrete.

Conflict of Interest

There is no conflict of interest associated with this work.

References

[1] Neville, A.M., (2011). *Properties of Concrete*, Pearson Education Limited, London.

[2] Shetty, M. S. (2005). *Concrete Technology: Theory and practice* (Multi-Color illustration ed.). New Delhi: S. Chand.

[3] Fowler, D. W., & Quiroga, P. N. (2003). The effect of aggregates characteristic on the performance of Portland cement concrete (ICAR 104-1F382 p.). International Center for Aggregates Research.

[4] Mehta, P.K. and Monteiro, P. J. M. (2011). *Concrete Microstructure, Properties, and Materials*, New York, McGraw Hill.

[5] Abdullahi, M. (2012). Effect of Aggregate Type on the compressive strength of concrete, *International Journal of Civil and Structural Engineering*, 2(3), 791 - 800.

[6] Olanipekun, E. A., Olusola, K. O. and Ata, O. (2006). A comparative study of

concrete properties using coconut shell and palm kernel shell as coarse aggregates, *Building and environment*, 41(3), 297-301.

[7] Siti T. A., and Sabarudin M., (2009). Investigate the combination of coconut shell and grained palm kernel to replace aggregate in concrete: A technical review.

[8] Adewuyi, A. P. and Adegoke, T. (2008). Exploratory study of periwinkle shells as coarse aggregates in concrete works, *ARPN Journal of Engineering and Applied Sciences*, 3(6), 1-5.

[9] Alengaram, U. J, Mahmud, H. and Jumaat, M. Z. (2010). Development of lightweight concrete using industrial waste material, palm kernel shell as lightweight aggregate and its properties, in *IEEE 2nd International Conference on Chemical, Biological, and Environmental Engineering*, 277-281.

[10] Gunasekaran, K., Kumar, P. S. and Lakshmipathy, M. (2011). Mechanical and bond properties of coconut shell concrete, *Construction and Building Materials*, 25(1), 92-98.

[11] Daniela I., Joe P., Bandita M., Jemily S. & David R. (2015). Alternative Aggregates for Concrete, *First International Conference on Science, Engineering & Environment Tsu City, Mie, Japan,* ISBN: 978-4-9905958-5-2 C3051 1

[12] Jerin M. G., Ashish B., George F., & Aseem A. P. (2016). Coconut shell as a substitute for coarse aggregate in concrete, *International Research Journal of Advanced Engineering and Science*, 1(4), 100-103.

[13] Bright B. W. & Muthukannanb M. (2018). Expanded Fly Ash Clay Aggregate a Sustainable Alternative Coarse Aggregate for Concrete, *Journal of Materials and Engineering Structures*, 5(1), 347–353

[14] Almograbi, M. (2010). Durability study of lightweight concrete material made from date palm seeds (DPS), *WIT Transactions on The Built Environment*, 112(1), 69 – 75.

[15] Aka A., Muhammad H. N., Ephraim T. K. & Idris A. W. (2013). Exploratory Study of Date Seed as Coarse Aggregate in Concrete Production, *Civil and Environmental Research*, 5(1), 85 – 92.

[16] Sama M. A., Dinesh B., & Dipesh P. (2018). Exploratory Study on Partial Replacement of Coarse Aggregate by Date Seed, *International Research Journal of Engineering and Technology (IRJET)*, 5(4), 730 – 734.

[17] British Standard Institute (2009) BS EN 12620-1:2009. *Aggregates for concrete*. British Standard Institute, London

[18] British Standard Institute (2011) BS EN 197-1:2011. *Composition, specifications and conformity criteria for common cements*. British Standard Institute, London

[19] BS 1881: Part 102, (1983). *Method for determination of slump*. British Standards Institution, Her Majesty Stationery Office, London.

[20] British Standard Institution, (1983). BS 1883: Part 116, *Method for determination of Compressive strength of Concrete Cubes factor*, British Standard Institution, 389 Cheswick High Road London

[21] Microsoft Excel (2010). Data Analysis [Computer software].

[22] British Standard Institution (1973). BS 882; Part 2, *Aggregate from Natural Sources for Concrete*, Cheswick High Road, London.

.[23] Mindess and Young (1981) *Concrete*, Prentice-Hall, Inc., Englewood Cliffs, NJ

[24] Montgomery, D.C., Peck, E.A., and Vining, G.G., (2001). *Introduction to Linear Regression*, 3rd ed. John Wiley and Sons, Inc. New York.

[25] Yusuf A. and Emmanuel, A. I. (2020). Flexural Strength of Revibrated Concrete Using Iron Ore Tailings (IOT) as Partial Replacement for River Sand, *USEP: Journal of Research Information in Civil Engineering*, 17(2), 4009 – 4019.

[26] Yusuf A., Mfon, B. E. & Aminulai, H. O. (2020). Strength Properties of Concrete Using Terrazzo Waste as Partial Replacement for Cement, *Epistemics in Science, Engineering and Technology*, 19(2), 677-684.

Covenant Journal of Engineering Technology (CJET) Vol.5 No.1, June, 2021
ISSN: p. 2682-5317 e. 2682-5325 DOI: xxxxxxxxxx

An Open Access Journal Available Online

Effects of the Partial Replacement of Cement with Cassava Peel Ash and Rice Husk Ash on Concrete

John Oloche Obute*, Oluwatobi Olufemi Akin, Yusuf Dada Amartey, Stephen Pinder Ejeh

Department of Civil Engineering, Ahmadu Bello University, Zaria, Nigeria
***Corresponding Email: jobute2@gmail.com**

Received: 18.06.2020 Accepted: 03.02.2021 Published: 30.06.2021

Abstract: Being the third-largest emitter of greenhouse gases (GHG) globally, the cement industry has come under scrutiny by the international community lately. In a bid to remedy the situation, researchers worldwide are keen on finding alternative materials to partially or fully replace Portland cement in concrete production. Materials such as industrial waste, biological waste, agricultural and domestic waste have been used. In this study, a ternary blend of Ordinary Portland Cement, Cassava Peel Ash (CPA), and Rice Husk Ash (RHA) were introduced as the binder System in concrete production to reduce the use of Portland cement. The concrete mix was prepared to put CPA at 5% for all combinations while the RHA was varied from 0 to 25% of the total binder content. With a 0.65 water/binder ratio, an optimum strength was reached at 20% replacement of CPA (5%) and RHA (15%). The partial replacement of cement with CPA – RHA in concrete has also positively affected concrete's water absorption properties. From the use of these materials, GHG emissions are reduced, and the waste generated from the pile of cassava peel and rice husk is eliminated.

Keywords: Concrete, Portland cement, Cassava Peel Ash, Rice Husk Ash, Ternary blend

1. Introduction

Food, clothing, and shelter. These, from the general point of view, are the three necessities of man. Shelter from the weather elements is not just leisure but a core necessity as well. Over the years, a great diversity of construction techniques and construction materials have been employed to meet this need. These structures have evolved with time from temporary and straightforward structures like huts, tents, and containers to more permanent and sophisticated structures such as skyscrapers, canals, and dams. Likewise, the early and perishable construction materials such as leaves, straws, tree branches, and animal skin were replaced with more durable materials like clay, stone, and timber. Synthetic materials such as brick, concrete, metal, and plastic have been developed for construction [1].

From the aforementioned, concrete is the single most widely used construction material in the world. With an annual production of over ten billion tons worldwide, it ranks second only to water in the list of human consumables [2]. Concrete is defined as a

composite material that comprises a mixture of Portland cement or any other hydraulic cement, fine aggregate, coarse aggregate, and water, with or without admixtures [3]. When fresh, it is highly workable and can be fashioned into a variety of shapes. On the other hand, it possesses a very high compressive strength when hardened. This strength is a function of age and can reach between 20 and 40 Mpa in commercially produced concrete. These two properties make concrete the most desirable construction material. However, if loaded in tension, the material fails at a stress typically of the order of 10% of the compressive strength. Because of this low (and unreliable) tensile strength, concrete is usually reinforced with steel bars [4].

Nonetheless, concrete does have its downsides. One of these is the negative impact inflicted on the environment when mining its aggregates and manufacturing Portland cement. For example, world cement production now contributes about 5 percent of annual anthropogenic global CO_2 output [5]. Also, cement production is costly, making it difficult for the masses in developing countries to afford modest housing. For example, in Nigeria, it was estimated by the United Nations Agency for Human Settlement UN-HABITAT that the housing deficit was 17 million as of 2006. The market value for this deficit was estimated at $363 billion [6].

The pollution of the environment is not entirely the fault of the construction industry alone, other sectors like the agricultural and power sectors also contribute, and are equally deserving of urgent attention. For instance, pollution studies in the Sagamu and Ewekoro environs in Ogun state revealed that many are suffering from health challenges due to the pollution from the cement factory close by [7]. Also, Nigeria is among the top producers of cassava and rice globally is bedeviled by tons of agricultural wastes, which loiters most of her towns and villages. CPA – RHA in cement will reduce the environmental pollution from cement production (by reducing the amount of cement needed per concrete mix) and provide a sustainable and economical way of managing the agricultural wastes from such crops.

This study investigates the strength of concrete containing Cassava peel ash and Rice husk ash as partial replacement of cement (5% CPA and varying percentage of RHA ranging from 5% - 25%) in the concrete of 1:2:4 mix ratio and 0.6 water binder ratio. Cassava peel ash (CPA) is produced after the combustion of cassava peel (CP), which is a byproduct from the processing of cassava, either for domestic consumption or industrial use [8]. The plant thrives in the Nigerian climate and is mostly cultivated in the country's southern and middle belt [9]. This has placed the country in a good light as the highest cassava producer, producing about 38 million tones (MT) per annum. It is expected that this value will double by the year 2020 [10]. This makes it suitable that adequate attention is given to finding effective ways of disposing or recycling waste. Salau [8] wrote that the cassava plant's major waste is the peelings and ranges between 20 – 35% by weight of the tuber, especially if it is peeled using the hands. From the estimate, using 20% by weight of the tuber, about 6.8 million tonnes of cassava peels are generated annually, and 12 million tonnes are expected to be produced in the year 2020. Failure to deal with this waste will inevitably lead to a serious environmental hazard. The reality of this is already dawning on some communities in the country. In Ado Ekiti, for example, a previous field survey revealed that the volume of cassava peel heaps around some factories had more than doubled within just three years. The resultant effect of this is the production of noxious and offensive odour and the emission of heat and gases, which attract flies and other vectors [11].

Oryza sativa – the botanical rice name - ranks next to maize as the most popular cereal in the world [12]. With an estimated 3.8 million tons production, Nigeria is the largest rice producer in West Africa and the second-largest in Africa after Egypt [13]. However, this falls below the yearly consumption of 5 million tons. About 365 billion nairas is spent yearly on rice importation. In essence, a higher production rate is expected, as the government's goal is to meet its local demand from local production.

There are two major wastes from rice: the husk, which constitutes about 20% of rice weight; the straw, which is almost the same weight as the rice grain. It is estimated that global rice production generates about 10^8 tonnes of rice husk annually [14]. The husk is sometimes burnt as fuel for cooking, heating air in rice driers, or power milling plants. However, just a small fraction is used for such purposes as most of it is dumped and burnt in the open [15]. Many refuse heaps have been formed in different country locations where they are dumped and posing as an environmental nuisance [14].

Rice husk ash (RHA) is a pozzolan produced after the burning of rice husk [12]. For the best pozzolans, the husk should be burnt at a controlled temperature below 700^0C and under the supply of adequate air to minimize carbon creation. This is because burning at temperatures above 700^0C produces a less reactive crystalline silica compared to the much more reactive amorphous silica formed at lesser temperatures. As a pozzolan, RHA is considered to possess the greatest potential due to its widespread availability and the large proportion of ash (containing about 90% silica) produced after burning. It is already being produced commercially in countries like Thailand, India, and Columbia for use as pozzolans [16].

2. Ternary Blending of Pozzolans

Blended cement refers to the partial replacement of cement (usually ordinary Portland cement) with one or more pozzolans. When OPC is partially replaced with a particular type of pozzolan, it is called a binary blended cement. However, when partially replaced with two different pozzolans, it is referred to as a ternary blended cement [17]. As earlier discussed, the aim of using pozzolans is because of its advantages, which include economic benefits, ecological benefits, and the improvement of concrete properties [18]. And when these pozzolans are used in ternary blends, research has shown that they often produce better results than binary blends. It is observed that the addition of a second pozzolan helps in overcoming the shortcomings of the first. However, it must not be assumed that the improvement is due to their properties' superimposition as the pozzolans could react with each other. The properties found in their ternary blend could be different from those found in their binary blends [19].

Quite a several researchers have looked into the ternary blend of pozzolans. In 2018, Datok et al. [17] investigated the behavior of binary and ternary blends of binding material in concrete. To achieve this, they blended OPC with 20% Acha Husk Ash (AHA), 10% Corn Cob Ash (CCA), and then the range of 5-15% was used for the ternary blend of OPC/AHA/CCA. Results from their research revealed that after 28 days of curing, the ternary blend of 5% developed a strength of 24.60 N/mm^2. This is about 96% of the control and higher than the highest strength developed by OPC/AHA and OPC/CCA's binary blends. In 2007, Ghrici et al. [20] blended Portland cement, limestone, and natural pozzolana. They then proceeded to test their resultant effect in concrete and compared them with the test results gotten from control mixtures of ordinary Portland cement, Portland cement and limestone, and Portland cement and natural pozzolana. The test results showed that the ternary blend not only offered more resistance to sulfate and chloride ion ingress than the control mixtures they also showed better early age and long-term compressive strength [19].

3. Materials and Methods

3.1 Materials

The materials used for the experiment were Ordinary Portland Lime cement, clean and dry river sand (fine aggregate), and crushed granite (coarse aggregate) of maximum nominal particle size. The water used was clean portable water. Cassava peels used were collected from cassava peels dumpsite at Oju Local Government, Benue State, Nigeria. The Cassava Peels were initially burnt to ash through open-air burning before being subjected to control burning in a kiln at a temperature of 650^{o}C for 90 minutes. It was ground into finer particles using local milling

machine and then sieved through 150µm sieve upon cooling down to room temperature. The analysis of its chemical composition was carried out using X-ray Fluorescence Analytical Method.

Rice husk was collected from Sabon Gari Local Government and subjected to -air burning at temperature, reaching up to 1000^{o}C for seven days. The ash was sieved through a 450µm sieve to rid it of dirt and ground into finer particles using a local milling machine upon cooling down to room temperature. Next, the milled RHA was sieved through 75µm, and analysis of its chemical composition was carried out using X-ray Fluorescence Analytical Method.

3.2 Methods

The tests employed in this research work are; oxide composition analysis using XRF, sieve analysis, specific gravity, crushing test, and impact value test. Others were consistency, setting time, soundness, Absolute Volume Method of concrete mix design, slump test, and compressive strength test All the tests were conducted in conformity with relevant standards.

Table 1: Physical Properties of Materials for Concrete

Materials	Specific Gravity	Moisture Content (%)	Bulk Density (Kg/m^3)
Cement	3.14	0.53	-
Fine Aggregate	2.56	7.50	1465.00
Coarse Aggregates	2.70	0.20	1795.00
Cassava Peel Ash	0.98	-	-
Rice Husk Ash	1.05	-	-

3.2.1 Tests on Concrete

The slump test is conducted on fresh concrete to determine how workable the concrete is. It was carried out following BS EN 12390 part 2 [21]. Compressive strength is a measure of the concrete's ability to resist the crushing load being applied directly. In essence, it reveals the maximum compressive load that the concrete can bear per unit area. This test was conducted following BS 1881, part 116 [22](1983). A total of one hundred and twenty cubes (120) were cast using 100mm × 100mm × 100mm steel moulds and cured in water for 3, 7, 14, 28, and 56 days, respectively tests.

Water absorption test, which is a test carried out to determine the level or rate at which concrete specimens absorb/retain water it, was done according to ASTM 140 [23]. The concrete cubes were surface dried after curing before being oven-dried at 100^{o}C for 24 hours. After the samples were removed from the oven, they were cooled and weighed before they were immersed in water for 24 hours and weighed again after removing them from water. Increases in mass as a percentage of initial mass is expressed as its water absorption and can be mathematically expressed as shown in equation (1);

$$\text{Water absorption} = \frac{\text{New Weight} - \text{Air dry weight}}{\text{Air dry weight!}} \text{ x } 100 \quad (1)$$

Where;
New weight = weight of saturated concrete cubes
Air dry weight = weight of oven-dried concrete cubes

3.2.2 Mixture Proportion

A Water-cement ratio of 0.60 was adopted for the mixes throughout the research work. The actual concrete mix proportions are presented in Table 2.

Table 2: material proportion used for producing concrete cubes (100× 100 × 100mm)

S/no	Description	Water (kg)	Cement (kg)	CPA (kg)	RHA (kg)	Fine aggregate (kg)	Coarse aggregate (kg)

1	C0%R0%	5.431	9.053	0.000	0.000	18.106	36.212
2	C5%R0%	5.431	8.600	0.453	0.000	18.106	36.212
3	C5%R5%	5.431	8.148	0.453	0.453	18.106	36.212
4	C5%R10%	5.431	7.695	0.453	0.906	18.106	36.212
5	C5%R15%	5.431	7.242	0.453	1.359	18.106	36.212
6	C5%R20%	5.431	6.790	0.453	1.812	18.106	36.212
7	C5%R25%	5.431	6.337	0.453	2.265	18.106	36.212

4. Results and Discussion

4.1 Oxide Composition of Cement, CPA, and RHA

Table 3 Oxide Composition of Cement, CPA, and RHA

Oxide (%)	Na_2O	MgO	Al_2O_3	SiO_2	P_2O_5	SO_3	Cl	K_2O	CaO
OPC	0.710	1.690	5.700	14.98	-	2.670	-	0.100	68.30
CPA	0.421	4.726	11.323	51.755	4.890	2.173	O.660	6.434	6.890
RHA	0.061	2.400	1.814	79.864	7.428	0.880	0.102	2.976	2.898
Oxide (%)	TiO_2	Cr_2O_3	Mn_2O_3	Fe_2O_3	ZnO	SrO			
OPC	0.220	0.010	-	4.100	-	-			
CPA	2.419	0.020	0.308	7.863	0.082	0.034			
RHA	0.198	0.002	0.236	1.065	0.058	0.017			

The chemical composition analysis of Cassava peel Ash (CPA) and rice husk ash (RHA) using XRF is presented in Table 3. It can be observed that the combined SiO_2, Al_2O_3, and FeO_3 content for CPA and RHA are 67.178% (class C pozzolana) and 82.743% (Class F pozzolana), respectively. This shows that the RHA is a very reactive pozzolan, having more than the 70% recommended in ASTMC618, [24] for good pozzolan. The CPA, however, is considered less reactive. The pozzolans' chemical composition also indicated that the K_2O content for CPA was 6.434% and 2.976% for RHA, higher than the 1.2% limit recommended in cement [25]. The high K_2O content may cause a delay in the setting time of concrete. It is also observed that the value of MgO for both pozzolans is lower than the 5% limit specified by ASTM C618-12 [24]. This indicates the possibility of improved soundness and hardness when they are used in concrete.

4.2 Sieve Analysis of a Coarse Aggregate

Coarse aggregate is crushed granite of nominal size of 20mm with a specific gravity of 2.7. The particle size grading curve shown in Figure 1 indicates that the coarse aggregate's particle size is majorly medium size granite.

The particle size distribution test for fine aggregates is shown in Figure 2. The test was carried out following BS EN 933-1 [26], and the fine aggregate was found to fall within zone 1 by BS 882 [27] classifications.

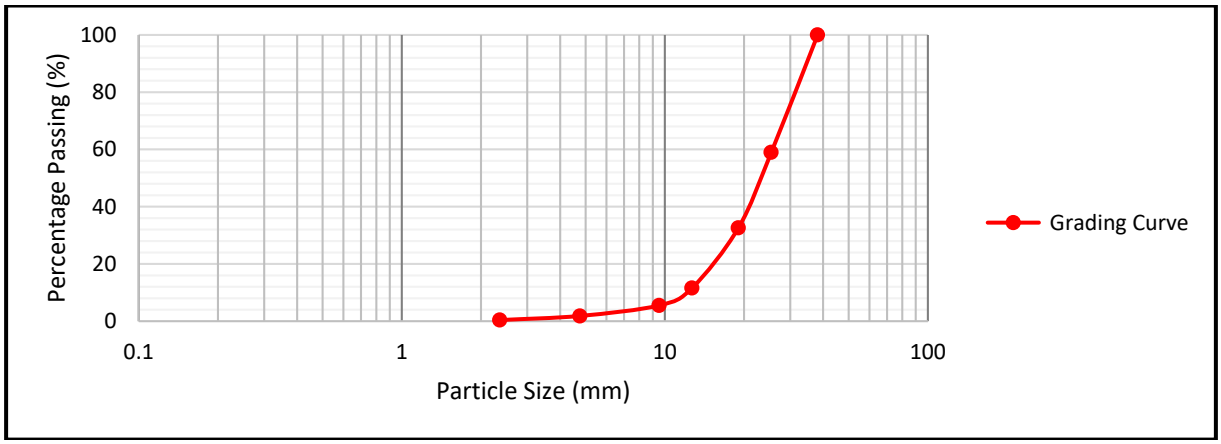

Figure 1: Particle Size Distribution Curve of coarse aggregate

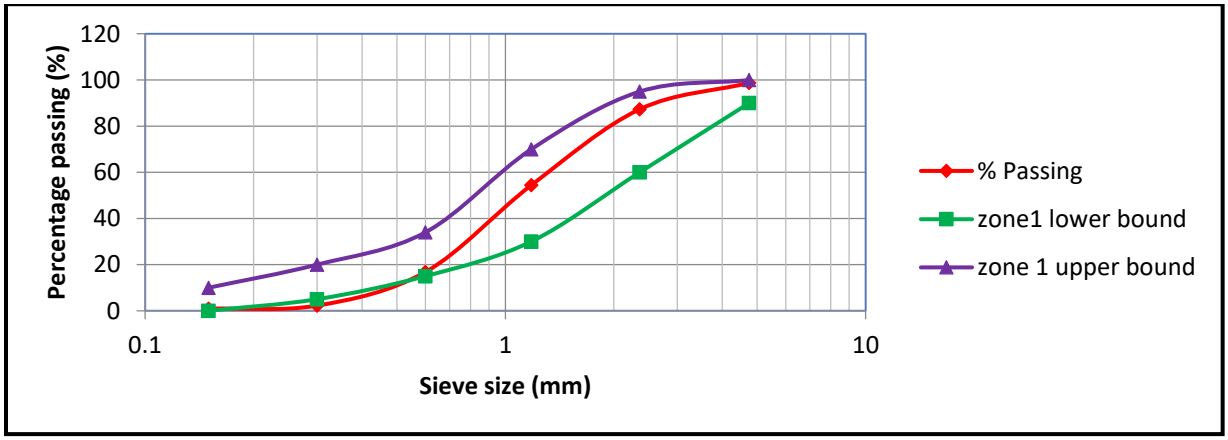

Figure 2: Particle Size Distribution Curve of Fine aggregate

4.3 Slump Test on Fresh Concrete

The slump values used to measure the fluidity, softness, or wetness of a batch of concrete as per ASTM C 143[28] are represented in Figure 3. As can be observed from the graph, the research results reveal that the slump decreased upon CPA - RHA inclusion as a partial replacement of ordinary Portland cement. It goes on to say that to attain the required workability, mixes containing CPA – RHA will require more water than the corresponding conventional mix.

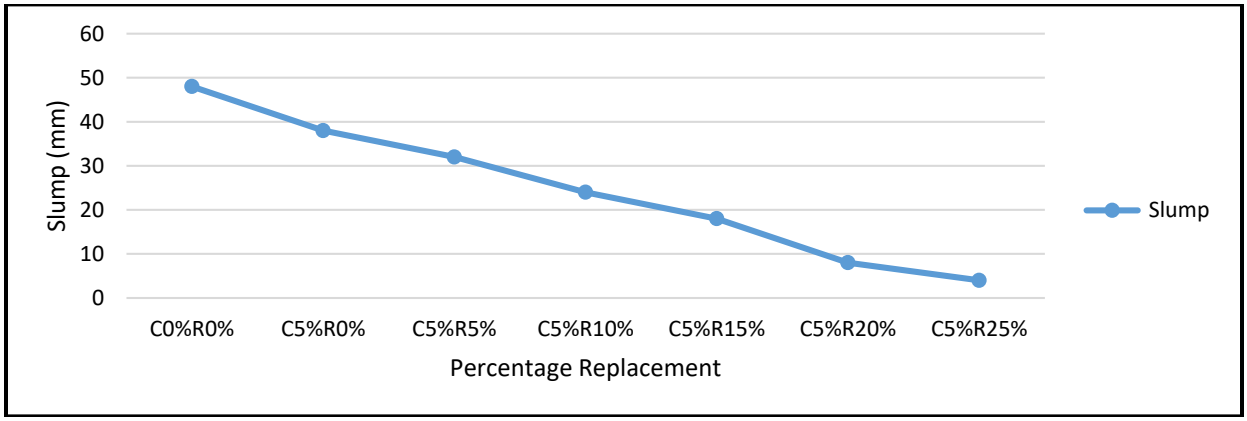

Figure 3: Slump Test of CPA - RHA Concrete

4.4 Compressive Strength of CSA-GSA Concrete

The compressive strength results shown in Figure 4 indicate that compressive strength increased with curing age and decreased with increased blended CPA - RHA content. The results show that the 3 days compressive strength decreased from 13.5N/mm^2 for OPC to 9.3N/mm^2 for 30% replacement with CPA – RHA. Similarly, after 28 days of curing, the strength decreased from 28.7N/mm^2 for OPC to 20.2N/mm^2 for 30% replacement with CPA – RHA. The optimal 28 and 56 days strength for CPA - RHA concrete is recorded at 20% replacement, i.e., 24.12N/mm^2 and 25.2N/mm^{2,} respectively. These results show that the ternary blend of OPC/CPA/RHA has a positive impact on concrete strength, especially at the later stages, and agrees with the previous works [17].

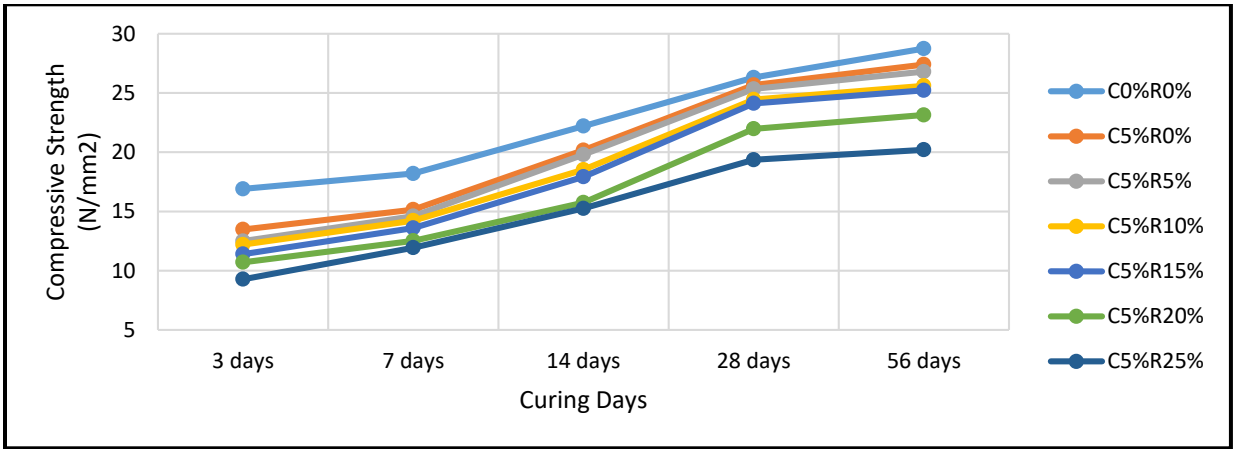

Figure 4: Compressive Strength of CSA-GSA Concrete

4.5 Water Absorption

The graph shows that the percentage water absorption of concrete reduced progressively as the percentage with CPA – RHA increased. The control it is observed had the highest percentage water absorption of 5.59%, while 5%CPA – 25%RHA had the least water absorption value of 3.25%. This is in line with the report by Malhotra and Mehta [29]. This decline in water absorption could be attributed to the fineness of CPA - RHA as reported by Pande and Makarande,[30]. Another explanation for this might also be due to the pore's extensive refinement in the matrix and the interface layer [31].

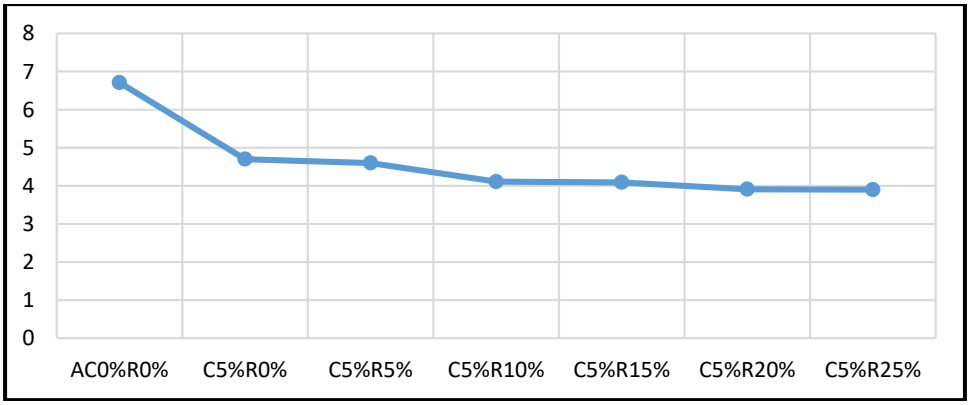

Figure. 5: Water Absorption of CPA - RHA Concrete (%)

5. Conclusions

This study looked into the effects of cement's partial replacement with cassava peel ash and rice husk ash on concrete. CPA is a class C pozzolan having combined SiO_2, Al_2O_3, and Fe_2O_3 content of 67.178 % (which is less than the recommended 70% for pozzolans). It is less reactive than RHA, a class F pozzolan having combined SiO_2, Al_2O_3, and Fe_2O_3 content of 82.743%. However, the ternary combination of CPA with RHA is complementary, producing a CPA – RHA concrete with satisfactory compressive strength. An increase in percentage replacement of cement with CPA – RHA results in a decrease in the compressive strength. However, an increase in curing age increases the compressive strength, with CPA – RHA concrete gaining a compressive strength comparable to that of the control when cured for 28 days or more. Hence, CPA – RHA concrete will be suitable for construction projects where early strength gain is not a major concern. A slump test carried out on fresh blended CPA – RHA concrete reveals that the workability of concrete reduces as the CPA – RHA percentage in concrete increases. Hence, more water will be required to maintain the fluidity of fresh CPA – RHA concrete than ordinary Portland cement concrete. An increase in percentage replacement of cement with CPA- RHA results in a decrease in the resulting concrete percentage water absorption.

Acknowledgment

The authors wish to acknowledge the staff and management of the concrete laboratory, Civil Engineering Department, Ahmadu Bello University, Zaria for their contribution to this work.

Conflict of Interest

The authors declare no conflict of interest.

References

[1] Strickland, Corol, and Amy Handy. (2001). The Annotated Arch: A Crash Course in History of Architecture. Kansas City, MO: Andrews McMeel Pub., 12. ISBN 0740710249

[2] Meyer, C. (2005). Concrete Materials and Sustainable Development in the United States.

[3] American Concrete Institute. (2018). Technical Questions. Retrieved July 23, 2018, from https://www.concrete.org/tools/frequentlyaskedquestions.aspx?faqid=640

[4] Meyer C., (2003) "Glass Concrete" Concrete International

[5] Crow, J. M. (2008). The Concrete Conundrum. *Chemistry World*, (March).

[6] BusinessDay NG. (2018, October). The Nigerian Construction Industry Outlook. *March 6, 2018, \ 4:28 Pm*. Retrieved from https://www.businessdayonline.com/research-reports/research-post/article/nigerian-construction-industry-outlook/

[7] Aigbedion, I., & Iyayi, S. E. (2007). Environmental effect of mineral exploitation in Nigeria. *International Journal of Physical Sciences*, *2*(2), 33–38.

[8] Salau, M. A. (2012). Structural Strength Characteristics of Cement-Cassava Peel Ash Blended Concrete. *Civil and Environmental Research*, *2*(10), 68–78.

[9] Ogunbode E.B and Akanmu W.P (2012) Turning waste to wealth: Potential of Laterised Concrete Using cassava Peel Ash (CPA) Blended Cement. International Journal of Engineering Research & Technology (IJERT) ISSN: 2278-0181. 1(3)

[10] United Nations Industrial Development Organisation [UNIDO], (2006) Annual Report

[11] Oladipo, I. O., Adams, J. O., & Akinwande, J. T. (2013). Using Cassava Peelings to Reduce Input Cost of Concrete : A Waste-to-Wealth Initiative in Southwestern Nigeria. *Universal Journal of Environmental Research and Technology*, *3*(4), 511–516.

[12] Zemke, N., & Emmet, W. (2009). RICE HUSK ASH, (June), 1–15.

[13] International Rice Research Institute [IRRI]. (2010). *Rice in the Global Economy: strategic research and policy issues for food security*. (S. Pandey, D.

Byerlee, D. Dawe, A. Dobermann, S. Mohanty, S. Rozelle, & B. Hardy, Eds.). Los Baños (Philippines): International Rice Research Institute.

[14] Oyetola, E. B., & Abdullahi, M. (2006). The Use of Rice Husk Ash in Low - Cost Sandcrete Block Production. *Leonardo Electronic Journal of Practices and Technologies*, (8), 58–70.

[15] Rice Knowledge Bank. (2017). Rice husk. Retrieved November 2, 2018, from http://www.knowledgebank.irri.org/step-by-step-production/postharvest/rice-by-products/rice-husk

[16] Practical Action. (2004). Rice husk ash (rha) and pulverised fuel ash (pfa). Retrieved July 24, 2018, from http://medbox.iiab.me/modules/en-practical_action/Construction/Cement and binders/KnO-100100_Pozzolanas - Rice husk ash pulverised fuel ash.pdf.

[17] Datok, E. P., Ishaya, A. A., Bulus, A. D., & Amos, N. G. (2018). AN INVESTIGATION OF THE BEHAVIOUR OF BINARY AND TERNARY BLENDS OF BINDING MATERIALS IN CONCRETE. *Scientific Research Journal (SCIRJ), VI*(III), 89–97.

[18] Erdem, T. K., & Kirca, O. (2008). Use of binary and ternary blends in high strength concrete. *Construction and Building Materials*, *22*, 1477–1483. https://doi.org/10.1016/j.conbuildmat.2007.03.026

[19] Gilliland, A. L. (2011). *Evaluation of Ternary Blended Cements for Use in Transportation Concrete Structures*. The University of Utah.

[20] Ghrici M, Kenai S, Said Mansour M (2007) Mechanical Properties and Durability of Mortar and Concrete Containing Natural Pozzolana and Limestone Blended Cements Cem Concr Compos 29:524-549

[21] BS EN 12390-3. Testing hardened concrete. Compressive strength of specimens. European standard adopted by Bristish Standards Institution, Methods of testing cement, 2009

[22] BS 1881-116: 1983 Testing Concrete Method of Determination of Compressive Strength of Concrete Cubes 1983

[23] ASTM C140 Standard Test Methods for Sampling and Testing Concrete Masonry Units and Related Units. American Society for testing and material International

[24] ASTM C618, (2008) Standard specification for coal fly ash and raw or calcined natural pozollan for use in concrete. American Society for testing and material International, West Coshohocken. PA.

[25] BS EN 197-1, Cement, composition, specifications and conformity criteria for common cements European standard adopted by Bristish Standards Institution, 2011.

[26] BS EN 933-1, Test for geometrical properties of aggregates. Determination of particle size distribution. Sieving method, European standard adopted by Bristish Standards Institution, 2012

[27] BS 882, Specification for aggregates for natural resources for concrete: sampling and testing, quality requirements and grading of coarse, fine and all-in-aggregate for use in concrete. European standard adopted by Bristish Standards Institution, Methods of testing cement. 1983

[28] ASTM C143 Standard Test Method for Slump of Hydraulic Cement Concrete. American Society for testing and material International

[29] Malhotra V.M amd Mehta P.K (2004) Pozzolanic and Cementitious Materials. CRC Press, 2004.

[30] Pande, A. M., & Makarande, S. G. (2013). Effect of rice husk ash on concrete. International Journal of Engineering Research and Applications (IJERA) ISSN, 2248-9622.

[31] Rodriguez-Camacho, R. E., & Uribe-Afif, R. (2002). Importance of using the natural pozzolans on concrete durability. *Cement and Concrete Composites*, *32*(42), 1851–1858.

Covenant Journal of Engineering Technology (CJET) Vol.5 No.1, June, 2021
ISSN: p. 2682-5317 e. 2682-5325 DOI: xxxxxxxxxx

An Open Access Journal Available Online

Effect of Temperature and Catalyst on Biofuel Yields from Pyrolysis of African Copaiba Balsam (*Daniellia Oliveri*) Sawdust

Pious O. Okekunle*, Abdulrasaq O. Olasupo and Ibrahim A. Adeyemi

Department of Mechanical Engineering, Faculty of Engineering and Technology, Ladoke Akintola University of Technology, P. M. B. 4000, Ogbomoso, Oyo State, Nigeria
*Corresponding author's email: pookekunle@lautech.edu.ng (+2348167643227)

Received: 18.02.2021 Accepted: 03.05.2021 Published: 30.06.2021

Abstract - The effect of sodium carbonate (Na_2CO_3) on biofuel yields from pyrolysis of *Daniellia oliveri* sawdust in a fixed bed reactor has been studied. The sawdust was procured from the New Sawmill, along Ilorin-Ibadan expressway, Ogbomoso, South-Western Nigeria. The sample was sundried for three days to reduce its moisture content. Catalytic pyrolysis of the sawdust was performed with different weight percentages of catalyst (10, 20, 30 and 40 wt.%) in the feed. Non-catalytic pyrolysis was also performed for the same temperatures and biofuel yields from both sets of experiments were compared. Char yield increased with an increasing percentage of catalyst and were higher than those from non-catalytic pyrolysis in all but one case, the highest being 49.42% at 500 ^oC (biomass/catalyst ratio of 60/40) and the lowest, 15.41% at a non-catalytic temperature of 400 ^oC. Bio-oil yields at 400 and 600 ^oC followed the same trend up to biomass/catalyst ratio of 70/30 while the yields at 500 ^oC, though higher than those from non-catalytic experiments in most cases, did not significantly change with an increasing percentage of catalyst. The highest yield of bio-oil (37.64%) was obtained at 600 ^oC (biomass/catalyst ratio of 90/10) and the lowest (16.41%) at 400 ^oC (biomass/catalyst ratio of 80/20). Gas yields in most cases decreased with an increasing percentage of catalyst and were all lower than those from non-catalytic experiments, the highest yield (62.77%) obtained at a temperature of 400 ^oC (non-catalytic) and the lowest (19.73%) at 500 ^oC (biomass/catalyst ratio of 60/40).
Keywords: Catalytic pyrolysis, biofuel, bio-oil, sodium carbonate, *Daniellia oliveri*, sawdust

1. Introduction

Fossil fuels remain the main sources of energy that are driving the global economy and industrialization. The awareness of the various havocs wrecked on earth by over-dependence on fossils has provoked a global campaign towards reducing their use. Although frantic efforts are being made to find alternatives to fossils, many works still have to be done in getting fuels from renewable sources, which are comparable in combustion characteristics to fossils. For decades, findings have shown that liquid fuel (bio-oil) from biomass pyrolysis can be used as boiler fuel [1] or

upgraded to transportation fuels [2-6]. However, high oxygenated compounds in the bio-oil, its high-water content [7] and low H/C ratios [8] have limited its applications. Besides, the acidity, instability and high viscosity [7] associated with pyrolysis-derived bio-oil are also serious concerns. Sequel to this, various chemical processes have been developed for upgrading the bio-oil [9,10]. Amongst these processes, catalytic cracking has been identified as a promising method [8, 11]. In order to understand the effects of catalysts on pyrolysis, several catalysts have been used on different biomass feedstock [12-16]. Aside from upgrading bio-oil, the use of catalysts in pyrolysis has a strong influence on product distribution and can be an interesting approach to product selectivity [17]. Findings from zeolite cracking of pyrolysis oil [18-24] have shown that though zeolite catalysts were effective in oxygen removal, liquid yields were low. Owing to this, less acidic catalysts can be used for bio-oil upgrading while at the same time enhancing liquid yields.

Furthermore, in most previous studies, woody biomass, typical of West African countries, was not used. This has made catalytic pyrolysis data on common West African woody biomass to be very scarce. Therefore, in this study, the effect of sodium carbonate on biofuel yields from pyrolysis of African copaiba balsam (*Daniellia oliveri*) sawdust was studied at different temperatures in a fixed bed reactor.

2. Materials and Methods

2.1 Materials

Daniellia oliveri sawdust was procured from the New Sawmill, along Ilorin-Ibadan expressway, Ogbomoso, South-Western Nigeria. The sawdust procured was the residue from the milling operation of *Daniellia oliveri* trunk at the sawmill. The sample was sundried for three days to reduce its moisture content. After sun drying, it was weighed and bagged in a cellophane bag for it to maintain its moisture content and it was kept at room temperature until it was used for pyrolysis experiments. Sodium carbonate (Na_2CO_3) was procured from a chemical vendor in Ogbomoso, South-Western Nigeria.

2.2 Experimental setup

Figure 1 shows the exploded view of the pyrolysis unit used for the experiments. A detailed description of this setup has been given elsewhere [25].

2.3 Experimental procedure

Experiments were carried out in two batches, the first with catalyst and the other without catalyst. The first batch of experiments was done to study the effect of catalyst on product distribution from *Daniellia oliveri* pyrolysis at different temperatures while the other was done to study product distribution without catalyst. In the first batch, *Daniellia Oliveri*/Na_2CO_3 weight ratios of 90/10, 80/20, 70/30 and 60/40, thoroughly mixed together, were fed into the crucible, one at a time, and the crucible was covered and fastened with bolts and nuts in preparation for a run. The furnace was then plugged to the mains, pre-set and heated with the aid of an electric heating element to a temperature 50 ^oC higher than the desired pyrolysis temperature in order to compensate for the heat loss during the insertion of the crucible. When the furnace attained the pre-set temperature, it was opened and the crucible was inserted into it. The furnace was covered again and reset to the actual pyrolysis temperature. This procedure was followed for the pyrolysis temperatures of 400, 500 and 600 ^oC with a residence time of 15 min. After each run, the bio-oil and char yields were weighed and expressed in percentages of the weight of the initial sample while gas yield was obtained by mass balance. In the second batch, 100 g of *Daniellia oliveri* (without catalyst) was measured and pyrolyzed at 400, 500 and 600 ^oC for 15 min. The bio-oil, char and gas yields were also

quantified following the same procedures as in catalytic pyrolysis.

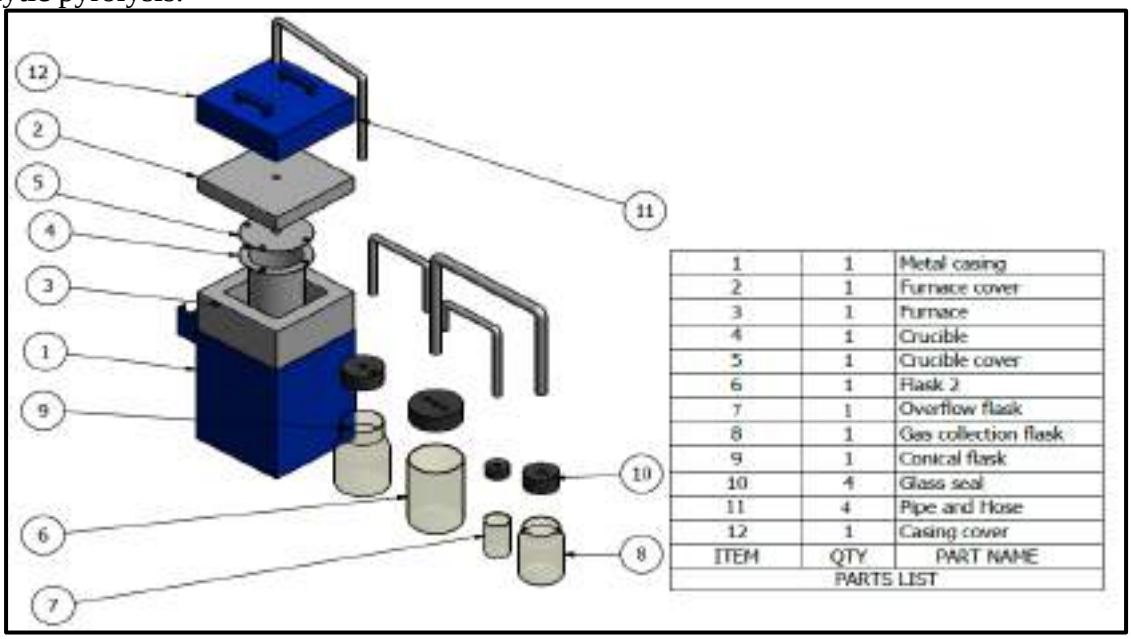

ITEM	QTY	PART NAME
1	1	Metal casing
2	1	Furnace cover
3	1	Furnace
4	1	Crucible
5	1	Crucible cover
6	1	Flask 2
7	1	Overflow flask
8	1	Gas collection flask
9	1	Conical flask
10	4	Glass seal
11	4	Pipe and Hose
12	1	Casing cover

PARTS LIST

Figure 1: The exploded view of the pyrolysis reactor

3. Results and Discussion

3.1 Effect of catalyst and temperature on char yield

Figure 2 shows char yields at different biomass/catalyst ratios for different pyrolysis temperatures. As shown in Figure 2, the yield of char increased with increasing catalyst percentage for all the temperatures considered. For a biomass/catalyst ratio of 90/10, the highest (32.5%) and lowest (21.69%) yields of char were obtained at 600 and 400 ^{o}C, respectively; for 80/20 ratio, the highest (37.03%) and lowest (33.44%) were at 400 and 600 ^{o}C; for 70/30 ratio, the highest (39.89%) and lowest (35.48%) were at 400 and 500 ^{o}C; and for 60/40 ratio, the highest (49.42%) and lowest (42.40%) were at 500 and 400 ^{o}C. These findings suggest that the effect of temperature on char yield in catalytic pyrolysis is dependent on biomass/catalyst ratio.

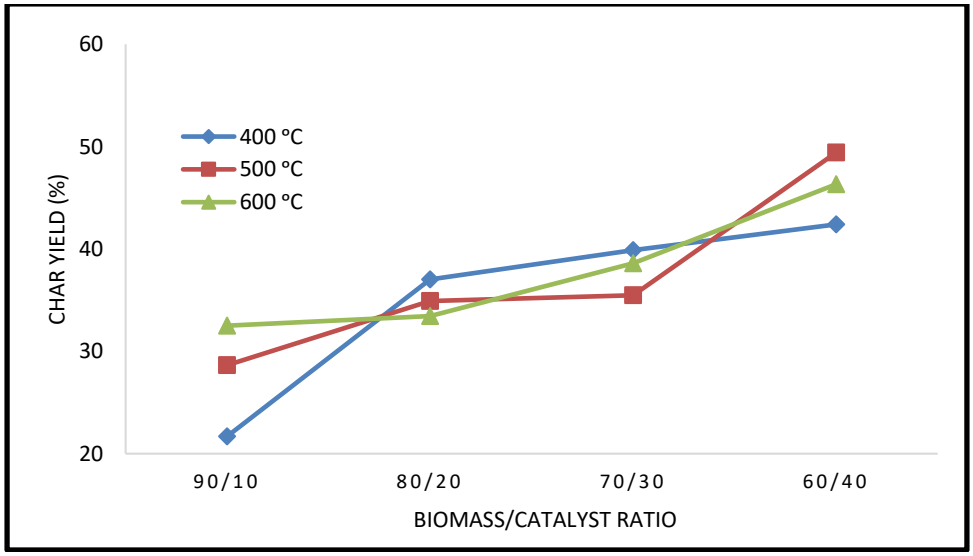

Figure 2: Char yields at different biomass/catalyst ratios and pyrolysis temperatures

3.2 Effect of catalyst and temperature on bio-oil yield

Figure 3 shows bio-oil yields at different biomass/catalyst ratios for different pyrolysis temperatures. As shown in Figure 3, bio-oil yields at 400 and 600 ^{o}C followed the same trend for different biomass/catalyst ratios. An increase from 10 to 20% of catalyst in the feed resulted in bio-oil yield reduction. A further increase in catalyst percentage to 30% in the feed increased bio-oil yield by 13.01% at 400 ^{o}C and by 1.55% at 600 ^{o}C. At a higher percentage of the catalyst (40%) in the feed, bio-oil yield decreased by 11.87% at 400 ^{o}C and by 1.91% at 600 ^{o}C. Unlike at 400 and 600 ^{o}C, different biomass/catalyst ratios at 500 ^{o}C did not cause any significant changes in bio-oil yields, the variation in the yields being in range -0.38 to $+3.45\%$. Figure 3 also shows that the effect of temperature on bio-oil yields at different biomass/catalyst ratios did not follow any consistent trend. However, aside from biomass/catalyst ratio of 90/10, bio-oil yields were maximum at 500 ^{o}C for all other ratios. This finding is very significant for catalytic pyrolysis of *Daniellia oliveri* where the yield of liquid bio-fuel is a priority.

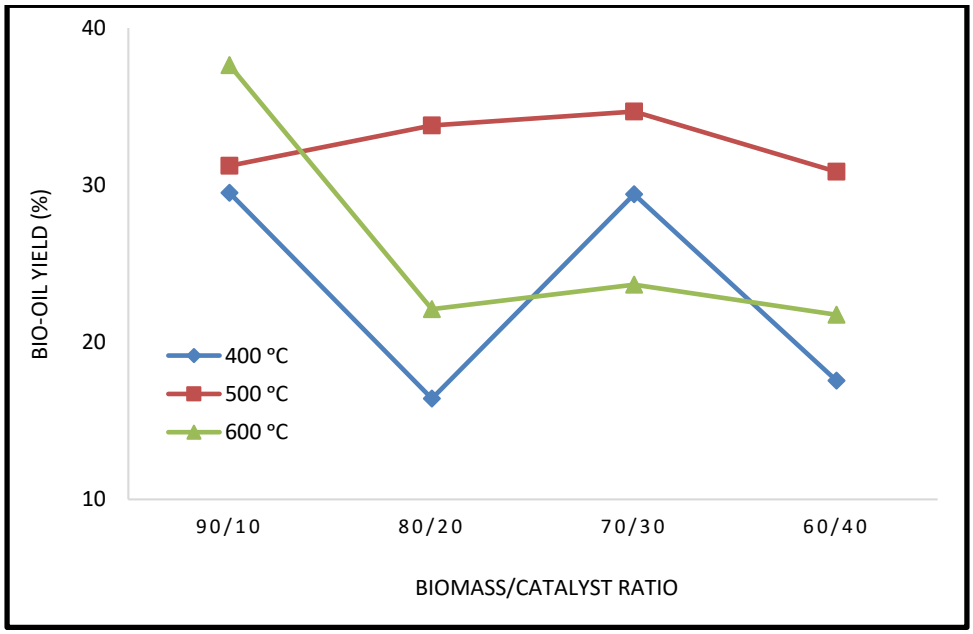

Figure 3: Bio-oil yields at different biomass/catalyst ratios and pyrolysis temperatures

3.3 Effect of catalyst and temperature on gas yield

Figure 4 shows gas yields at different biomass/catalyst ratios for different pyrolysis temperatures. As shown in Figure 4, gas yields at 400 and 500 ^{o}C followed the same trend up to biomass/catalyst ratio of 70/30. An increase in catalyst percentage in the feed from 10 to 20% resulted in a reduction in gas yield by 2.24% at 400 ^{o}C and by 8.85% at 500 ^{o}C. A further increase in catalyst percentage to 30% in the feed further reduced gas yield by 15.87% at 400 ^{o}C and by 1.44% at 500 ^{o}C. However, at a higher percentage (40%) of catalyst in the feed, gas yield increased by 9.36% at 400 ^{o}C while it decreased by 10.11% at 500 ^{o}C. It is necessary to point out, as shown in Figure 4, that gas yield decreased consistently with increase in catalyst percentage at 500 ^{o}C, with the lowest yield (19.73%) in all of the catalytic

experiments obtained at this temperature at biomass/catalyst ratio of 60/40. Unlike the trends observed at 400 and 500 °C, an initial increase in catalyst percentage from 10 to 20% in the feed increased gas yield by 14.59% at 600 °C. Beyond this catalyst percentage, any increase in catalyst percentage resulted in a continuous decrease in gas yield at 600 °C.

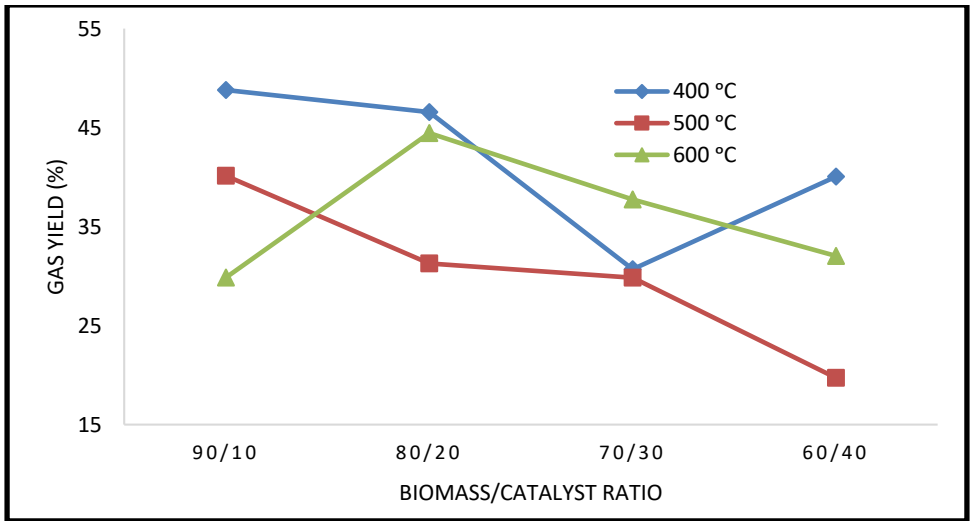

Figure 3: Gas yields at different biomass/catalyst ratios and pyrolysis temperatures

3.4 Comparison of catalytic and non-catalytic product distribution

3.4.1 Char yield

The comparison between char yields from non-catalytic and catalytic pyrolysis of *Daniellia oliveri* is shown in Figure 5. It is shown that char yield increased with the percentage of catalyst at all temperatures in the catalytic experiments. It can also be seen from Figure 5 that char yields from the catalytic runs at all biomass/catalyst ratios at

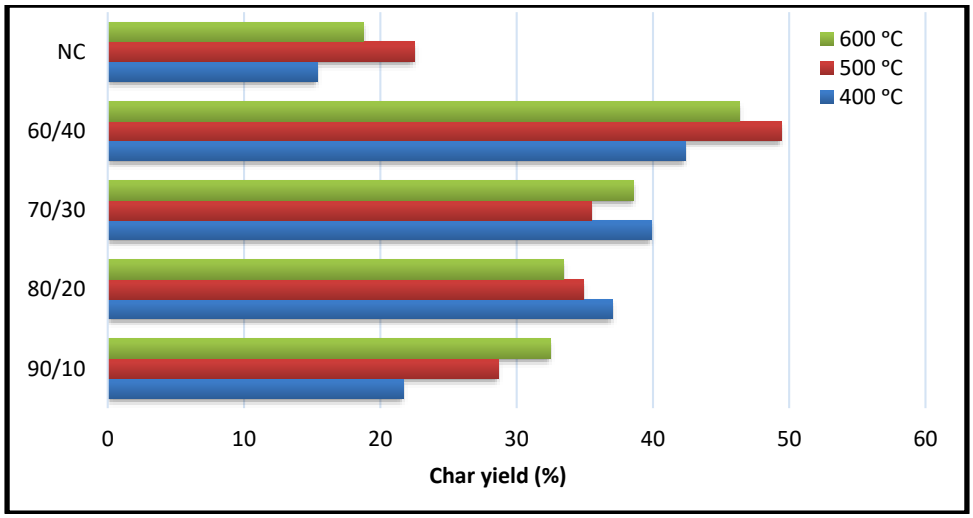

Figure 5: Comparison of char yields from non-catalytic (NC) and catalytic pyrolysis

a particular temperature are higher than the yields from non-catalytic runs at the same temperature. Moreover, it is shown that char yields from all the cases but one (at 400 °C and biomass/catalyst ratio of 90/10) of catalytic runs were higher than those from non-catalytic

runs. These results show that the use of sodium carbonate as catalyst increased the yield of char from pyrolysis of *Daniellia oliveri*.

3.4.2 Bio-oil yield

Figure 6 shows the comparison between bio-oil yields from non-catalytic and catalytic pyrolysis. It can be seen that in most cases, bio-oil yields from catalytic pyrolysis at 500 ^{o}C were higher than all the yields from non-catalytic runs. Figure 6 also shows that the highest yield of bio-oil in all the runs (catalytic and non-catalytic) was obtained at 600 ^{o}C and biomass/catalyst ratio of 90/10. These results, considered together with char yield trends, can inform the choice of the appropriate conditions for maximizing the yield of liquid fuel from catalytic pyrolysis of *Daniellia oliveri*.

3.4.3 Gas yield

Gas yields from non-catalytic and catalytic experiments are compared in Figure 7. It is shown that gas yields from non-catalytic experiments were higher than all the yields from catalytic pyrolysis. These results show that the use of sodium carbonate as catalyst reduced the yield of gas from pyrolysis of *Daniellia oliveri.*

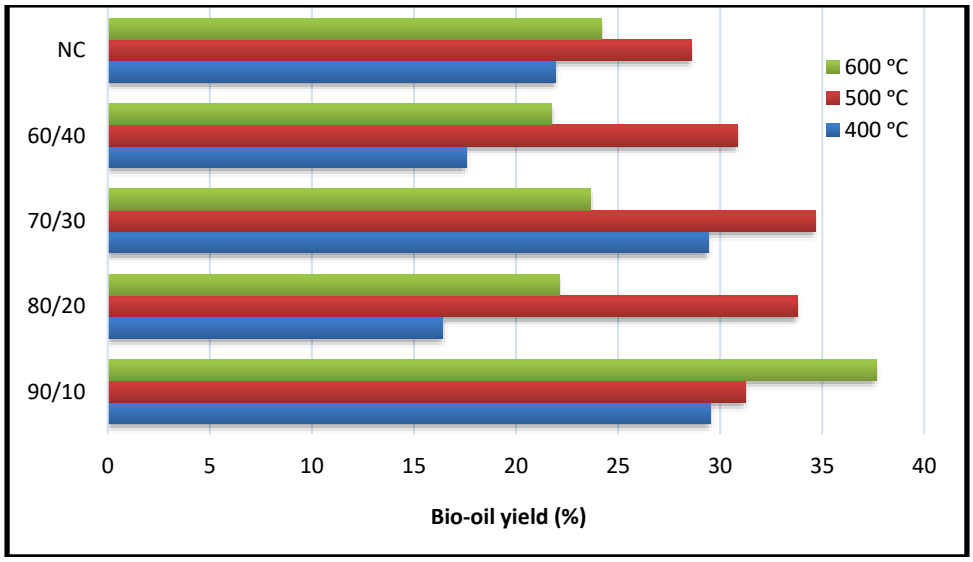

Figure 6: Comparison of bio-oil yields from non-catalytic (NC) and catalytic pyrolysis

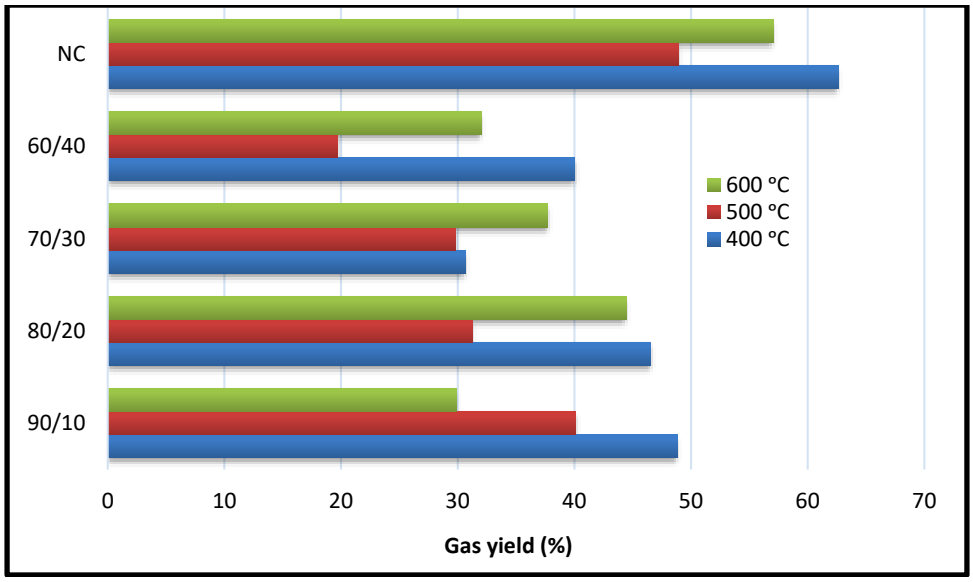

Figure 6: Comparison of gas yields from non-catalytic (NC) and catalytic pyrolysis

4. Conclusions

In this study, the effect of sodium carbonate catalysts on biofuel yields from pyrolysis of *Daniellia Oliveri* sawdust has been studied. Char, bio-oil and gas yields from catalytic pyrolysis were compared with those from non-catalytic experiments. Based on the findings from this work, the following conclusions were drawn:

i. Char yield increased with an increasing Na_2CO_3 catalyst in the feed for all the pyrolysis temperatures considered.
ii. Gas yield decreased with an increasing Na_2CO_3 catalyst in the feed for all the pyrolysis temperatures considered.
iii. Bio-oil yields at 500°C were not significantly affected by increasing the percentage of Na_2CO_3 catalyst in the feed.
iv. Bio-oil and char yields from Na_2CO_3 – assisted pyrolysis were generally higher than those from non-catalytic experiments.
v. The presence of Na_2CO_3 in the feed reduced gas yield for all the temperatures considered.

References

[1] Mullen, C.A., Boateng, A.A., Hicks, K.B., Goldberg, N.M. and Moreau, R.A. (2010). Analysis and comparison of bio-oil produced by fast pyrolysis from three barley biomass/byproduct streams. Energy Fuel 24, 699 – 706.

[2] Mohan, D., Pittman, C.U., Jr., and Steele, P.H. (2006). Pyrolysis of wood/biomass for bio-oil: A critical review. Energy Fuels 20(3), 848 – 889.

[3] Huber, G.W., Iborra, S. and Corma, A. (2006). Synthesis of transportation fuels from biomass: Chemistry, catalysts, and Engineering. Chemical Reviews 106(9), 4044 – 4098.

[4] Bridgwater, A.V., Cottam, M.L. (1992). Opportunities for biomass pyrolysis liquids production and upgrading. Energy Fuels 6(2), 113 – 120.

[5] Czernik, S. and Bridgwater, A.V. (2004). Overview of application of biomass fast pyrolysis oil. Energy Fuels 18(2), 590 – 598.

[6] Bridgwater, A. (2012). A review of fast pyrolysis of biomass and product upgrading. Biomass and Bioenergy 38, 68 – 94.

[7] Thangalazhy-Gopakumar, S., Adhikari, S., and Gupta, R.B., (2012). Catalytic pyrolysis of biomass over H^+ZSM-5 under hydrogen pressure. Energy Fuels 26, 5300 – 5306.

[8] Pütün, E., (2010). Catalytic pyrolysis of biomass: Effects of pyrolysis temperature, sweeping gas flow rate and MgO catalyst. Energy 35, 2761 – 2766.

[9] Elliott, D.C. (2007). Historical development in hydroprocessing bio-oils. Energy Fuels 21(3), 1792 – 1815.

[10] Samolada, M.C., Papafotica, A. and Vasalos, I.A. (2000). Catalyst evaluation for catalytic biomass pyrolysis. Energy Fuels 14, 1161 – 1167.

[11] Zhou, L., Yang, H., Wu, H., Wang, M., and Cheng, D. (2013). Catalytic pyrolysis of rice husk by mixing with zinc oxide: Characterization of bio-oil and its rheological behaviour. Fuel Processing Technology 106, 385 – 391.

[12] Pütün, E., Ateş, F. and Pütün, A.E., (2008). Catalytic pyrolysis of biomass in inert and steam atmospheres. Fuel 87, 815 – 824.

[13] Foster, A.J., Jae, J., Cheng, Y.-T., Huber, G.W. and Lobo, R.F. (2012). Optimizing the aromatic yield and distribution from catalytic fast pyrolysis of biomass over ZSM – 5. Applied Catalysis A: General 423 – 424, 154 – 161.

[14] Zabeti, M., Nguyen, T.S., Heeres, H.J. and Seshan, K. (2012). In situ catalytic pyrolysis of lignocellulose using alkali-modified amorphous silica alumina. Bioresource Technology 118, 374 – 381.

[15] Mansur, D., Yoshikawa, T., Norinaga, K., Hayashi, J., Tago, T. and Masuda, T. (2013). Production of ketones from pyroligneous acid of woody biomass pyrolysis over an iron-oxide catalyst. Fuel 103, 130 – 134.

[16] Yu, Y., Li, X., Su, L., Zhang, Y., Wany, Y. and Zhang, H. (2012). The role of shape selectivity in catalytic fast pyrolysis of lignin with zeolite catalysts. Applied Catalysis A: General 447 – 448, 115 – 123.

[17] Uzun, B.B. and Sarioğlu, N. (2009). Rapid and catalytic pyrolysis of corn stalks. Fuel Processing Technology 90, 705 – 716.

[18] Encinar, J.E., Beltrán, F.B., Ramiro, A. and González, J.F. (1997). Catalyzed pyrolysis of grape and olive bagasse. Influence of catalyst type and chemical treatment. Industrial and Engineering Chemistry Research 36(10), 4176 – 4183.

[19] Sharma, R.K. and Bakhshi, N.N. (1991). Catalytic upgrading of biomass derived oils to transportation fuels and chemicals. Canadian Journal of Chemical Engineering 69, 1071 – 1081.

[20] Pütün, E., Uzun, B.B. and Pütün, A.E. (2006). Fixed-bed catalytic pyrolysis of cottonseed cake: Effect of pyrolysis temperature, natural zeolite content and sweeping gas flow rate. Bioresource Technology 97, 701 – 710.

[21] Ateş, F., Pütün, A.E. and Pütün, E. (2005). Fixed bed pyrolysis of *Euphobia rigida* with different catalysts. Energy Conversion and Management 46(3), 421 – 432.

[22] Ioannidou, O., Zabaniotou, A., Antonakou, E.V., Papazisi, K.M., Lappas, A.A. and Athanassiou, C. (2009). Investigating the potential for energy, fuel, materials and chemicals production from corn residues (cobs and stalks) by non-catalytic and catalytic pyrolysis in two reactor configurations. Renewable and Sustainable Energy Review 13(4), 750 – 762.

[23] Vitolo, S., Seggiani, M., Frediani, P., Ambrosini, G. and Politi, L. (1999). Catalytic upgrading of pyrolytic oils to fuel over different zeolites. Fuel 78(10), 1147 – 1159.

[24] Pütün, E., Uzun, B.B. and Pütün, A.E. (2006). Production of bio-oils from cottonseed cake by catalytic pyrolysis under steam atmosphere. Biomass and Bioenergy 30, 592 – 598.

[25] Okekunle, P.O., Itabiyi, O.E., Adetola, S.O., Alayande, I.O., Ogundiran, H.O., and Odeh, K.G., (2016). Biofuel production by pyrolysis of cassava peel in a fixed bed reactor. International Journal of Energy for a Clean Environment 17(1), 57 – 65.

Covenant Journal of Engineering Technology (CJET) Vol.5 No.1, June, 2021
ISSN: p. 2682-5317 e. 2682-5325 DOI: xxxxxxxxxx

An Open Access Journal Available Online

Development of a New Air Compressor System for Ship Operations

Thaddeus C. Nwaoha* and Fabian I. Idubor

Marine Engineering Department, Federal University of Petroleum Resources, Delta State, Nigeria

Received: 18.04.2021 Accepted: 28.05.2021 Published: 30.06.2021

Abstract: An optimal operation of compressors used onboard vessels for various purposes is very important. In this study, the drawbacks of conventional air compressors are addressed. Interruption of the operations by unpredictable electrical power blackout and corrosion are the key drawbacks. The corrosion occurs due to a manual drain, which depletes the life of the air tank, thereby causing damages to the compressors. To address this challenge, the need for modification of conventional air compressors is imperative. Hence, this study entails the design and fabrication of an air compressor system with rechargeable characteristics, well equipped with an automatic drain sensor and pressure switch, to obtain optimal system efficiency and reliability. From the obtained results of the test and performance of the compressor, it is obvious that it is efficient and reliable for onboard ship operations.

Keywords: Air compressor, Design, Fabrication, Ship operations, Rechargeable

1. Introduction

Compression technology has made a significant impact in industries [1]. Air compressors are used in various marine vessels to provide compressed and pressurized air for many applications, such as starting the main engine, auxiliary engine, emergency generator, and emergency fire pump [2]. Various compressors design and experiments have been conducted in different publications [3-7]. Air compressors such as main air compressors, emergency air compressors, and topping up air compressors are used onboard vessels. The mechanism of the air compressor is used to force air into a storage tank, which causes a gradual pressure increase in the tank [8-9].

The underlying engineering science supporting the design practices of compressors is demonstrated in various research [10-11]. Shuts off of air compressor occurs whenever the pressure of tank reaches its upper limit. The compressed air is stored in an air tank for utilization. Whenever the air is released from the tank, it releases kinetic energy that can be used for pneumatic device activation, transfer of air, and cleaning operations. The tank depressurizes when the air is released from them. Once tank pressure reaches its lower limit, the air compressor turns on again and re-pressurizes it.

Xu and Muller [1] studied the volute flow mechanisms in a compressor to provide comprehensive design guidance. They demonstrated how the viscous Navier-Stokes equations simulate the flow inside the vane-less diffuser and volute of air compressor to improve efficiency and operating range. The numerical calculation obtained from the study is in line with the experimental data [1]. In Shin *et al.* [8], a rotary-type compressor with a

novel structure design is proposed to improve the cooling capacity and mechanical efficiency. The novel structure used the inner space of the roller as an additional working volume to compress more refrigerant under the same main dimensions of the compressor. Thus the cooling capacity is improved by 31.28–37.99% compared to the conventional rolling piston-type rotary compressor [8]. In Langa *et al.* [12], the impact of Profiled End Wall (PEW) on the performance and working range of centrifugal compressors is demonstrated. PEW is an effective method used to reduce secondary flows and associated losses to improved efficiency. The numerical simulations conducted for different PEW treatments are recorded and benchmarked against experimental data from the exemplar open test case called 'Radiver.' The results produced from the research illustrated that the compressor operating range is significantly extended to 39%, with no significant decrease in efficiency or pressure ratio. Conventional air compressors tend not to meet today's demand for onboard services because of operational failure caused by unpredictable electrical power blackout and corrosion. One of the corrosion causes is the manual drain, which depletes the tank's life. To improve the efficiency and reliability of compressors onboard vessel, a compressor with unique characteristics such as the ability to recharge, possess automatic drain with less human intervention, more ease of operation and transportation, and operating silently with high thermal efficiency be developed.

In view of this, the research aims to design and fabricate a rechargeable and automatic drain air compressor system. The design and fabrication exercise accommodated a hermetic compressor. The hermetic compressor will make it noiseless and reduce the condensate level accumulated in the air receiver tank to an acceptable level. An automatic condensate drain sensor or solenoid valve, an inverter, battery charger, pressure switch, pressure relief valve, pressure regulator, hermetic compressor, control panel, pressure gauge, air gun or quick connect, dampers, moisture absorber, and a mobile body frame will be used to design and fabricate the air compressor. The research structure is outlined as material and methods in Section 2, results and discussion in Section 2, and conclusion in Section 4.

2. Material and Methods

The various air compressor components such as air storage tank or air receiver, a hermetic compressor, a solenoid valve, a 12volts DC battery, a pressure control unit, control panel, inverter, battery charger, air gun and hose, cooling fan, air filter, dryer, a non-return valve or check valve, damper, body frame, battery terminals, tires, and foam or moisture absorber are used in the design and fabrication. The usability of various systems has been detailed in various literature [13-20]. The component specification and rating are described as follows: The air tank's capacity: The air tank's volume is 0.0160 m^3, which is equivalent to 16litres. Material of the air tank or air receiver: The material used for producing the air tank is Alloy steel. The properties are of great permeability and durability, high tensile, and yield strength. The color is blue. The maximum pressure capacity of the tank is 250Psi (17.24bar). The maximum safe operating pressure is 145Psi (10bar). The length of the air tank is 380mm (0.38m), the diameter is 232mm (0.232m), and the radius is 116mm (0.116m).

- Compressor ratings: The compressor brand is Samsung. The type of material used is steel, and the motor type is RSIR with a frequency of 50Hz. The power is 225watt with a voltage rating of 220/240volts.
- Battery ratings: The battery rating is 24 volts and 18 amperes for voltage and current, respectively. The inverter has a similar rating as the battery.

Storage capacity of the air tank analysis

The storage capacity of the air tank is calculated using Equation 1.

$$V = \pi r^2 l \qquad (1)$$

where the radius, $r = \frac{d}{2} = \frac{0.232}{2} = 0.116m$

Length, = $0.38m$; Therefore,

$V = \pi \times 0.116^2 \times 0.38(m^3)$

$V = 0.0160m^3 \approx 16litres$

2.1 Free Air Delivery Analysis

The capacity of the Free Air Delivery (FAD) can be calculated using Equation (2).

$$FAD = Q = \frac{P_2 - P_1}{P_o} \times \frac{V}{t}\left(m^3/\min\right) \qquad (2)$$

Where P_2 in the bar is the final pressure after filling.

P_1 in the bar is the initial pressure after bleeding.

P_0 is the atmospheric pressure which is equal to 1.0135bar.

V is the storage volume in m^3 which includes the receiver and delivery pipes.

t is the time it takes to build up pressure to P_2. Its unit is minutes.

From the International Standard Organization (ISO), free air delivery can be calculated in standard cubic feet per minute (SCFM) at conditions between 1 to 7bars. Therefore,

P_2 = 7bar, P_1 = 1bar, P_0 = 1.0135 bar

Standard FAD = $\frac{7-1}{1.0135} \times \frac{0.016}{4.4} = 0.0215m^3/\min$

Also, SCFM = 0.0215×35.31=0.76 (CFM)

Calculating the actual FAD from the experiment at values of the following:

P_2 = 10bar, P_1 = 4bar, t = 4.30minutes

Actual FAD = $\frac{10-4}{1.0135} \times \frac{0.0160}{4.30} = 0.0220m^3$ / min.

Therefore, ACFM = 0.0220 × 35.31 = 0.78CFM.

Volumetric efficiency of the compressor

The volumetric efficiency of the compressor is the ratio of actual capacity to piston or compressor displacement. Mathematically, it is expressed as:

$$\eta_V = \frac{FAD}{D_P} \times 100\% \qquad (3)$$

Piston displacement denoted as D_P is the swept volume of the piston per unit time. It is expressed in cfm.

$$D_P = \frac{\pi d^2}{4} \times 1 \times n \times N \qquad (4)$$

Where the *b*ore diameter, d=25mm, stroke = 24mm, *n*umber of cylinders, n=1, and several *r*evolution = 3000rpm.

$$D_P = \frac{\pi \times 0.025^2}{4} \times 1 \times 0.024 \times 3000 = 0.0353m^3/\min$$

Substitution of D_P in Equation (3) gives:

$$\eta_V = \frac{0.022}{0.0353} \times 100\% = 62.30\%$$

2.2 Battery Charging Time Analysis

The calculation of the time it takes the 18 amp battery to charge and drain is expressed below. The charging current is 10 Ampere. Then, the charging time for the 18 Amps battery is given as shown in Equation (5):

$\frac{18}{10} = 1.8hrs$ (This is an Ideal case)

It is practically noted that 40% of losses occur in the case of battery charging. Then,

$18 \times \left(40/100\right) = 7.2amps$

$$\text{Charging time of battery} = \frac{\text{Ah (Amp Hour)}}{\text{Charging current}} \quad (5)$$

$$= \frac{50.4}{10} = 5.04hrs \text{ (in real case)}$$

Therefore, an 18 Amp battery would take 5.04 hours to be fully charged.

2.3 Battery Draining Time Analysis

The backup time of a battery depends essentially on power consumption, battery voltage, and battery capacity. Most batteries have a nominal voltage of 12volts and may require a back–up for effectiveness. Mathematically, it is given by the expression in Equation (6):

$$\text{Back up time} = \frac{\text{Power consumption (watt)} \times \text{Battery backup (hours)}}{\text{Voltage of the battery}} \quad (6)$$

In this research, the power consumption is 225 W. The power of the battery = 18 Amp × 24 = 432 W

$$\text{Therefore, Back-up time} = \frac{432}{225} = 1.92 \approx 2hrs$$

This means that the battery will take 2 hours to drain.

2.4 Design and Assembly Drawing of the Automated Compressor

The various design views of the automated compressor are shown in Figures 1-4 as model design overall dimensions, exploded view of the system showing more of the electrical parts, exploded view of the compressing unit of the system. And complete design model of the rechargeable compressor and automatic drain system, respectively. Figure 5 shows the prototype of the locally fabricated Rechargeable and automatic drain air compressor system

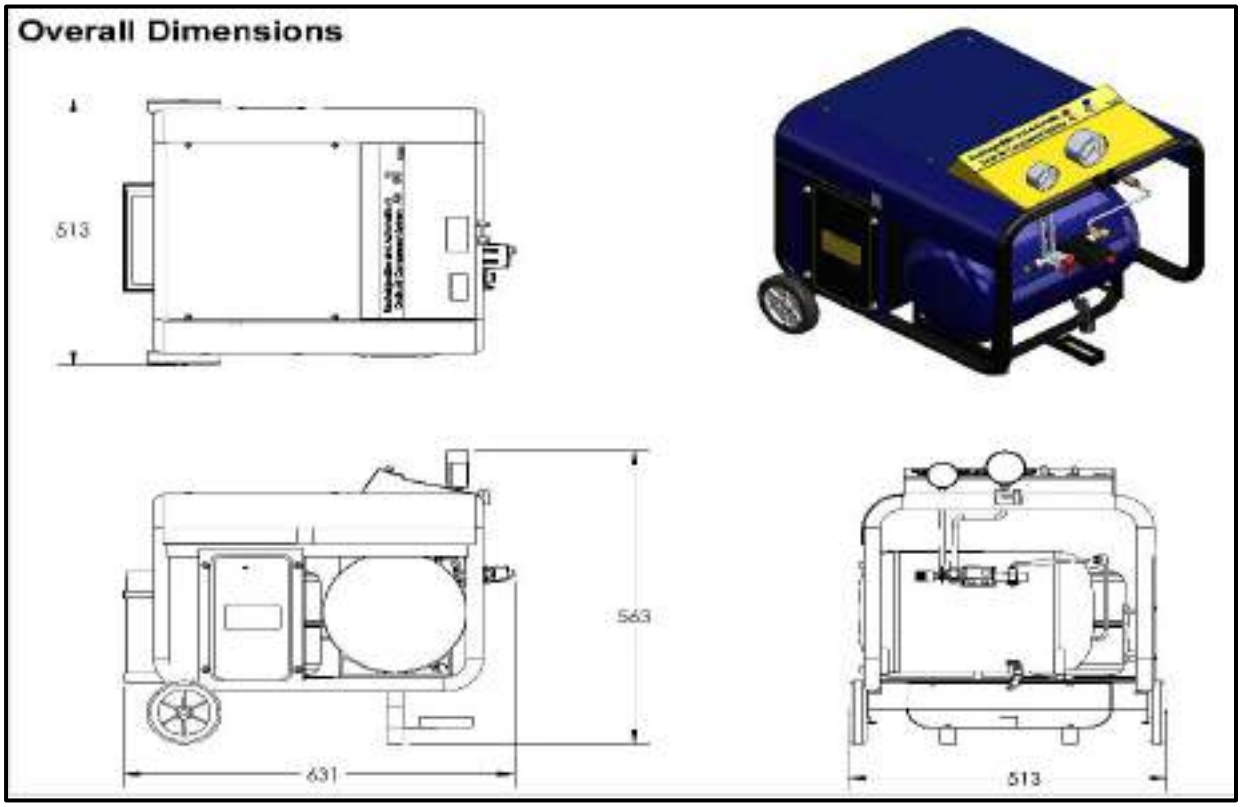

Figure 1: Model design overall dimensions

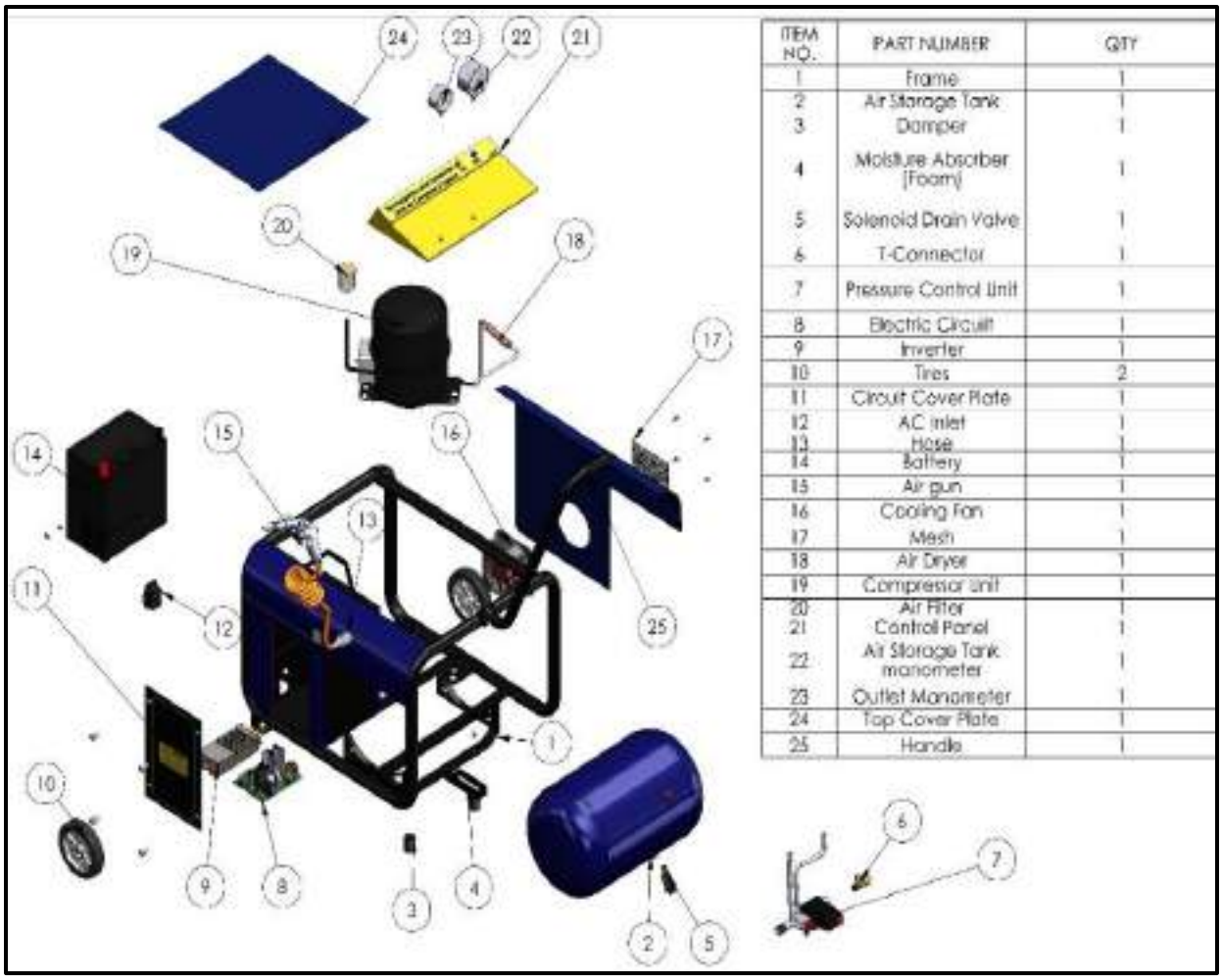

ITEM NO.	PART NUMBER	QTY
1	Frame	1
2	Air Storage Tank	1
3	Damper	1
4	Moisture Absorber (Foam)	1
5	Solenoid Drain Valve	1
6	T-Connector	1
7	Pressure Control Unit	1
8	Electric Circuit	1
9	Inverter	1
10	Tires	2
11	Circuit Cover Plate	1
12	AC inlet	1
13	Hose	1
14	Battery	1
15	Air gun	1
16	Cooling Fan	1
17	Mesh	1
18	Air Dryer	1
19	Compressor Unit	1
20	Air Filter	1
21	Control Panel	1
22	Air Storage Tank manometer	1
23	Outlet Manometer	1
24	Top Cover Plate	1
25	Handle	1

Figure 2: The exploded view of the system showing more of the electrical parts

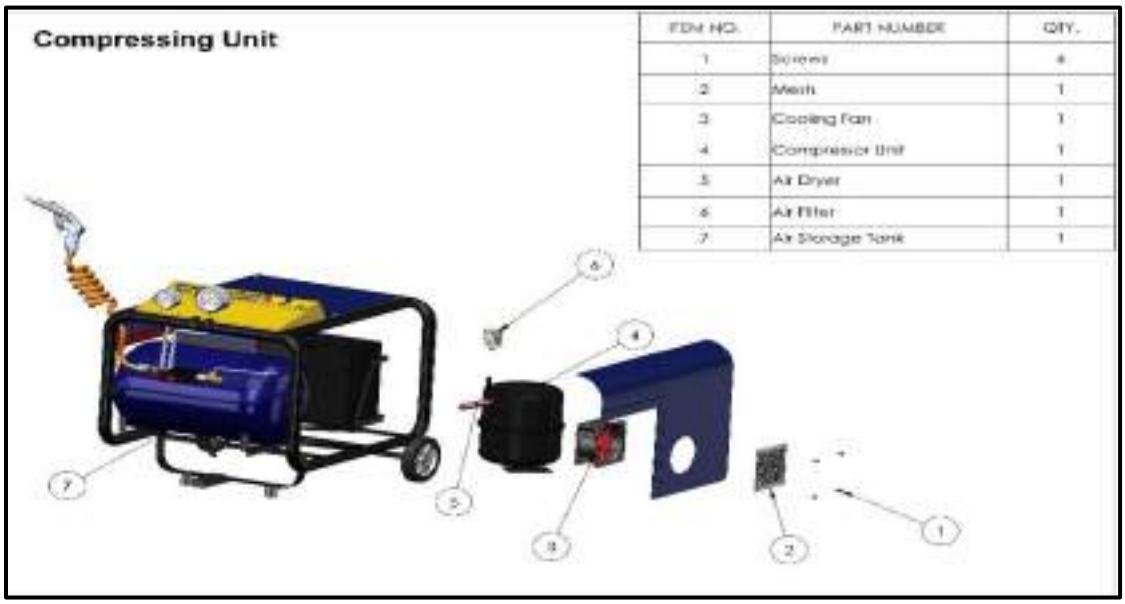

ITEM NO.	PART NUMBER	QTY.
1	Screws	4
2	Mesh	1
3	Cooling Fan	1
4	Compressor Unit	1
5	Air Dryer	1
6	Air Filter	1
7	Air Storage Tank	1

Figure 3: Exploded view of the compressing unit of the system.

Figure 4: The Complete design model of the rechargeable compressor and automatic drain system

Figure 7: Picture of the Locally Fabricated Prototype

3. Results and Discussion

The volume of the air tank is 0.0160m^3, which is equivalent to 16litres. In calculating the quantity of compressed air stored in the air tank, 28.33litres of free air at 7.58bar was reduced to 1/10 original volume. Therefore, for a 16 litres tank pressurized to 7.58bar, the tank would store about 4.623 × 10 = 42.3 gallons (160litres) of air. For the Compressor, the value of the airflow rate at standard condition (SCFM) is 0.0215m^3/min (0.76CFM), and that of the airflow rate at any reference point (ACFM) is 0.0220 m^3/min (0.78CFM). These results imply that the actual quantity of compressed air delivered to the discharge system at rated speed and underrated conditions between 4 to 10bar. At 4.30 minutes is 0.78 cubic feet of air per minute (22litres of air per minute) of the work cycle. Various rated conditions for calculating the Actual

FAD at P_0=1.035 bar, P_1= 4*b*ar, gave the results as shown in Table 1. From the illustration in Figures 6 and 7, it is clear that the FAD is dependent on the operating pressure. This can be seen as the FAD increases with an increase in operating pressure. The rating of FAD is usually associated with pressure. It is also a function of time. As the time increases with an increase in operating pressure, the FAD increases. In Figure 7, the actual FAD is 0.0220 m^3/min at 10.0 bar. According to the Compressed Air and Gas Institute (CAGI) ratings of air compressors, the rechargeable and automatic drain air compressor system is perfect for light pneumatic duties. The complete results of the calculations are expressed in Table 2.

Table 1: Relationship between operating pressure and ACFM at various time intervals

P_2 (bar)	Volume (m^3)	Time (minutes)	FAD (m^3/min)
10.0	0.0160	4.30	0.0220
9.0	0.0160	4.17	0.0189
8.0	0.0160	4.13	0.0152
7.0	0.0160	3.98	0.0118
6.0	0.0160	3.80	0.0082

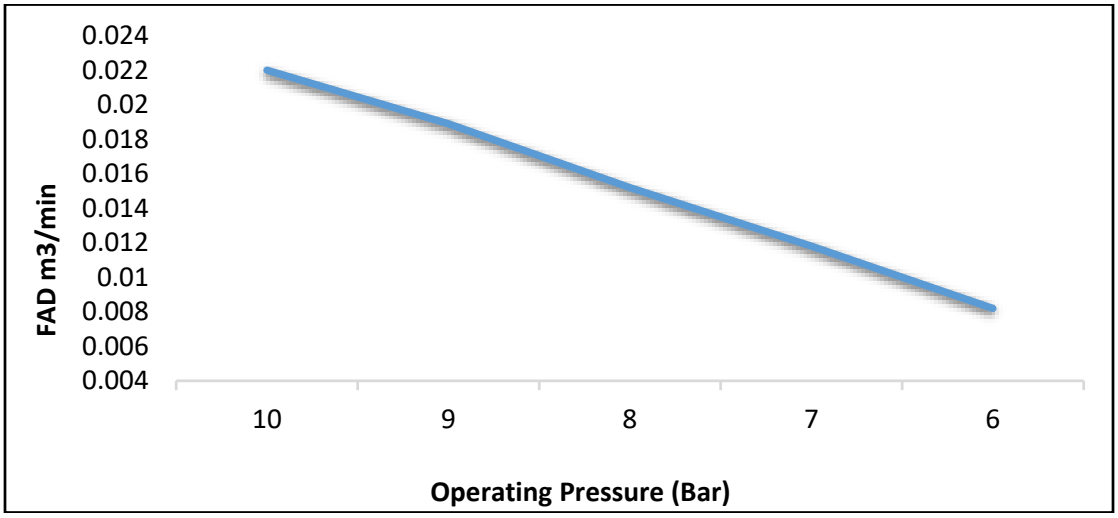

Figure 6: The graph of air delivery against operating pressures airflow diagram

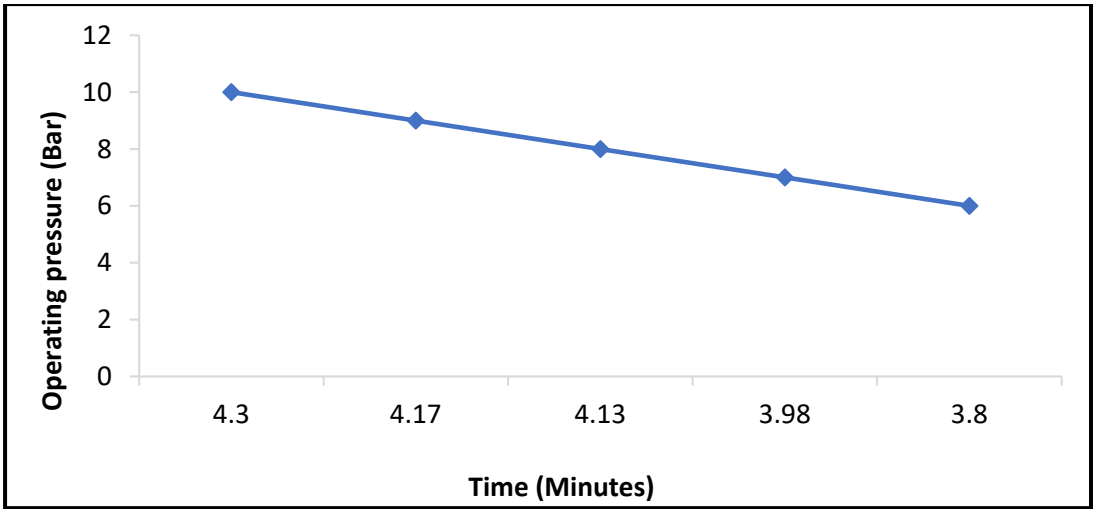

Figure 7: The graph of operating pressures against time

Table 2: The results of the calculations

PARAMETERS	VALUES
The capacity of Tank (V)	0.0160 m^3 (16litres)
Maximum Safe Operating Pressure (P_2)	145 Psi (10 Bar)
Power	225 Watt
SCFM	0.76 CFM
ACFM	0.78 CFM
Standard FAD	0.0215 m^3/min
Actual FAD	0.0220 m^3/min
Volumetric Efficiency	63.2%
Piston Displacement	0.0353 m^3/min
Battery Charging time	5.04 Hours
Battery Drain time	2 Hours

4. Conclusion

The research aims to design and fabricate a rechargeable and automatic drain air compressor system for shipboard services. The 16litres capacity system was designed to safely and reliably compress air at a maximum operating pressure of 10bar. The material selection, design considerations, calculations, drawings, and assembly were made before the project was fabricated. The materials used were selected to meet standard requirements. The air storage tank volume was determined using the basic parameters. Tank Length of 0.38m and a diameter of 0.232m were used. The other parameters required were determined and are stated in Table 2. The fabrication was done using locally available materials. The test results show that the performance of the fabricated air compressor system was found to be satisfactory, and the output of the compressor is up to the expected level.

References

[1] Xu, C, and Muller, M. (2005). Development and design of a centrifugal compressor volute. International Journal of Rotating Machinery, 3, 190–196.

[2] Mohit, K. (2016). Efficiency of air compressor and uses of compressed air on a ship.. http://www.marineinsight.com/tech/air-compressor/efficiency-of-air-compressor-and-uses-of-compressed-air-on-a-ship/ Retrieved October 27, 2016.

[3] Zhang, X., Ziviani, D., Braun, J. E., and Groll, E. A. (2020). Experimental validation and sensitivity analysis of a dynamic simulation model for linear compressors. International Journal of Refrigeration, 117, 369-380.

[4] Egger, A., Almbauer, R., Dür, L., Hopfgartner, J., and Lang, M. (2020). Multi-Response optimization applied to a mechanically assisted reed valve of a hermetic reciprocating compressor. International Journal of Refrigeration, 119, 119-130.

[5] Ghorbanian, K. and Gholamrezaei, M. (2009). An artificial neural network approach to compressor performance prediction. Applied Energy, 86(7), 1210-1221.

[6] Tanveer, M. M. and Bradshaw, C. R. (2020). Quantitative and qualitative evaluation of various positive-displacement compressor modeling platforms. International Journal of Refrigeration, 119, 48-63.

[7] Wang, J., Guo, Y., Zhou, K., Xia, J., Li, Y., Zhao, P., and Dai, Y. (2020). Design and performance analysis of compressor and turbine in supercritical co2 power cycle based on system-component coupled optimization. Energy

Conversion and Management.221, 113179.

[8] Shin, M., Na, S., Lee, J., Min, B. and Choi, G. (2019). Model analysis of a novel compressor with a dual chamber for high-efficiency systems. Applied Thermal Engineering. 158, 113717.

[9] Wang, M., Sun, H., Wang, Z., Wang, Y., Magagnato, F. and Luan, Y. (2020). Numerical investigation of the effects of system volume and average mass flow on the surge characteristics of an axial compressor. Aerospace Science and Technology. 106, 106172.

[10] Came, P. M. and Robinson, C. J. (1999). Centrifugal compressor design. Proceedings of the Institution of Mechanical Engineers. Part C, Journal of Mechanical Engineering Science, 213 (2), 139-155.

[11] Hobbs, D. E. and Weingold, H. D. (1984). Development of controlled diffusion airfoils for multistage compressor application. Journal of Engineering for Gas Turbines and Power. 106 (2), 271-278.

[12] Langa, J., Chu, W., Spence, S., An, G. and Galloway, L. (2021). Performance enhancement of a centrifugal compressor stage using profiled end wall (pew) treatments in the radial vaned diffuser. Aerospace Science and Technology.110, 106488.

[13] Zagorowska, M., Skourup, C. and Thornhill, N. F. (2020). Influence of compressor degradation on optimal operation of a compressor station. Computers & Chemical Engineering. 143, 107104.

[14] Xiao, B., Huang, T., He, L., Yan, Y., Sun, Y. and Wang, W. (2019). Experimental study of an improved air-source heat pump system with a novel three-cylinder two-stage variable volume ratio rotary compressor. International Journal of Refrigeration. 100, 343-353.

[15] Reddy, K. M., Vasanth, M. H., Kumar, N. Y. B., Dwivedi, D. (2019). Design and analysis of multiplier using approximate 4-2 compressor. AEU - International Journal of Electronics and Communications. 107, 89-97.

[16] Ozsipahi, M., Kose, H. A., Cadirci, S. Kerpicci, H. and Gunes, H. (2019). Experimental and numerical investigation of lubrication system for the reciprocating compressor. International Journal of Refrigeration. 108, 224-233.

[17] Nathalal, G. K. (2018). A review on the study of an air compressor. Journal of Emerging Technologies and Innovative Research, 5(4), 26-34.

[18] Naveenkumar C., Ashkai M; Athul, M., Balakumaran, R and Balaji, S. (2018). Design, fabrication & simulation of compressed air hybrid vehicle. International Research Journal of Engineering & Technology (IRJET). 5(2), 183-184.

[19] Ganesan, S., Senthil, S. K., Balamurugan, M. and Lokesh, B. (2019). Design and fabrication of a mobile air compressor. Global Scientific Journal. 7(5), 174-193.

[20] Brown, R. N. (2005). Compressors: selection and sizing. Elsevier, ISBN: 9780750675451.

Covenant Journal of Engineering Technology (CJET) Vol.5 No.1, June, 2021
ISSN: p. 2682-5317 e. 2682-5325 DOI: xxxxxxxxxx

An Open Access Journal Available Online

Emission Comparison of Air-Fuel Mixtures for Pure Gasoline and Bioethanol Fuel Blend (E20) Combustion on Sparking-Ignition Engine

M.A. Muregi [1], M.S. Abolarin [1], O.J. Okegbile [1], E.J. Eterigho [2], I.P. Okokpujie [3,4]

[1]Department of Mechanical Engineering, School of Infrastructure, Process Engineering and Technology, Federal University of Technology
[2]Department of Chemical Engineering, School of Infrastructure, Process Engineering and Technology, Federal University of Technology, Minna, Niger State, Nigeria.
[3]Department of Mechanical Engineering, Covenant University, Ota, Ogun State, Nigeria
[4]Department of Mechanical and Industrial Engineering Technology, University of Johannesburg, Johannesburg, 2028, South Africa
***Corresponding author's email:** imhade.okokpujie@covenantuniversity.edu.ng[3], muregi.pg718024@st.futminna.edu.ng[1]

Received: 18.02.2021 Accepted: 01.05.2021 Published: 31.06.2021

Abstract: This study analyses and compared the exhaust gas emission of two different air-fuel mixture, Pure Gasoline and Bioethanol Fuel blend (E10 and E20), in a spark-ignition (S.I.) engine. Proximate and ultimate analyses of pure gasoline and bioethanol blend were carried out for their respective percentage (%) elemental composition for each fuel (i.e., carbon, hydrogen, oxygen, sulphur, nitrogen, metals, and water). The analysis reveals that pure gasoline has high carbon (C) content of 86%, and bioethanol has a carbon content of 52.2%. Oxygen content stands at 33-35% and was carried out at varying load conditions. To ascertain their CO., CO_2, HC., NO, lambda, and the calorific values of exhaust emission. The result clearly shows that bioethanol's calorific value is lower than that of gasoline, which gives a remarkable increase in mechanical efficiency, which was attributed to an increase in the oxygen content in bioethanol, ethanol blend during combustion gives an air-fuel mixture lean in an unmodified engine. Hence the mixture strength (charge) burns more rapidly. Bioethanol blends in gasoline engines reduce CO. emissions, unlike gasoline, which gave higher CO emissions. The gas emission test was conducted on E10, and E20.and effective combustion was determined and completed much earlier in the expansion stroke, thereby decreasing the probability of CO emissions due to flame quenching. At the end of the investigation, it was found that bioethanol blend reduces CO and HC in exhaust stroke by 40% and gives a higher compression ratio (high speed) thus, causes a decrease in CO_2 NO_X. E20 for both idle and high speed recorded a remarkable reduction in comparison. Therefore, bioethanol fuel blends in gasoline engines are recommended as mitigation against the greenhouse gas effect.

Keywords— Bioethanol fuel blend; the calorific value of blend; exhaust gases; emission; and petrol engine

1. Introduction

Due to the growing industrialization and the expanding transportation sector worldwide, increasing demand for energy, specifically fossil-oriented energy. The world energy consumption is expected to increase to 180,000 GWh/year by 2020 [1]. Extensive use of fossil fuels over the years has resulted in increased prices of petroleum and electricity as well as a negative impact on the environment resulting from increases in greenhouse gas (GHG) emissions [2]. It is estimated that 81% of the world energy requirement utilization is obtained from fossil fuels [3].

Thus, the limit of fossil fuel reserves is quite clear. Global warming is growing. The increasing demand of crude oil (gasoline/diesel) is escalating by the day. The emission regulations are rhythm out from its utilization. Gasoline is a refined product of petroleum consisting of a mixture of hydrocarbons, its composition widely varies depending on the crude oils, gasoline is the second product to be extracted from crude oil by heating to boiling point of 110^{o}c.

Flammable liquid, transparent liquid primarily used as a fuel in most spark ignition (SI) engines. EIA (2020), it remains the world most important source of energy today. Due to its chemical contents mainly BTEX it as many harmful effects (environmentally) [3]. Alternatively, biofuel (bioethanol and biodiesel) is being perpecturateted to reduce the gassy emissions regimen. Studies have been reported on the application of bioethanol on S.I. and CI engines, which is the focus of these studies, and it is based on three aspects [4-5]. The application methods of bioethanol on petrol engines, fuel properties of bioethanol-gasoline blends, and out-there on the combustion and its resulting emission characteristics. To minimize the over-reliability of oil and contribute to the raising efforts of decarburizing the transport sector. Bioethanol fuel (ethyl alcohol) is a clear burning alternative fuel made from feedstock (wood, corn, cassava, sugar cane, vegetable matters, animal fats, to mention but a few) it is oxygenated (high oxygen content) with high octane rating and naturally burns, it can be renewed again and again without depleting its original source

Ethanol is a biodegradable and sustainable energy of organic chemical compound comprising of hydrogen, carbon and oxygen. It is a clean and clear liquid that looks like water (colourless), completely miscible with water [25]. Bioethanol has a somewhat sweet flavour when diluted with water which is part of its resource base, its pungent, and naturally denotes, with burning taste when concentrated, odourless, it is more volatile than water, flammable, burns with a light blue flame, and has excellent fuel properties for spark ignition internal combustion engines. Biofuels also have the budding/latent to minimize CO., HC., $NO_{X,}$ and chapped emissions resulting from combustion in comparison a liter of ethanol contains about two-thirds as much energy as a liter of gasoline. [21] However, pure ethanol has high octane value, which improves the performance of gasoline when blended and reduces the likelihood of engine knock problems, which occurs when fuel combusts too soon in an engine cylinder when a vehicle is working hard to accelerate. Since ethanol molecules contain (oxygen) unlike gasoline molecules ethanol fuel is referred to as "oxygenated". The oxygen in ethanol can improve the fuel combustion process thereby reducing emission such as carbon monoxide, ozone from unburned hydrocarbons, car inorganic particulates amongst other [21].

However, for related reasons, ethanol combustion reacts more with atmospheric nitrogen, which can marginally increase emissions of ozone-forming nitrogen oxide (NO_2) gases. It also contains a negligible amount of Sulphur compared to petroleum, blending ethanol with gasoline helps to reduce the sulphur content. However, even at high concentrations of ethanol, minimal amounts of water will draw the ethanol out of the blend away from the gasoline. Ethanol and gasoline are very similar in specific gravity. The two fuels mix readily with minimal agitation, since the biomass used to produce ethanol is created by photosynthesis and the carbon dioxide formed by the combustion of ethanol is recycled back to the air. The net reduction in greenhouse gases related to ethanol's displacement of petroleum fuel can vary substantially depending upon the amount of fossil fuel used in the ethanol fuel production process. Therefore, bioethanol produced through fermentation or synthesis provides a way of shifting to low-carbon, non-petroleum fuels, and chemical catalysts [6]. While improving vehicle efficiency is by far the essential low-cost way of reducing carbon dioxide (CO_2) emissions in the transport sector. Biofuels also have the potential to reduce C.O., H.C., NOx, and particulates emissions [7]. There are many parameters available in automobile engine that determines performance and emission of an engine. First is to determine the yield process and desire combustion quality, (required standards) and secondly is to give maximum output power requirements. The investigation indicated a considerable reduction in smoke and NO level. This was accompanied by an increase in brake thermal efficiency at high output, ignition delay

and pressure rate went up. The rate of heat release in the premixed burn period was higher, when oxygen concentration in the intake was enhanced by 25% step up along with the use of water diesel emulsion the brake thermal efficiency improved and there was a further reduction in smoke level HC and CO levels also dropped alongside with NO emission went up due to temperature increase and oxygen availability. The variable compression ratio on a spark-ignition engine is designed to run on pure gasoline and ethanol-gasoline blend based on different ratios (EER) 10% and 20% by volume. In comparison with Manoel et al. [8], where a Binary search algorithm was used to determine the level of emission, and Ejilah et al. [9] reported a multicommuted flow analysis approach on TD110-115 Petrol Engine to engulf with an SV-5Q motor vehicle silencer gas analyser was used to determine the influence of fuel blends samples and lambda on heat and emissions of a petrol engine base on different loadings on the effect of lambda, silencer gas temperature, heat loss in the engine, and silencer gas analysis.

2. Materials and Methods

2.1 Preparation of Gasoline Ethanol Blend

The synthesis of catalysts and bioethanol production by the non-conventional method has earlier been reported [10]. A given volume (four litres) of unleaded gasoline sourced from Total Nigeria and AYM Shafa Plc were blended with half a litre. One litre of bioethanol produced from cassava using a non-conventional method (the use of synthesized heterogeneous catalyst) in a beaker marked E10 and E20 (10 and 20 percent by a ratio of the bioethanol to 90 and 80 percent of petrol, respectively). The blend was stirred continuously for a quarter of an hour at room temperature to attend a homogenous state and ensure relative phase stability and consistency of the blend on short-term measure. The choice of EER blend (E10 and E20) adopted for this study is in line with the U.S (FFR) [11].

2.2 Proximate and Ultimate Analysis

SV-5Q Automobile gas analyser was used to carry out the proximate and ultimate analysis. The equipment model, TD110-115, 45kg net weight with CR of (compression ratio) 20.5:1, temperature between 5 – 40 ^{0}C, humidity < 95% atmosphere and pressure was set at between 60-106 KPa. Fuel moisture was first carried out by weighing a required quantity of the sample, which was subjected to heat at103°C in an oven, then allowed for cooling. It was then reweighed. This analysis was to guarantee complete drying of the sample, and the procedure was repeated until its weight remained constant. The variance in the weight between the dry and fresh sample gives the moisture content in the fuel, and subsequently, readings of other various elemental compositions in the bioethanol, gasoline, and its blend was recorded. This is in line with [12-13].

2.3 Engine Exhaust Gas Emission Analysis

Peugeot 406 Nigeria's four-stroke internal combustion engine (E10 model) was used to investigate gas emission analysis on ethanol energy ratio (EER) of E10, E20, and pure gasoline fuel additives to determine engine performance. Furthermore, the comparative analysis for air-fuel mixture exhaust gas emission based on technical specifications was carried out; which is in agreement with the standard of SAE practice SAE J1312 for the four-stroke engine. The process was carried out on each of the three EER blends for idle and high-speed loadings, respectively, as in Plate 1.

The vehicle in which the analysis was carried out was placed (parked) on a computerized weighbridge. The emission analyser code was inserted in the exhaust. While the engine remained running (under all loads) the respective emission elements (calorific value (air/fuel ratio), lambda, H.C. (ppm), CO%, CO_2%, O_2% and NO in ppm) were displayed on the monitor of the computer for reading/recording. The results were recorded for each fuel sample for both idle and high-speed load (Tables 1 to 4). At the same time, a comparison was made manually based on the results obtained and the benchmark of the gasoline test, in agreement with the standard of SAE practice SAE J1312, in agreement with Abdulkarim et al. [14] and Artur et al. [15].

Plate 1: Gas Emission Test device and the test

3. Results and Discussion

In this section, the investigational results of emission and its comparison for fuel-air mixture combustion for pure gasoline and gasoline bioethanol blend on the pollutant emissions emitted from the engine are reported and discussed. It must be brought up here that Ethanol Energy Ratio (EER) represents the ratio of ethanol blend.

2.1 Proximate and Ultimate Analysis of Raw Ethanol Produced

Proximate and ultimate analysis carried out to determine various elemental compositions of the three fuels; (pure gasoline, pure ethanol, and gasoline-ethanol blend (E10 and E20) with particular reference to oxygen, carbon, and hydrogen content of their respective fuels combustion and emissions comparison. It was observed that pure gasoline contains 86% carbon and oxygen 0%, compared with bioethanol and its blend, which contains 50.10% – 52.20% of carbon and 33.35% - 34.80% oxygen (Figure 1). H.C. and C.O. are products of incomplete combustion or inappropriate catalytic converter from pure gasoline combustion, which results from flame quenching on the surface of the piston crown containing a high carbon percentage.

Moreover, oxygen deficiency could result in incomplete combustion and subsequent power loss. Therefore, resulting in carbon monoxide formation compared with bioethanol blend. This gives better combustion developed from lean fuel mixture with high oxygen content, as shown in Figure 1.

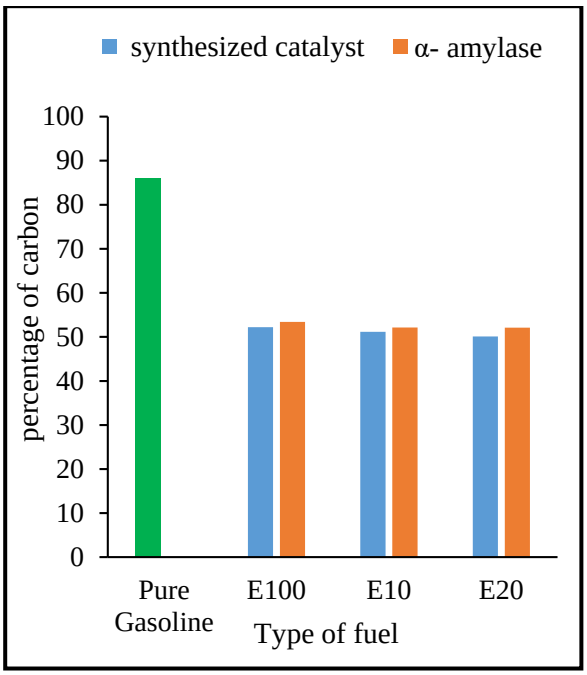

Figure 1: Carbon Content in Pure Gasoline and the Fuel produced using synthesized catalyst and α-Amylase

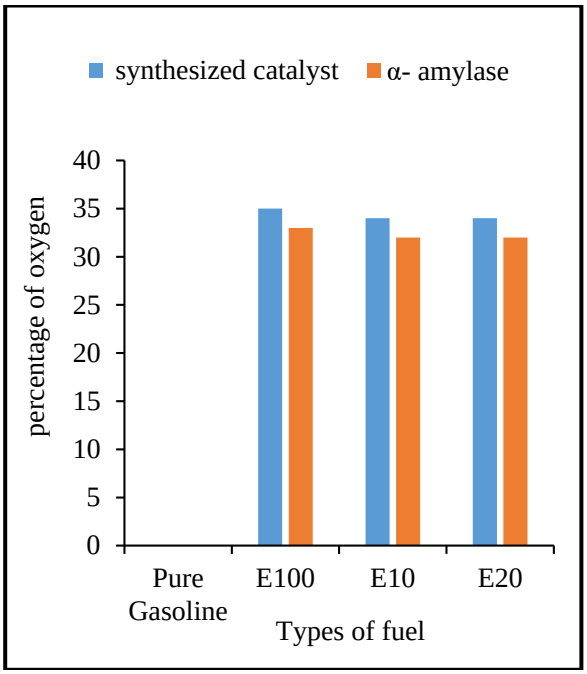

Figure 2: Oxygen Content in Pure Gasoline and the Fuel produced using synthesized catalyst and α-Amylase

The carbon monoxide focus diminishes as the EER mix builds due to the expansion of bioethanol, which is exceptionally oxygenated. Making the combination slenderer and gave better ignition with less C.O. creation. Figure 2 portrays the rates of oxygen present in the various energizes by close and extreme examination. This is in concurrence with Haroun et al. [16] discoveries. The H.C. emanation diminishes with the expanding EER mix. Rapid outcomes in stable ignition measures and quicker fire, along these lines, discharges fewer outflows after burning on account of its higher octane rating, which has the chance of motor thump event. High oxygen content in bioethanol additionally lessens nitrogen oxide emanation from the ignition, higher warmth vaporization, and fire speed. It gives more oxygen to the ignition cycle prompting a "learning impact" in adaptation [17].

When contrasted with conventional unleaded gas, bioethanol gives clean-consuming and without particulate fuel when combusted. The final result is carbon dioxide and water. The NOx focus relies on burning temperature, accessibility of oxygen (lambda), and better ignition time. The NOx increments as the EER mix increments close by with load increment. This is because of a superior burning cycle because of a higher ignition temperature, which favours NOx development. As motor speed was expanded, the NOx discharges for all mixing proportions were additionally slowly expanded. Unadulterated fuel during the burning cycle for a complete transformation of carbon and hydrogen, lacking oxygen was challenging to accomplish, prompting particulates and carbon monoxide exhaust discharge. Hence, oxygen-enhanced ignition is essential and a critical factor for contamination control and improved motor burning; this is in confirmative [18].

2.2 Engine Exhaust Gas Emission

Tables 1 to 4 showed the gas emission test, C.O., and CO_2 emissions and were compared for all fuel mixtures as depicted in Figure 3 and 4. It was seen that the bioethanol mix is reasonable at all heaps because lesser carbon monoxide outflow was recorded contrasted with unadulterated gas. Base on the examination in this investigation, bioethanol at 10% and 20% by volume are better at all heaps, and high-pressure proportions were accomplished; this is in arrangement [19].

Table 1: Gas Emission Test Result for Pure Gasoline: IDLE SPEED

Gas Emission Test	Max.	Min.	Average	Status
HC (ppm)	201	443	332	X
CO (%)	0.75	2.05	1	V
Lambda	1.01	1.07	1	V
CO_2 (%)	11	13	12	
O_2 (%)	0.9	0.99	0.94	
NO (ppm)	171	788	479.5	

"X" refers to incomplete combustion for idle speed loading for all cases of H.C. emission. At the same time, C.O. represents inappropriate combustion resulting from catalytic converter or oxygen deficiency. Also, "V" means complete combustion in all loading.

Table 2: Gas Emission Test Result for Pure Gasoline: HIGH SPEED

Gas Emission Test	Max.	Min.	Average	Status
HC (ppm)	201	391	269	X
CO (%)	0.73	2.87	1.8	X
Lambda	0.97	1.07	1.02	V
CO_2 (%)	11	13	12	
O_2 (%)	1.65	1.72	1.68	
NO (ppm)	84	341	212.5	

Table 3: Gas Emission Analysis Test for Bioethanol Blend (E20): IDLE SPEED

Gas Emission Test	Max.	Min.	Average	Status
HC (ppm)	168	334	260	X
CO (%)	0.51	1.69	1	V
Lambda	0.96	1.01	1	V
CO_2 (%)	10	12	11	
O_2 (%)	1.69	1.75	1.72	
NO (ppm)	84	380	232	

The investigation carried out from the experimental analysis in this study shows that the engine performance increased. And pollutant emission was decreased using bioethanol–gasoline blend in an S.I. engine against pure gasoline (Figure 5).

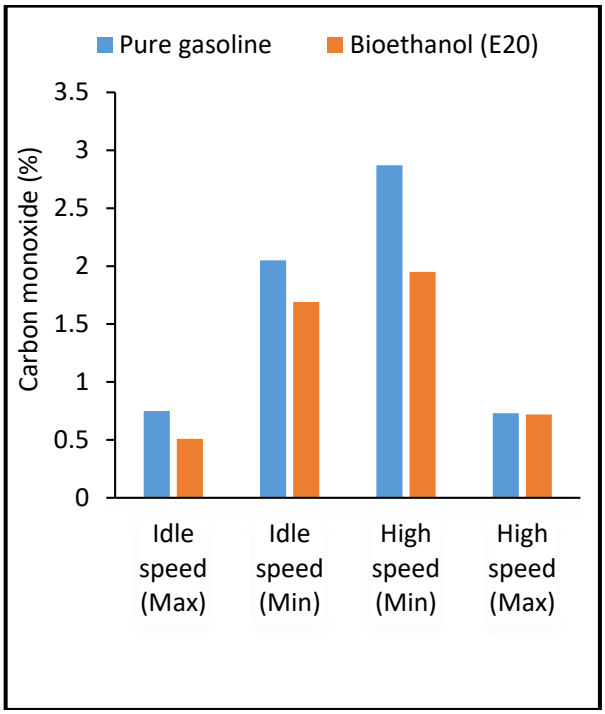

Figure 3: Gas Emission Test for Carbon monoxide at Idle and High Speed

There are many parameters available in automobile engine that determines performance and emission of an engine. First is to determine the yield process and desire combustion quality, (required standards) and secondly is to give maximum output power requirements. The investigation indicated a considerable reduction in smoke and NO level. This was accompanied by an increase in brake thermal efficiency at high output, ignition delay and pressure rate went up. The rate of heat release in the premixed burn period was higher, when oxygen concentration in the intake was enhanced by 25% step up along with the use of water diesel emulsion the brake thermal efficiency improved and there was a further reduction in smoke level HC and CO levels also dropped alongside with NO emission went up due to temperature increase and oxygen availability.

The results reveal that when bioethanol was blended, the heating value of the blended fuel decreased, this result is in line with [20-22]. At the same time, the octane rating increased. This implies that lambda (air-fuel ratio mixture for the combustion process is normal), confirmative with standard specification.

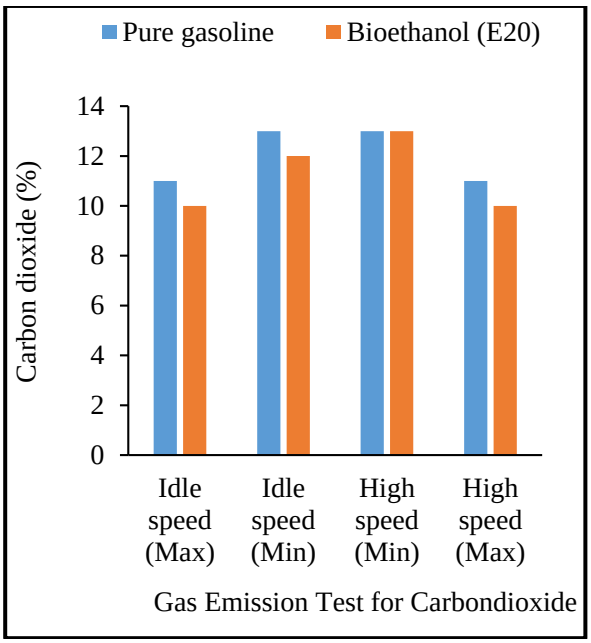

Figure 4: Gas Emission Test for Carbon dioxide at Idle and High Speed

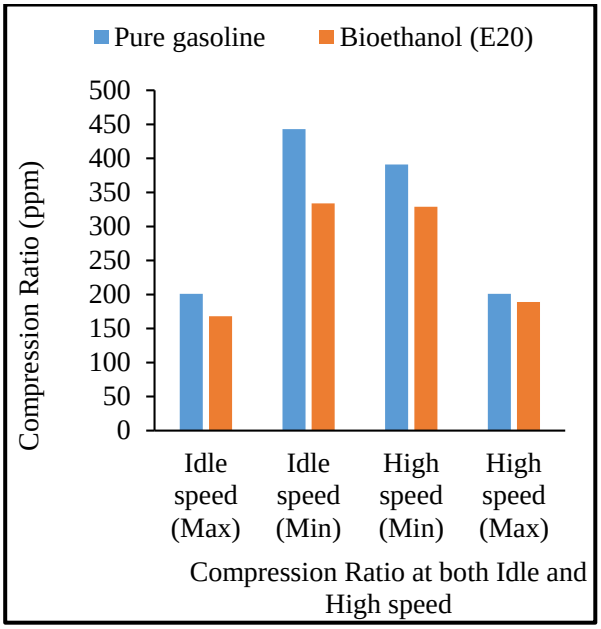

Figure 5: Compression Ratio for both fuels at both Idle and High speed

And must not exceed "1" as recorded for ethanol blend as well as" 1.07" as recorded for pure gasoline (Figure 6). In contrast, CO_2 emission from ethanol blend recorded 10% as against 13% for pure gasoline and HC. for ethanol blend 168 ppm against 201 ppm for gasoline for idle speed loadings. Where "V" represents complete combustion in all cases, from Table 4, it could be observed the increase in EER has improved for all exhaust emission of the elements (HC., CO, and Lambda). Furthermore, as the motor forces increases and transparent fuel utilization diminishes, and CO. emanation from the motor reductions. Because of the inclining impact brought about by the expansion of bioethanol HC. discharge. The results also show that there were decreases in similar working conditions of the CO_2 release from oxygen and water reduction on account of the improved burning [20], [23-25]. The life cycle of SI engine also depends on the ethanol blend for maximum performance all through the life span [27-30]. This analysis will assist the manufacturing industry to produce quality fuel blend that will reduce environmental pollution thereby improving the economical of the nation.

Table 4: Gas Emission Analysis Test for Bioethanol Blend (E20): HIGH SPEED

Gas Emission Test	**Max.**	**Min.**	**Average**	**Status**
HC (ppm)	189	329	259	V
CO (%)	0.72	1.95	1.34	V
Lambda	0.96	1.01	0.99	V
CO_2 (%)	10	13	11.5	
O_2 (%)	0.85	0.91	0.88	
NO (ppm)	158	760	459	

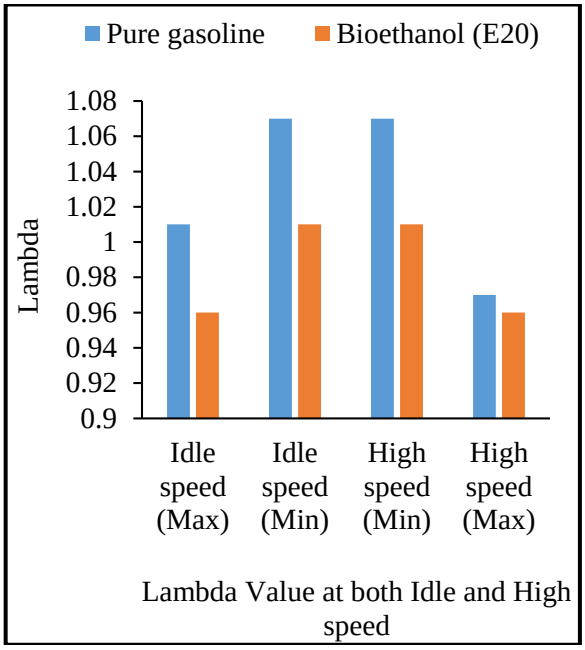

Figure 6: Lambda Value at both Idle and High speed

4. Conclusions

The investigation revealed from the proximate and ultimate analysis that pure

gasoline has high carbon (C) content of 86%, compared to bioethanol with a carbon content of 52.2%. In comparison, higher exhaust emission of carbon dioxide was recorded when pure gasoline was combusted, resulting in greenhouse gas and global warming. In contrast, a remarkable decrease in emission was recorded using a gasoline bioethanol blend for combustion, which will contribute to the transport sector's decarbonisation if implemented. The result reveals that bioethanol blends (E20) status indicate complete combustion, which is quite suitable in replacing pure gasoline in the transport sector

It was also observed that the concentration of bioethanol increases alongside with reduction in lambda. In contrast, gasoline fuels were found to have the lowest silencer temperature output under the same conditions. The increase in EER blends concentration (E10 and E20) shows a remarkable higher trend. Due to their higher tendency from oxidation, lower C.O. emission was recorded in the blends than gasoline during the combustion process.

References

[1] F. M. Luna, J. A. Cecilia, R. M. Saboya, D. Barrera, K. Sapag, Rodríguez-Castellón E, Cavalcante CL. Natural and modified montmorillonite clays as catalysts for synthesis of biolubricants. Materials. 2018 Sep;11(9):1764.

[2] P. Zulu, B. Ilori, and A.S. Sambo, Biogas technology in Nigeria. Journal of Renewable Energy. 4(2) Pp 81, 2017.

[3] K. Srirangan, L. Akawi, M. Moo-Young, C. P. Chou. Towards sustainable production of clean energy carriers from biomass resources. Applied Energy. 2012 Dec 1; 100:172-86.

[4] H. Huang, M. Khanna, H. Önal, X. Chen. Stacking low carbon policies on the renewable fuels standard: Economic and greenhouse gas implications. Energy Policy. 2013 May 1; 56:5-15.

[5] M. J. Lima, B. F. Reis. Automatic Procedure to Determine Acidity in Fuel Ethanol by Photometric Titration Using Binary Search and Multicommuted Flow Analysis. Journal of the Brazilian Chemical Society. 2018 Nov; 29(11): 2326-33.

[6] Isah AN, Eterigho EJ, Olutoye MA, Garba MU, Okokpujie IP. Development and test performance of heterogeneous catalysts on steam reforming of bioethanol for renewable hydrogen synthesis: A review. J Advance Res Fluid Mechanics Therm Sciences 2020;73(73):69-108.

[7] E. J. Eterigho, M. A. Musa, S. E. Ejejigbe, I. P. Okokpujie. Optimization of Process Parameters Influencing Biogas Production from Rumen and municipal waste: Analytical Approach. Covenant Journal of Engineering Technology. 2019 Dec 16;3(2).

[8] I. R. Ejilah, B. A. Gambo, and K. Dahuwa. Influence of Air-Fuel Mixtures and Gasoline, Bioethanol Fuel Mixtures on Emissions of a Spark Ignition Engine. The International Journal of Engineering and Science. Pp 2-7 2017.

[9] F. M. Luna, J. A. Cecilia, R. M. Saboya, D. Barrera, K. Sapag, Rodríguez-Castellón E, Cavalcante CL. Natural and modified montmorillonite clays as catalysts for synthesis of biolubricants. Materials. 2018 Sep;11(9):1764.

[10] P. Zulu, B. Ilori, and A.S. Sambo, Biogas technology in Nigeria. Journal of Renewable Energy. 4(2) Pp 81, 2017.

[11] K. Srirangan, L. Akawi, M. Moo-Young, C. P. Chou. Towards sustainable production of clean energy carriers from biomass resources. Applied Energy. 2012 Dec 1; 100:172-86.

[12] H. Huang, M. Khanna, H. Önal, X. Chen. Stacking low carbon policies on the renewable fuels standard: Economic and greenhouse gas implications. Energy Policy. 2013 May 1; 56:5-15.

[13] M. J. Lima, B. F. Reis. Automatic Procedure to Determine Acidity in Fuel Ethanol by Photometric Titration Using Binary Search and Multicommuted Flow Analysis. Journal of the Brazilian Chemical Society. 2018 Nov; 29(11): 2326-33.

[14] Isah AN, Eterigho EJ, Olutoye MA, Garba MU, Okokpujie IP. Development and test performance of heterogeneous catalysts on steam reforming of bioethanol for renewable hydrogen synthesis: A review. J Advance Res Fluid Mechanics Therm Sciences 2020;73(73):69-108.

[15] E. J. Eterigho, M. A. Musa, S. E. Ejejigbe, I. P. Okokpujie. Optimization of Process Parameters Influencing Biogas Production from Rumen and municipal waste: Analytical Approach. Covenant Journal of Engineering Technology. 2019 Dec 16;3(2).

[16] I. R. Ejilah, B. A. Gambo, and K. Dahuwa. Influence of Air-Fuel Mixtures and Gasoline,

Bioethanol Fuel Mixtures on Emissions of a Spark Ignition Engine. The International Journal of Engineering and Science. Pp 2-7 2017.

[17] M. A. Muregi, M. S. Abolarin, O. J. Okegbile and E. J. Eterigho· Development and Characterization of Local Content Catalyst (Montmorillonite Clay) Supported Nickel Oxide. Pp 50, 2019.

[18] L. J. Nunes, J. C. Matias, J. P. Catalao. Torrefaction of Biomass for Energy Applications: From Fundamentals to Industrial Scale. Academic Press; 2017 Nov 21.

[19] L. Fryda, K. Panopoulos, P. Vourliotis, E. Kakaras, E. Pavlidou. Meat and bone meal as secondary fuel in fluidized bed combustion. Proceedings of the Combustion Institute. 2007 Jan 1;31(2):2829-37.

[20] N. Abdulkarim, P. BoriIge, B. Shiru and M. Abubakar. Analysis of Exhaust Gas Emissions from Gasoline Engine-powered Passenger vehicles in Nigeria. International Journal of Engineering, Trends and Technology 34(1) Pp 405-408; 2016.

[21] J. Artur, K. Hubert, U. Adam, B. Krzysztof, L. Kazimierz and W. Paweł. Analysis of the repeatability of the exhaust pollutants emission research results for cold and hot starts under controlled driving cycle conditions. Journal of Environmental Science and Pollution Research 18(25) Pp 17862–17877; 2018.

[22] H. A. Shahad, S. K. Wabdan. Effect of operating conditions on pollutants concentration emitted from a spark ignition engine fueled with gasoline bioethanol blends. Journal of Renewable Energy. 2015 May 14;2015.

[23] E. J. Eterigho, and U. Habib. Production of Green Ethanol" 6th Edition of Nigerian Universities Research and Development Fair (NURESDEF). 2016, P.P. 21-22

[24] P. Baskar, A. Senthilkumar. Effects of oxygen enriched combustion on pollution and performance characteristics of a diesel engine. Engineering Science and Technology, an International Journal. 2016 Mar 1;19(1):438-43.

[25] G. Juozas and N. Seshaiah. Influence of Composition of Gasoline – Ethanol Blend Parameters of Internal Combustion Engines, Journal of Kones, Internal Combustion Engines. 2013, Vol.10 Pp 3-4.

[26] A.D. Bhetalu, S. S. Patil and N. Ingole. An Overview Ethanol as Motor Fuel. Journal of Engineering Research and Studies. 2012; 3(2) Pp 112-120

[27] D. C. Vasconcelos, E. H. Nunes, W. L. Vasconcelos. AES and FTIR characterization of sol–gel alumina films. Journal of non-crystalline solids. 2012 Jun 1;358(11):1374-9.

[28] B. Q. He, J. X. Wang, J. M. Hao, X. G. Yan, J. H. Xiao. A study on emission characteristics of an EFI engine with ethanol blended gasoline fuels. Atmospheric Environment. 2003 Mar 1;37(7):949-57.

[29] A.A. Yusuf, F.L. Inambao. Progress in alcohol-gasoline blends and their effects on the performance and emissions in SI engines under different operating conditions. International Journal of Ambient Energy. 2021 Mar 12;42(4):465-81.

[30] M. Göktaş, M.K. Balki, C. Sayin, M. Canakci. An evaluation of the use of alcohol fuels in SI engines in terms of performance, emission and combustion characteristics: A review. Fuel. 2021; 286:119425.

[31] M.K. Mohammed, H.H. Balla, Z.M. Al-Dulaimi, Z.S. Kareem, M.S. Al-Zuhairy. Effect of Ethanol-Gasoline Blends on SI Engine Performance and Emissions. Case Studies in Thermal Engineering. 2021 Feb 17:100891.

[32] B. Zhang, S.M. Sarathy. Lifecycle optimized ethanol-gasoline blends for turbocharged engines. Applied Energy. 2016 Nov 1; 181:38-53.

[33] Sarah M., Edward A. B. (2015) New Paradigms for Engineering Plant Cell Wall Degrading Enzymes. Pp 129-149

[34] World Watch Institute London Stealing (2017) Biofuels for Transport. Global Potential and implication was for sustainable Energy and Agriculture. Earth Scan Publications Ltd, London P 3-29, 45 – 55, Pp 169 – 261.

[35] I. Dunmade, M. Udo, T. Akintayo, S. Oyedepo, & I. P. Okokpujie. Lifecycle impact assessment of an engineering project management process - A SLCA approach. Paper presented at the IOP Conference Series: Materials Science and Engineering, 2018, 413(1). doi:10.1088/1757899X/413/1/012061.

[36] A. Onawumi, M. Udo, E. Awoyemi, & I. P. Okokpujie. Alternate maintainability evaluation technique for steering system of used automobiles. Paper presented at the IOP Conference Series: Materials Science and Engineering, 2018, 413(1) doi:10.1088/1757899X/413/1/012062.

[37] I. P. Okokpujie, O. S. I. Fayomi, & R. O. Leramo. The role of research in economic development. Paper presented at the IOP Conference Series: Materials Science and Engineering, 2018, 413(1). doi:10.1088/1757899X/413/1/012060.

[38] M.K. Mohammed, H.H. Balla, Z.M. Al-Dulaimi, Z.S. Kareem, M.S. Al-Zuhairy. Effect of Ethanol-Gasoline Blends on SI Engine Performance and Emissions. Case Studies in Thermal Engineering. 2021 Feb 17:100891

Covenant Journal of Engineering Technology (CJET) Vol.5 No.1, June, 2021
ISSN: p. 2682-5317 e. 2682-5325 DOI: xxxxxxxxxx

An Open Access Journal Available Online

Mechanical and Chemical Properties of Reinforcement Bars Manufactured in Nigeria

***Oluwaseun B. Hassan, Oluwatobi O. Akin, Adamu Lawan and Yusuf D. Amartey**

Department of Civil Engineering, Ahmadu Bello University, Zaria, Nigeria
***Corresponding email: oluwaseunbhassan@gmail.com**

Received: 11.03.2021 Accepted: 15.06.2021 Published: 30.06.2021

Abstract: Reinforcement bars, or REBAR for short, are mainly produced from metal scrap or iron ore, or a combination of both. Their manufacturing process has a significant effect on their properties, so also are the percentage concentration of various constituent elements and the cooling rate in the production process. This research work aims to study the physical and chemical properties of rebars manufactured in Nigeria vis-à-vis their suitability for construction purposes. The effect of chemical composition in rebar on steel stresses was studied. Rebar samples were collected at various points in Abuja and its environs and tested for their mechanical and chemical properties. The results show some tolerable and intolerable deviations from provisions of BS 4449 B500B 2005 indicating that some of the rebars are satisfactory for use in reinforced concrete works while others are not. Tests conducted on the rebars include Tensile Strength, Relative Rib Area, Percentage Elongation, Bend and Rebend, and Spectrometer tests, among other physical examinations. In some rebars, results showed moderate to vast deviation from minimum acceptable standard values as specified in BS 4449 B500B 2005 for yield stress, elongation, bar diameter, mass per kilogram, carbon equivalent, while there is satisfactoriness for other tested samples.

Keywords: Reinforcement bars, Ultimate Tensile Strength, Yield Strength, Elongation, Rib Geometry, Carbon Equivalent.

1. Introduction

A reinforcement bar is described as a steel product with a circular or practically circular cross-section suitable for the reinforcement of concrete. Steel is at the heart of the economic and sustainable development of any nation. It is one of the materials most widely used by all sectors of the economy, from building structures to transport and infrastructural development. The world's most advanced economies produce and consume large quantities of steel [1-3]. Steel is indeed a versatile material. About twenty-six different elements are used in various proportions and combinations to manufacture both carbon and low alloy structural steels. [4]. In reinforced concrete structures, reinforcement bars play a role as a construction material whose properties must be known to the users before application in either design or construction purposes. Codes such as BS4449: 1967, 1969, 1997, 2005, +A2:2009, and many others have specified limits on the properties of reinforcement bars and their testing procedures amongst others [5]. A reinforcement bar is found in virtually every concrete and masonry structure. It refers to the steel rods installed inside the concrete to help them keep their shape and ensure safe, durable

structures that will be reliable for years. Without them, the natural expansion and contraction of concrete will cause weak areas to develop, which will ultimately collapse in the long run. The tensile strength of concrete is only about 10% of its compressive strength. Owing to this fact, nearly all reinforced concrete structures are designed on the assumption that concrete does not resist any tensile stress, and this is where the steel come to play a major role in tensile stress resistance [6].

The manufacturing process of reinforcement bars have a significant effect on their properties even though BS 4449 [7] contains no specific requirements for rebar manufacturing process [8]. It is important that quality norms are exercised in the case of reinforcement bars which should invariably have been rolled from tested billets [9].

In Nigeria, investigation showed that steel of recognizable origin satisfies both local and International Standard Organization (ISO) requirements for strength and ductility. On the other hand, steel of non-recognizable origin failed to satisfy the above requirements for high-yield ribbed bars but satisfies the local specifications if used as mild steel [10]. A lot of behavioral and durability issues affect the performance of this composite material. The in-depth understanding of these issues depends partly on environmental factors, and in this case, Nigeria is peculiar [11]. Reinforcement bars testing in most construction sites have been restricted to tensile tests with little or no information about other mechanical properties such as rebend, elongation, rib geometry and the chemical properties. [5].

The role reinforcement bars play in the construction industry is very important as a result, many researches have been done on reinforcement bars used in Nigeria in the past, but there is still need to constantly revisit it and carry out studies on it as the properties and qualities are always changing, so study should be carried out at regular intervals [12]. Another reason for this is the worrisome trend of building collapse in Nigeria. [13-17]. Some previous studies have shown the suitability of locally produced reinforcement bars in structural works, especially where strength and ductility are of great importance [10, 12]. In a comparative study of four locally-produced steel bars and foreign steel imported to Nigeria, it was discovered that both the local steels and the foreign product met the standard for use in the construction industry [18]. Some researchers reported different results from others, a review by Balogun et.al., [19] showed that some locally manufactured steel in Nigeria and some West African countries fall short of the international standard according to the world average specification for high yield steel bar report [20].

2. Material and Methods

2.1. Material

Reinforcement Bars: The sample materials used in this study are 25mm, 20mm, 16mm, 12mm, and 10mm bars, collected from some Steel Mills across Abuja and its environs (but their product samples are tagged to conceal their identities in the course of the testing), open markets, and construction sites.

Physical Requirements: The finished steel bars for reinforced work were rolled and made ready for construction works, irrespective of their actual weight, dimensions, and defects but free of rust and dust.

Table 1. BS4449:2005 A3 2005 – Nominal Cross -Sectional Area and Mass per Metre

Nominal Diameter (mm)	Cross-Sectional Area (mm)	Mass per Metre (Kg)
6[a]	28	0.222
7[a]	38.5	0.302
8	50.3	0.395
9	63.6	0.499
10	78.5	0.617
12	113	0.888
16	201	1.58
20	314	2.47

25	491	3.85
32	804	6.31
40	1257	9.86
50	1963	15.4
[a] Preferred diameters for the manufacture of welded fabric to BS 4483 only ***Tolerance: Permissible deviation from normal mass/m shall not be more than+/-4.5 on nominal diameters greate than 8mm, and +/-6mm on nominal diameters less than or equal to 8mm.***		

2.2 Methods: Steel Testing for Mechanical Properties

(a) Ultimate Tensile Strength

This test helps in determining the maximum stress that the tested material can withstand while being stretched or pulled before necking, that is, when the specimen's cross section starts to contract significantly.

Test equipment: Universal Testing Machine

(b) Yield Strength

It is the lowest stress that produces a permanent deformation in the tested material.

(c) Elongation

This is the increase in length of the gauge length, expressed as a percentage of the original length.

(c) Rib Geometry

The following are determined under rib geometry for the reinforcement samples tested:

i. Rib inclination angle (α)
ii. Relative rib area (*f*R)
iii. Rib height (h)
iv. Rib spacing (c)

Test Specimen

The length of the test specimen was 400mm to allow for gripping by the RRA machine and to allow automatic measurements of the geometrical characteristics of the test sample for calculating the relative rib area.

Test equipment: Automatic Relative Rib Area Machine (RRA machine)

The relative rib area ***fR*** is calculated using Equation (1) in accordance with BS4449 B500B 2005 by using the results of measurements of the geometrical characteristics discussed:

It is derived mathematically using the formula:

$$fR = (\pi d - \sum e) \times 2a_m / 3\pi dc \quad (1)$$

Where;

*f*R = Relative rib area
a_m = Centre height of the rib
e = Ribless spacing between two rib rows
d = Nominal diameter
c = Centre to centre spacing of two ribs

Table 2: BS4449 – Standard Rib Geometry (mm)

Transverse Rib										**Longitudinal Rib**	**Relative Rib Area (RRA)**
Bar Dia (d)	Rib Height (h)		Rib Spacing (C)		Rib Inclination (β)		Row Distance	Flank Inclination(α)		Rib Height	
	Min	Max	Min	Max	Min	Max	Min	Max		Max	
	0.03d	0.15d	0.4d	1.2d	35^0	75^0	(∑i)	45^0		0.10d	Min
8	0.24	1.20	3.20	9.60	35^0	75^0	6.28	45^0		0.80	0.040
10	0.30	1.50	4.00	12.00	35^0	75^0	7.85	45^0		100	0.040
12	0.36	1.80	4.80	14.40	35^0	75^0	9.42	45^0		1.20	0.040

16	0.48	2.40	6.40	19.20	35^0	75^0	12.57	45^0		1.60	0.056
20	0.60	3.00	8.00	24.00	35^0	75^0	15.71	45^0		2.00	0.056
25	0.75	3.75	10.00	30.00	35^0	75^0	19.64	45^0		2.50	0.056
32	0.96	4.80	12.80	38.40	35^0	75^0	25.13	45^0		3.20	0.056

The characteristic relative rib area is expected to meet the requirement of Table 3.

Table 3: BS4449:2005 – Characteristic Relative Rib Area

Nominal Bar Size, d (mm)	**Relative Rib Area**
$d \leq 6$	0.035
$6 < d \leq 12$	0.040
$d > 12$	0.056

(d) Rebend Test

This test determines the susceptibility of samples to fracture or irregular bending deformation.

Test equipment: Steel Bending Machine

(e) Verification of Mechanical Properties

Test samples were selected from different bars of a batch and they are required to pass the tests to be considered to have conformed to International Standard (BS4449 B500B 2005)

2.3 Chemical Concentration

All the elements in the test samples would be identified, and their concentration in percentage by weight determined.

Test equipment: Spectrometer

Determination of Carbon Equivalent

This property is required to set the cooling parameters in TMT (Thermo mechanically treated) process, and a slight variation in carbon equivalent may alter the physical properties.

The Carbon Equivalent is calculated using the following formula:

$$C_{eq} = C + (Mn/6) + (Cr+Mo+V)/5 + (Ni + Cu)/15 \quad (2)$$

Where: ***Mn*** is the percentage Manganese content

Cr is the percentage Chromiun content

V is the percentage Vanadium content

Mo is the percentage Molybdenum content

Cu is the percentage Copper content

Ni is the percentage Nickel content

3. Results and Discussions

3.1 Mechanical Properties

(a) Physical Properties of Rebar Samples

From the result of the mass per metre of tested rebar samples, 57.7% of rebars tested fell below -4.5% lower limit nominal mass per metre, while the remaining 42.3% fell within the lower limit range. Figure 1 showed that 40% of tested samples conformed to BS4449:2005 [7], even though their mass per metre fell below code standard, they remain within the lower limit of -4.5%.

Out of the fourteen rebar samples tested in the relative rib area machine, twelve samples have precise cross-sectional area while two samples (samples G and M) fell below their factory specified diameter of 16mm by (2mm in each). The RRA machine precisely measured them as 14mm rebars.

From the results presented in Figure 2, the percentage elongation at fracture of the tested samples falls within 16% - 21% while the average percentage elongation within gauge length falls within 6.0% - 8.5%. As per BS 4449:2005 B500B; the total elongation at maximum force, AGT is given as 5.0.

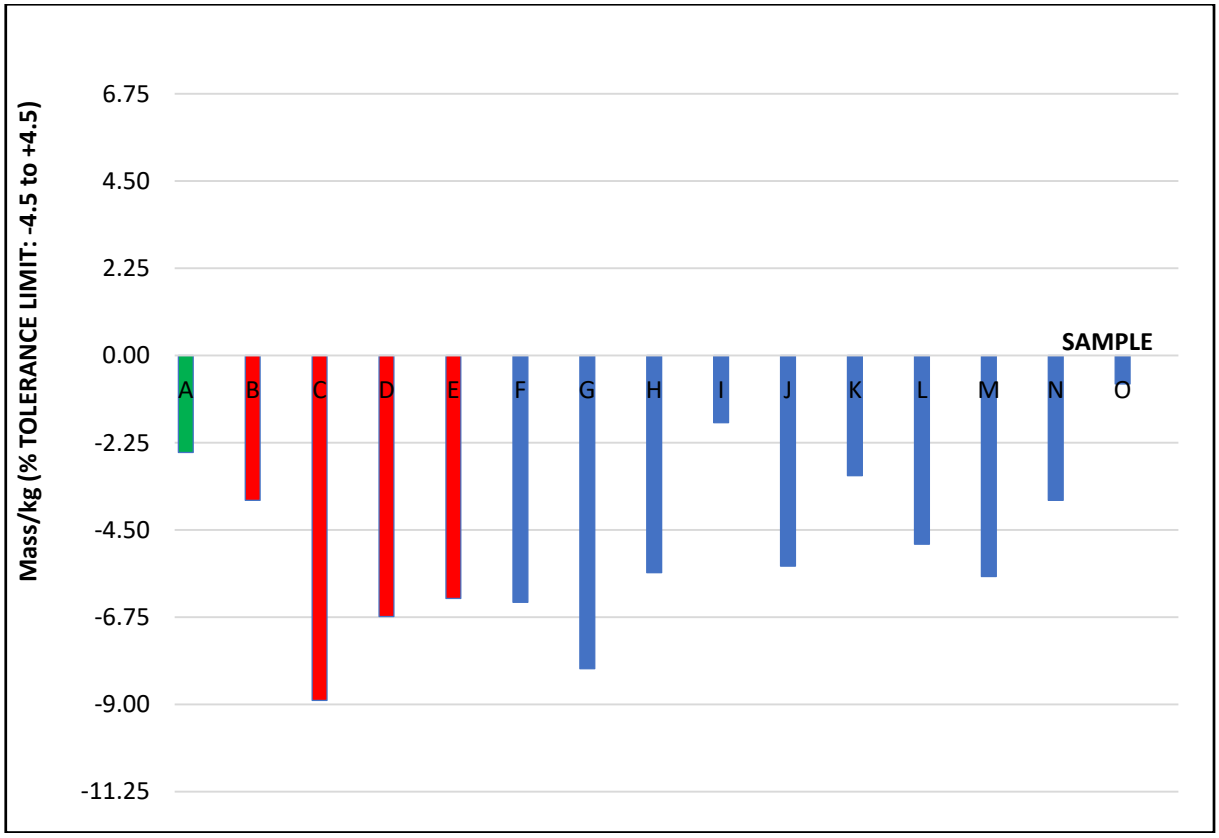

Figure 1: Bar Chart Showing Mean Permissible Deviation from Nominal Mass Per Metre

(c) Elongation

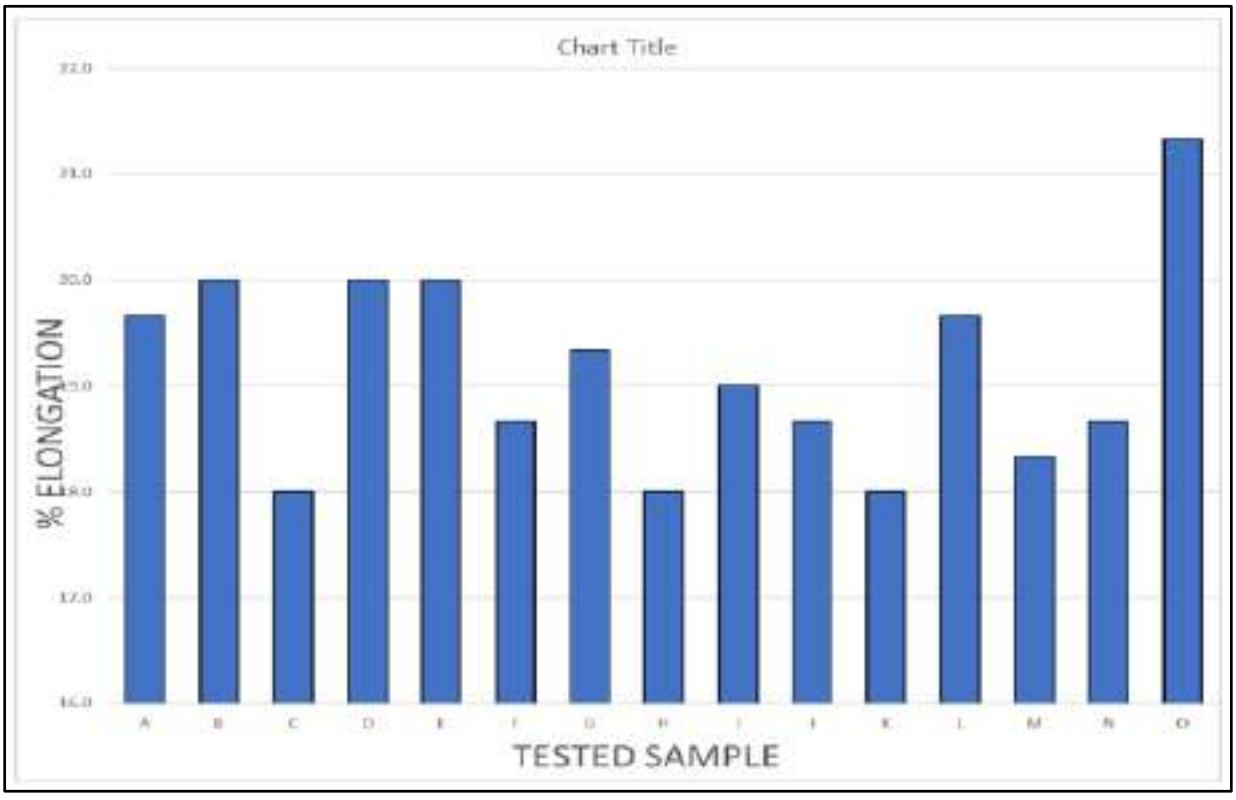

Figure 2: Percentage Elongation at Fracture

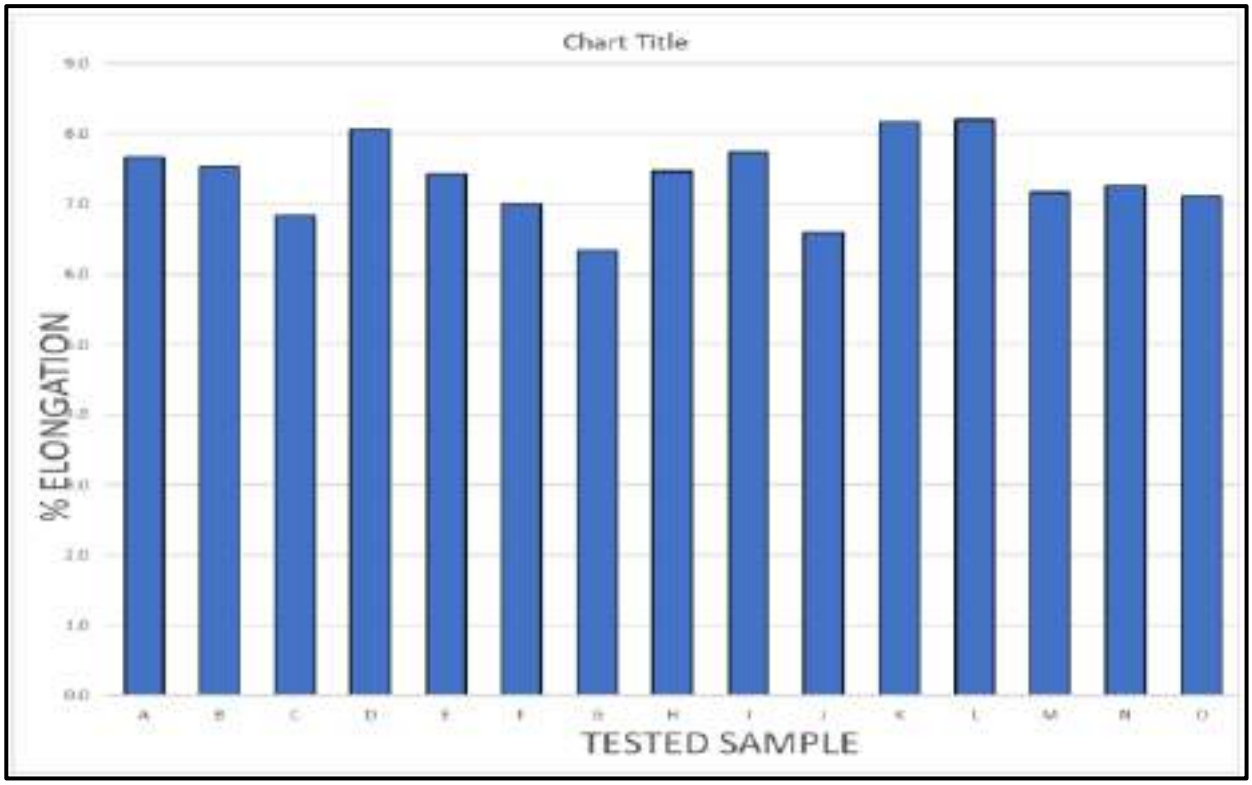

Figure 3: Percentage Elongation at Average Gauge Length

(c) Yield Stress.

Table 4 Mean and Maximum Yield Stress

	Yield stress (n/mm^2)						Ultimate stress (n/mm^2)				
Sample	**1**	**2**	**3**	**Mean**	**Standard Deviation**		**1**	**2**	**3**	**Mean**	**Standard Deviation**
C	503	401	458	454	51.12		565	494	541	533	36.12
D	561	568	571	567	5.13		640	643	637	640	3.00
E	343	329	304	325	19.76		434	418	422	425	8.33
O	434	445	444	441	6.08		615	628	630	624	8.14
B	564	564	567	565	1.73		661	658	659	659	1.53
G	341	355	458	385	63.89		493	541	500	511	25.93
H	458	513	488	486	27.54		576	627	611	605	26.08
M	500	502	503	502	1.53		622	625	621	623	2.08
N	475	468	474	472	3.79		570	565	565	567	2.89
F	327	328	329	328	1.00		501	483	503	496	11.02
J	535	522	530	529	6.56		607	599	605	604	4.16
L	492	498	497	496	3.21		663	654	653	657	5.51
A	567	579	573	573	6.00		684	688	688	687	2.31
K	608	577	594	593	15.52		682	683	683	683	0.58
I	625	525	623	591	57.17		761	702	766	743	35.59

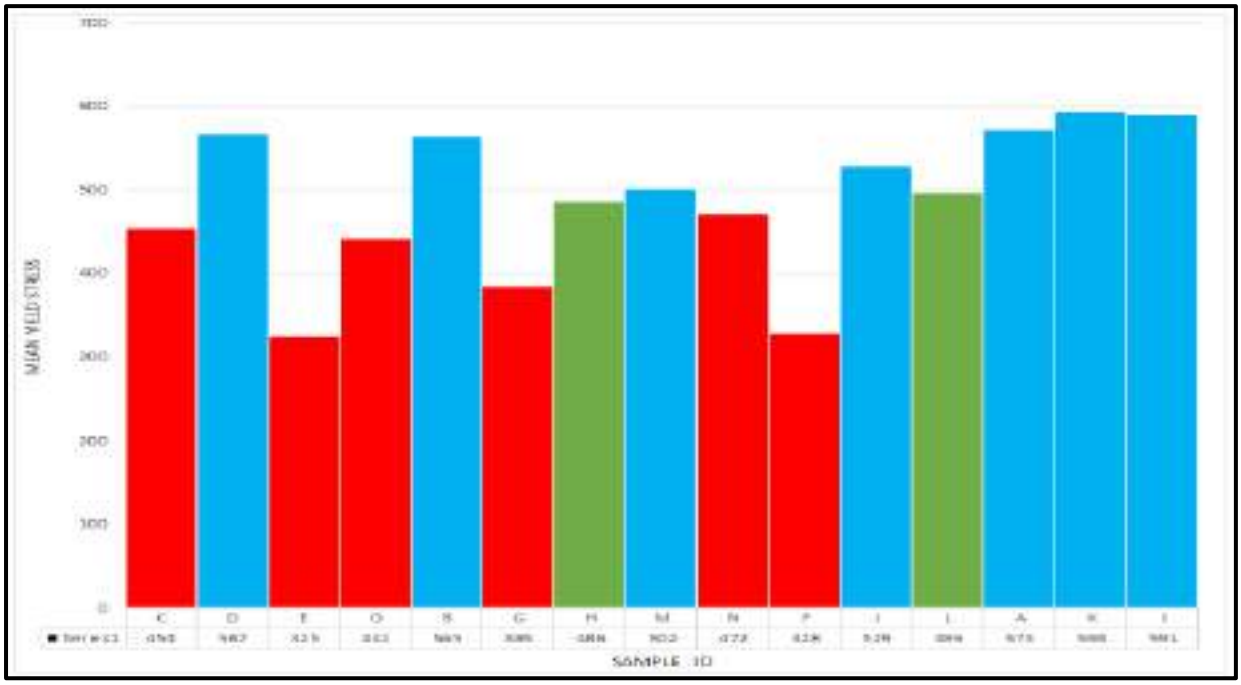

Figure 4: Mean Yield Stress of Tested Rebar Samples

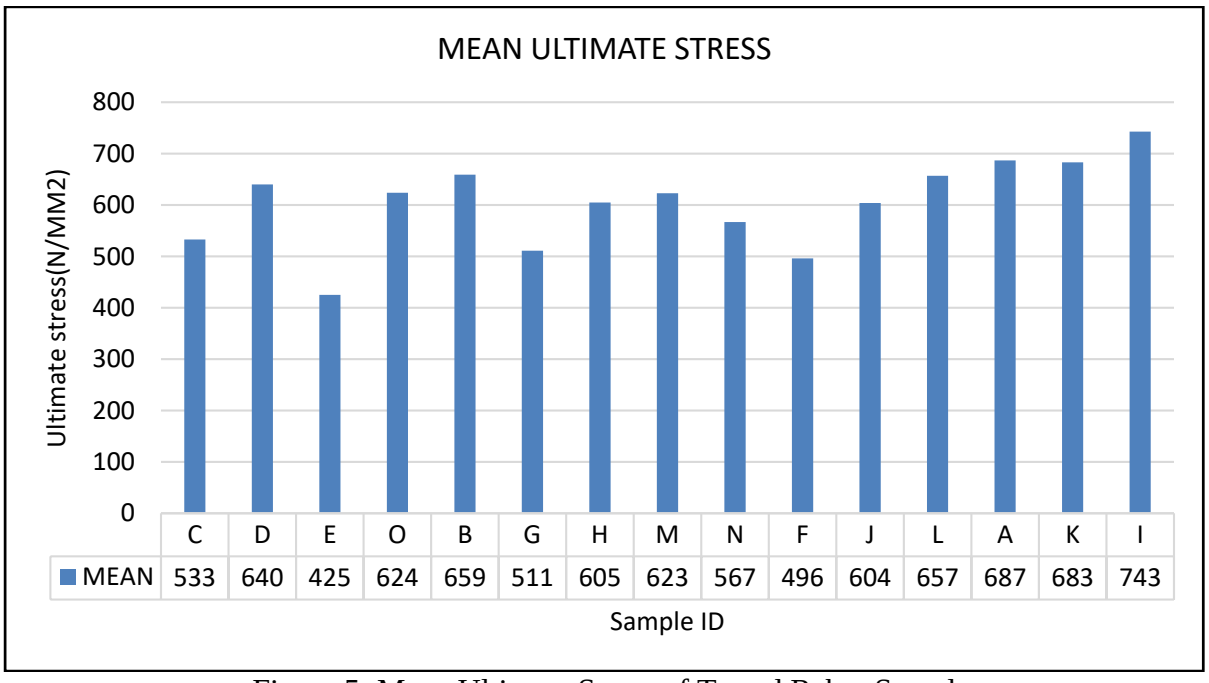

Figure 5: Mean Ultimate Stress of Tested Rebar Samples

From Figure 4, of the fifteen samples tested, only seven have their mean yield stress exceeding 500N/mm^2 as per BS4449:2005 [7], two others fell within the minimum tolerance limit of 485N/mm^2 (BS4449:2005 [7] – Absolute minimum and maximum values of tensile properties), while the remaining six samples fell below the minimum value. These findings are in accordance with the report from Alabi et.al. [21], and other works on yield strength and ultimate tensile strength [18, 22]. Table 4 also indicates the standard deviation (SD) of yield stress results, higher value of SD indicates disparity in individual values of a group of samples which is a pointer to incoherence in properties of the rebar in that group

(d) Relative Rib Area.

Table 5 Computation of Relative Rib Area (Rra) of Tested Samples

S/No	ROW NO	DIAMETER (mm)	RIB HEIGHT (mm)			RIB DIST. C (mm)	INCLINATION		ROW DIST. E (mm)	HEAD WIDTH (mm)	RIB LENGTH (mm)	LONG RIB		RELATIVE RIB AREA fR	RRA Remark
			centre	1/4 pnts	3/4 pnts		Alpha	Beta				height (mm)	width(mm)		
B	1	16	0.93	0.95	1	10.4	50	56	4.08	1.7	23.7	0.53	2.78	0.051*	Failed
	2		1.1	1.04	1.13	10.2	55	56	6.89	1.6	23.7	0.28	3.18		
	Mean		1.02	1	1.07	10.3	53	56	∑: 10.97	1.65	23.7	0.41	2.98	-8.9%	
K	1	25	1.52	1.21	1.44	14.7	53	63	4.9	2.7	36.9	0.85	2.89	0.062	Passed
	2		1.8	1.37	1.35	15	51	62	7.93	1.9	37.2	0.86	3.17		
	Mean		1.66	1.29	1.4	14.9	52	63	∑: 12.83	2.3	37	0.86	3.03	+10.7%	
C	1	10	0.87	0.66	0.72	10.2	38	39	1.8	2.7	19	0.16	1.93	0.043	Passed
	2		0.87	0.64	0.76	10.2	39	40	5.65	2.6	18.6	0.17	1.99		
	Mean		0.87	0.65	0.74	10.2	39	40	∑: 7.45	2.65	18.8	0.17	1.96	+7.5%	
F	1	20	1.76	1.24	1.1	21	32	39	4.64	3.2	41.2	1.29	3.23	0.043*	Failed
	2		1.69	1.34	0.99	22.7	34	39	6.35	4.1	41.2	0.99	3.33		
	Mean		1.73	1.29	1.05	21.9	33	39	∑: 10.99	3.65	41.2	1.14	3.28	-23.2%	
D	1	10	0.61	0.45	0.29	6.9	48	55	2.17	0.7	16.5	0.15	1.28	0.06	Passed
	2		0.83	0.51	0.27	6.9	53	55	2.29	0.8	16.5				
	Mean		0.72	0.48	0.28	6.9	51	55	∑: 4.46	0.75	16.5	0.08	0.64	+50.0%	
E	1	10	0.83	0.83	0.55	7.7	48	49	3.88	1.1	16.5	0.7	2.13	0.054	Passed
	2		0.75	0.66	0.57	7.8	48	48	2.63	1.1	16.8	0.81	2.3		
	Mean		0.79	0.75	0.56	7.8	48	49	∑: 6.51	1.1	16.6	0.76	2.22	+35.0%	
G	1	14*	1.32	1.21	0.69	13.2	40	41	5.83	2.5	25.6	1.2	2.96	0.044*	Failed
	2		0.98	0.95	0.59	13.5	33	41	4.62	2.5	25.6	1.52	3.08		
	Mean		1.15	1.08	0.64	13.4	37	41	∑: 10.45	2.5	25.6	1.36	3.02	-21.4%	
O	1	12	1.28	0.5	1.48	14.3	48	44	6.44	2.3	17.4	-5.34	3.83	0.037*	Failed
	2		1.14	0.81	0.97	13.7	47	46	7.13	1.9	16.8	1.04	4.27		
	Mean		1.21	0.66	1.23	14	48	45	∑: 13.57	2.1	17.1	-2.15	4.05	-7.5%	
M	1	14*	1.45	1.24	1.33	12	56	57	2.87	2	21.9	0.52	2.5	0.064	Passed
	2		1.28	1.2	0.89	11.9	60	58	4.3	1.7	21.7	0.27	1.95		
	Mean		1.37	1.22	1.11	12	58	58	∑: 7.17	1.85	21.8	0.4	2.23	+14.3%	
H	1	16	0.72	0.62	0.6	10	51	52	5.87	1	24.7	0.5	3.43	0.042*	Failed
	2		0.9	0.56	0.58	10	56	52	5.54	0.9	24.7	0.55	3.5		
	Mean		0.81	0.59	0.59	10	54	52	∑: 11.41	0.95	24.7	0.53	3.47	-25.0%	
N	1	16	1.12	0.57	0.8	16.9	51	46	6.21	2.1	26.6	0.88	3.15	0.036*	Failed
	2		1.31	0.45	1.01	17	51	46	5.8	2.1	26.6	0.27	3.05		
	Mean		1.22	0.51	0.94	17	51	46	∑: 12.01	2.1	26.6	0.58	3.1	-37.5%	
J	1	20	1.06	1.07	0.81	14.1	47	56	3.38	1.4	33.5	0.33	2.97	0.042*	Failed
	2		0.97	0.9	0.51	14.1	46	57	3.86	1.5	33.1	1	3.14		
	Mean		1.02	0.99	0.66	14.1	47	57	∑: 7.24	1.45	33.3	0.67	3.06	-0.25%	

L	1	20	1.61	1.12	1.35	21.3	31	41	7.14	3.5	35.8	0.95	3.9	0.041*	Failed
	2		1.51	0.25	0.99	16.6	33	40	8.69	3.8	36.6	0.34	1.98		
	Mean		1.56	0.69	1.17	19	32	41	∑: 15.83	3.65	36.2	0.65	2.94	-26.8%	
A	1	25	2.18	1.11	1.48	14.5	51	56	5.62	2.1	40	1.72	2.89	0.084	Passed
	2		2.18	1.82	1.5	14.6	55	63	6.58	2.3	37.2	1.78	2.56		
	Mean		2.18	1.47	1.5	14.6	53	60	∑: 12.20	2.2	38.6	1.75	2.73	+50.0%	

* Characteristic RRA limit not satisfied.

3.2 Chemical Composition

Table 6 Percentage Chemical Composition

ELEMENTS	Sample I.D and % composition of the elements														
	K	F	I	M	B	C	D	E	G	H	I	N	O	Z	A
Carbon ©	0.16	0.25	0.21	0.2	0.14	0.12	0.12	0.12	0.26	0.17	0.26	0.12	0.25	0.13	0.22
Manganese(Mn)	0.68	0.64	1.44	0.51	0.72	0.55	0.75	0.38	0.42	0.62	0.7	0.53	0.69	0.52	0.94
Silicon (Si)	0.25	0.27	0.3	0.19	0.21	0.19	0.21	0.13	0.16	0.16	0.23	0.26	0.34	0.23	0.2
Copper (Cu)	0.21	0.13	0.25	0.17	0.17	0.22	0.22	0.3	0.17	0.25	0.12	0.25	0.28	0.26	0.033
Phosphorus (P)	0.051	0.029	0.038	0.033	0.038	0.047	0.042	0.045	0.029	0.034	0.054	0.036	0.055	0.039	0.021
Sulphur (S)	0.047	0.037	0.05	0.038	0.038	0.047	0.047	0.062	0.029	0.053	0.058	0.046	0.059	0.055	0.038
Chromium (Cr)	0.31	0.17	0.14	0.13	0.25	0.22	0.16	0.23	0.19	0.33	0.13	0.28	0.26	0.28	0.035
Molybdenum (Mo)	0.02	0.012	0.023	0.012	0.017	0.013	0.015	0.027	0.011	0.016	0.008	0.024	0.03	0.025	0.001
Nickel (Ni)	0.097	0.065	0.11	0.078	0.092	0.1	0.095	0.11	0.088	0.2	0.064	0.096	0.11	0.099	0.018
Vanadium (V)	0.003	0.003	0.04	0.001	0.003	0.003	0.002	0.003	0.003	0.003	0.002	0.004	0.005	0.004	0.001
Nitrogen (N)	0.0066	0.0194	0.0128	0.014	0.0073	0.0066	>0.0381	0.018	0.0045	0.0062	0.0143	0.007	0.002	0.0063	0.0132
Boron (Bo)	0.0011	0.0003	<-0.0004	<-0.0002	0.001	0.0013	<0.0000	0.0009	<0.0001	<-0.0004	<-0.0001	0.0003	<-0.0005	<-0.0007	<-0.0003
Aluminum (Al)	0.003	0.006	0.003	0.002	0.002	0.004	0.002	0.003	0.005	0.002	0.004	0.008	0.002	0.006	0.006
Calcium (Ca)	0.002	0.002	0.0006	0.0002	0.0003	0.0001	0.001	0.0003	0.0002	0.0006	0.006	0.01	0.0006	0.004	0.002
Cobalt (Co)	0.009	0.005	0.015	0.007	0.008	0.008	0.007	0.009	0.009	0.008	0.006	0.007	0.006	0.006	<0.0003
Zinc (Zn)	<-0.0002	0.001	<0.0004	0.001	<-0.0003	<-0.0002	<0.0001	<-0.0003	0.005	<-0.0004	0.003	<-0.0002	<-0.0004	<-0.0003	<0.0001
Arsenic (As)	0.004	0.003	0.007	0.003	0.002	0.003	0.002	0.001	0.002	0.002	0.004	0.002	0.002	0.002	0.003
Antimony (Sb)	0.012	0.008	0.011	0.008	0.009	0.011	0.009	0.008	0.008	0.009	0.006	0.007	0.009	0.011	0.005
Tin (Sn)	0.029	0.01	0.016	0.013	0.024	0.021	0.034	0.025	0.023	0.037	0.014	0.019	0.019	0.021	0.002
Titanium (Ti)	<0.0001	0.0007	<-0.0001	<-0.0003	<-0.0003	0.0003	<-0.0008	<-0.0006	0.0007	<0.0001	0.0006	0.0009	<-0.0002	0.0003	0.0002

Carbon Equivalent Results

Table 7 Chemical Composition and Computation of Carbon Equivalent of Samples

SAMPLE LABEL	%N	% C	% Mn	% Cr	% Mo	% V	% Ni	% Cu	%P	%S	C_{eqv}
A2	0.0132	0.22	0.94	0.035	0.001	0.001	0.018	0.033	0.021	0.038	0.3875
B1	0.0073	0.14	0.72	0.25	0.017	0.003	0.092	0.17	0.038	0.038	0.3315
C1	0.0066	0.12	0.55	0.22	0.013	0.003	0.1	0.22	0.047	0.047	0.2802
D1	0.0381	0.12	0.75	0.16	0.015	0.002	0.095	0.22	0.042	0.047	0.3014
E1	0.0180	0.12	0.38	0.23	0.027	0.003	0.11	0.3	0.045	*0.062	0.2627
F1	0.0194	*0.25	0.64	0.17	0.012	0.003	0.065	0.13	0.029	0.037	0.4067
G1	0.0045	*0.26	0.42	0.19	0.011	0.003	0.0045	0.17	0.029	0.029	0.382
H1	0.0062	0.17	0.62	0.33	0.016	0.003	0.2	0.25	0.034	0.053	0.3731
I1	0.0128	0.21	1.44	0.14	0.023	0.04	0.11	0.25	0.038	0.05	0.5146
K1	0.0066	0.16	0.68	0.31	0.02	0.003	0.097	0.21	0.051	0.047	0.3604
L1	*0.0143	*0.26	0.7	0.13	0.008	0.002	0.064	0.12	0.054	*0.058	0.4169
M1	0.0002	0.2	0.51	0.13	0.012	0.001	0.078	0.17	0.033	0.038	0.3301
N1	0.0070	0.12	0.53	0.28	0.024	0.004	0.096	0.25	0.036	0.046	0.293
O1	0.0020	*0.25	0.669	0.26	0.03	0.005	0.11	0.28	0.055	*0.059	0.4465

* % by mass exceeded.

Fourteen samples were tested and diameter of rebars range from 10mm – 25mm. of the fourteen samples, six crossed the minimum threshold specified in Table 9 of BS4449:2005 [7]. The remaining nine samples failed, indicating that their rib geometry did not conform to standard.

This is an indication that the bonding of the rebars which failed the RRA test when used in reinforced concrete works will be unreliable.

(e) Bend and Rebend

After the bend and rebend tests, all fifteen (15) tested rebar samples were checked. They showed no sign of fracture or cracks visible to a person of normal or corrected vision. Therefore, the requirements of BS4449:2005 [7] Clause 7.2.5 were satisfied by the rebar samples

The twenty elements discovered in this test are Aluminium (Al), Boron (Bo), Calcium (Ca), Carbon (C), Chlorine(Cl), Chromium(Cr), Copper (Cu) antimony (Sb) Arsenic (As), Iron(Fe), Manganese (Mn), Molybdenum(Mo), Nickel (Ni), Nitrogen (N), Phosphorus (P), Silicon(Si), Sulphur, Titanium (Ti), Vanadium (V), Zinc (Zn).

The asterisked data under the columns: %carbon %Sulphur and % Nitrogen in Table 7 indicate that Carbon, Sulphur, and Nitrogen contents by mass for the samples were exceeded, however, for Carbon for instance. The values are permitted to exceed the maximum values 0.03% by mass, provided that the carbon equivalent value is decreased by 0.02% by mass.

The carbon equivalent, C_{eqv}, for all the tested samples fell below the maximum of 0.52% by mass in accordance with BS4449:2005 [7].

4. Conclusion

The following conclusions were drawn based on the results presented and practical observations made on the mechanical and chemical properties of reinforcement bars manufactured in Nigeria:

i. About 15% of the tested rebar samples have their measured diameter smaller than their nominal diameter, which may indicate the level of quality control of the local bar manufacture.

ii. It was observed that 57% of the tested rebar samples failed the RRA test, which indicates that the surface geometry of the tested rebars did not conform to the standard.

iii. It was found that only 40% of tested rebars fall within permissible deviation from nominal mass per meter, while the remaining 60% weigh less than the tolerant limit of the permissible mass per meter.

iv. About 47% of the tested rebars have yield stresses above the BS4449:2005 stipulated minimum standard, 13% fall within allowable minimum while 40% others failed. This is an indication that there is a 40% chance of procuring rebars from local manufactures which would not pass the yield stress test

v. It was found that the chemical composition of tested rebars conformed very largely to standards, and where values marginally exceeded (in the case of carbon %) the corresponding values carbon equivalent fall below the maximum specified in the code.

Acknowledgement

The authors would like to acknowledge the management and laboratory staff of African Foundries Limited, Lagos, for the access to their sophisticated and world-class laboratories to carry out the experiments of this study.

Conflict of Interest

The authors declare no conflict of interest.

References

[1] Ajayi J.A (1998): "*Materials and Metallurgical Engineering: Nigeria's link to Technological Development in the next millennium":* Lecture delivered at the National Association of Metallurgical and Materials Engineering Students week, Obafemi Awolowo Branch, Ile-Ife, Nigeria. p.4.

[2] M. Jibrin, Characterization of reinforcing steel bars in the Nigeria Construction Industry, Ph.D. thesis, Department of Civil Engineering, Ahmadu Bello University, Zaria, Kaduna State (2012)

[3] Ponle, E. A., Olatunde, O. B., & Awotunde, O. W. (2014). Mechanical properties of reinforcing steel rods produced from recycled scraps. *Int. J. Eng. Sci*, *3*(2), 14-34.

[4] MIT Department of Civil and Environmental Engineering, (1999). Design of Steel Structures. Pp 1-2

[5] Jibrin M.U. and Ejeh S.P. (2013). "*Chemical Composition of Reinforcing Steel Bars in the Nigerian Construction Industry*": Accepted by The International Journal of Civil & Environmental Engineering, IJCEE-IJES, Vol 13. Pp. 01-05.

[6] Adetoro A.E., Oladapo A.S. (2017): *"Assessment of suitability of selected reinforcement Bars Used for Construction in Nigeria"*. Published by Journal of Multidisciplinary Engineering Science and Technology. www.jmest.org. ISSN:2458-9403. Vol 4, Issue 5. Pp 7308-7312.

[7] British Standards Institutions. BS 4449 (2005) "*Carbon Steel Bars for the Reinforcement of concrete. Weldable reinforcing steel- bar, coil and decoiled product. Specification*" London. pp.5-11

[8] UK CARES - "*Guide to Reinforcing Steels* - PARTS 1, 2, 3, 7 and 8. (Certification Authority for Reinforcing Steels)

[9] Singh, B., & Kaushik, S. K. (2002). Influence of steel-making processes on the quality of reinforcement. *Indian Concrete Journal*, *76*(7), 407-412.

[10] Arum, C. (2008). Verification of properties of concrete reinforcement bars: Nigeria as case study. African Research Review, 2(2), 234-252.

[11] Anthony N.E., Oluwarotimi M.O. and Opeyemi J. (2014): *"Experimental investigation of Yield Strengths of Steel Reinforcing Bars Used in Nigerian Concrete industries."* Published by International Journal of Science and EngineeringResearch www.ijser.com Volume 5, Issue 4. Pp 76-82

[12] Odusote, J. K., Shittu, W., Adeleke, A. A., Ikubanni, P. P., & Adeyemo, O. (2019). Chemical and Mechanical Properties of Reinforcing Steel Bars from Local Steel Plants. Journal of Failure Analysis and Prevention. doi:10.1007/s11668-019-00695-x

[13] Olateju, O.T., The Need for Quality Control in the Nigeria Building Industry, Journal of Studies in Environmental Design in West Africa 10 (1993) 22-25.

[14] Chinwokwu, O., The Role of Professional in Averting Building Collapse, in: Proceedings of 2days' seminar of NIOB (Lagos state chapter) on Building Collapse, Prevention and Remedies, Lagos Airport Hotel, Lagos 3rd -4th May 2000.

[15] Folagbade, S.O., Case Studies of Building Collapse in Nigeria, in: Proceedings on Building Collapse: Causes, Prevention and Remedies, D.R. Ogunyemi (Ed.), Ondo State, Nigeria. The Nigeria Institute of Building, 2002, pp. 183-187.

[16] Fagbenle O.I. and Olawumi, A.O., Building Failure and Collapse in Nigeria. The Influence of Informal Sector, Journal of Sustainable Development, 3(4) (2010) 268-276.

[17] Odusote, J. K., & Adeleke, A. A. (2012). Analysis of Properties of Reinforcing Steel Bars: Case Study of Collapsed Building in Lagos, Nigeria. Applied Mechanics and Materials, 204-208, 3052–3056.

doi:10.4028/www.scientific.net/amm.204-208.3052

[18] Alabi, A. G. F., & Onyeji, L. I. (2010). Analysis and comparative assessment of locally produced reinforcing steel bars for structural purposes. Journal of Research Information in Civil Engineering, 7(2), 49-60.

[19] Balogun, S., Esezobor, D., Adeosun, S., & Sekunowo, O. (2009). Challenges of producing quality construction steel bars in West Africa: Case study of Nigeria steel industry. *Journal of Minerals & Materials Characterization & Engineering*, *8*(4), 283-292

[20] Vlad, C. M., 1986, "A comparison between the TEMPRIMAL and TEMPCORE processes for high strength rebars", 27th Mechanical Working and Steel Processing Conference Proceedings, Iron and Steel Society, Vol.23, pp. 908-912

[21] Alabi, A. G. F., Ayoade, A. O., Odusote, J. K., & Akanni, A. A. (2016). Assessment of suitability of Nigerian made steel bars for structural applications. The Journal of the Association of Professional Engineers of Trinidad and Tobago, 44(2), 17-23.

[22] Chukwudi, B.C. (2010). "Assessment of the quality of steel rods available in Onitcha market: In view of the role of poor quality rods in building failures in Nigeria", Pacific Journal of Science and Technology, Vol. 11, No 1, pp.55-59.